Wnt/β-catenin signaling in malignant mammary tumor progression and metastasis formation

&

Mechanisms of evasive resistance to sorafenib in hepatocellular carcinoma

Inauguraldissertation

zur
Erlangung der Würde eines Doktors der Philosophie
vorgelegt der
Philosophisch-Naturwissenschaftlichen Fakultät
der Universität Basel

von

David Martin Büchel

aus Rüthi (SG), Schweiz

Basel, 2019

Genehmigt von der Philosophisch-Naturwissenschaftlichen Fakultät auf Antrag von:

Prof. Dr. Gerhard Christofori

Prof. Dr. Markus Heim

Basel den 19.02.2019

Prof. Dr. Martin Spiess
Dekan

Table of contents

1. General Introduction

1.1 Cancer

Cancer is a general term for a group of diseases which can originate and affect nearly all organs and tissues and is the second leading cause for death worldwide (WHO, 2018). These malignancies share some but also have their own characteristics, risk factors and treatment approaches. Each cell in our body has a specific function and a functioning tissue architecture underlies stringent control mechanisms as for example precise control of cell division and function to ensure homeostasis. Cancer cells, on the other hand, manage to escape these mechanisms resulting in uncontrolled growth and acquisition of altered functions that may hamper the function of non-cancerous cells around them. The majority of such neoplasms arise from epithelial cells. They can be either benign or be/become malignant. Benign tumors remain confined to the location of origin and do not spread or invade the surrounding tissue. Malignant tumors, however, are able to invade the surrounding tissue and spread throughout the body via blood and/or the lymphatic system. Most cancer deaths are not caused by the primary tumor itself but rather by the metastatic outgrowth [1]. Cancer development also depends on the interaction and collaboration with the tumor microenvironment. The tumors are not only composed of cancer cells but also of several other cell types, such as immune cells, endothelial cells, pericytes and fibroblasts [2]. The probability to develop cancer increases with age and thus more cancer are diagnosed rather late in life with an increase at approximately 50 years of age. Some of the known risk factors include genetic predisposition, environmental / lifestyle influences, chronic inflammation and viral infections [3-6]. The development of cancer is a multistep process requiring the acquisition of genomic alterations often involving tumor suppressor genes as well as proto-oncogenes. The common features that collectively dictate malignant growth acquired during this multistep development of cancer have been proposed in 2000 by Weinberg A. and Hanahan D and comprised six hallmarks that were revised in 2011 and updated due to observations and progress in cancer research [7, 8]. These hallmarks are:

- Sustaining proliferative signaling: The ability of cancer cells to sustain chronic proliferation by deregulation of mechanisms controlling tissue homeostasis.

- Evading growth suppressors: To evade regulation of cell number and tissue homeostasis, cancer cells are able to circumvent or even eliminate negative regulators of cell proliferation. These regulatory genes – mostly belonging to the family of the so-called tumor suppressor genes – operate as central points of intersection acting on decisions of proliferation or, alternatively, activate senescence and thus apoptotic pathways.

- Deregulating cellular energetics: The deregulated proliferation of cancer cells requires an adjustment of the energy household. Under normoxia, cells rely on oxidative phosphorylation and switch to glycolysis under hypoxic conditions. However, cancer cells are able to use glycolysis even in the presence of oxygen (aerobic glycolsis) also called “Warburg effect”.

- Resisting cell death: The balance between cell proliferation and cell death that would maintain tissue homeostasis is disturbed in cancer cells. Apoptosis has been found being attenuated in high-grade and therapy-resistant tumors.

- Genomic instability & mutation: Certain epigenetic changes and/or genomic mutations can confer a growth advantage of certain cells leading to clonal expansions of altered cells. An increased sensitivity to mutagenic agents and ablation of the genomic maintenance machinery can increase the mutation rate, respectively impair the repair mechanisms, leading to accumulation of mutations by impairing genomic integrity surveillance which would force genetically damaged cells into senescence or apoptosis. Thus, increasing the chance of mutation acquisition with evasion of genome maintenance systems facilitates tumor cell growth.

- Inducing angiogenesis: To ensure and sustain the increased nutrient and oxygen supply as well as disposal of metabolic wastes and carbon dioxide during tumor growth, an angiogenic switch is activated leading to the expansion and generation of the normally quiescent vasculature.

- Activating invasion and metastasis: Progression to higher pathological grades is often associated with local invasion and distant metastasis formation. The cancer cells adapt their cell morphology and alterations in cell-cell attachment as well as cell attachment

to the ECM are found. This enables intravasation into lymphatic vessels or blood vessels and spreading into distant tissues and organs in a multistep process termed “invasion-metastasis cascade”. Within this process, the developmental regulatory program referred as the epithelial-mesenchymal transition (EMT) by which epithelial cells undergo a transformation by which they gain migratory and invasive capabilities which will be further discusses later in this thesis (see chapter “Epithelial-to-mesenchymal transition”).

- Tumor-promoting inflammation: Infiltration of cells of the innate and adaptive immune system in neoplastic tissue is known for a long time and has been thought to only reflect an antagonizing effort of the immune system on tumor cells. The current state of scientific knowledge also adds an unanticipated and paradoxical effect of promoting tumorigenesis and progression by releasing factors to the tumor microenvironment, such as survival-factors, ECM-modifying enzymes, growth factors and enzymes facilitating angiogenesis, invasion and metastasis.

- Avoiding immune destruction: The immune system monitors cells and tissues and is suggested to contribute to tumor eradication by recognizing and eliminating cancer cells. Hence, for cancer cells to outgrow, they have to evade immune surveillance or limit their removal by immune cells.

- Enabling replicative immortality: The ability to form macroscopic tumor tissue requires a prolonged life span and thus abolishment of senescence and crisis in tumor cells. This transition, called immortalization, has been observed in various immortalized cell cultures as well as in tumor tissue and was associated with enhanced activity of the specialized DNA polymerase Telomerase, an enzyme responsible for adding telomere repeats to the ends of telomeric DNA. The length of telomeric DNA has been shown indicative of the cells lifespan or ability to further replicate, since without these hexamer repeats, the protection from end-to-end fusions ending up in unstable dicentric chromosomes in mitosis leads to unbalanced chromosomes and thus threatens cell viability. The maintenance of telomeric DNA by enhanced telomerase activity or less frequently by an alternative recombination-based telomere maintenance mechanism hence provides means to protect the chromosomal ends enabling cancer cells to have an unlimited replicative potential.

2. Project I: Wnt/β-catenin signaling in malignant mammary tumor progression and metastasis formation

2.1 Summary

β-catenin exerts a dual role as the key nuclear effector of the canonical Wnt signaling pathway and as a crucial component of the E-cadherin-mediated cell-cell adhesion complex. In breast cancer, aberrations in the canonical Wnt signaling pathway have been found in correlation with poor prognosis. To provide a better understanding of β-catenin's function in breast tumor progression and metastasis formation, we have performed functional *in vivo* analysis in the MMTV-PyMT mouse model. We first analyzed breast cancer progression and metastasis formation in the complete absence of β-catenin by conditional knockout. We found that the knockout of β–catenin and hence the loss of its signaling and adhesion function leads to apoptosis *in vitro* and *in vivo*. To specifically dissect its transcriptional function without affecting its role in cell adhesion, we have used mice expressing mutant forms of β-catenin which retained their function in cell adhesion but lacked either the N- or C-terminal transcriptional output or both, resulting in the abrogation of β-catenin's transcriptional activity and thus the canonical Wnt signaling output. Introducing the N-terminal mutation D164A abrogates the interaction of β-catenin with its coactivators BCL9 and BCL9L, deletion of the C-terminus (ΔC) on the other hand prevents binding of multiple coactivators to the C-terminus. The double mutant (dm) combines both, the D164A mutation and the C-terminal truncation and thereby completely abrogates Wnt signaling. From the different mouse tumor genotypes, cell lines have been established to further characterize and examine the effects of an altered canonical Wnt signaling output. As compared to the β-catenin knockout cells, these cells were viable, suggesting a key role of β-catenin's adhesion function in cell survival. Here, we demonstrate that selective abrogation of the N- and/or C-terminal transcriptional output of β-catenin affects tumor progression and tumor cell proliferation. Lack of the N-terminal transcriptional output only or the complete abrogation of Wnt signaling activity in the dm form of β-catenin also affects metastasis formation *in vivo* and epithelial-to-mesenchymal transition (EMT) *in vitro*. Furthermore, the different mutant forms exert a dominant-negative effect. RNA sequencing analysis to examine global changes in transcription and signaling pathways affected by the expression of the different β-

catenin mutant forms upon activation of the Wnt pathway and during EMT by Wnt3a or TGFβ treatment, respectively, has been performed. With this approach we were able to identify candidate genes, which seem to be either regulated by N- and C-terminal or specifically by N- or C-terminal coactivators binding to β-catenin. Furthermore, preventing the binding of coactivators to β-catenin in the β-catenin$^{dm/-}$ cell line resulted in the almost complete abrogation of the canonical Wnt pathway showing only minor expression changes in some known Wnt target genes as well as pathway components. Moreover, also upon TGFβ treatment we detected target genes that seem to be specifically regulated by either the N- or the C-terminal coactivators during EMT. The mutant forms of β-catenin were able to alter and partially ablate the EMT response as compared to wild-type β-catenin, however, the cell lines are still able to upregulate most of the mesenchymal markers examined so far. In summary this study provides new insight of the involvement of the canonical Wnt signaling pathway in breast tumor progression and metastasis formation and allows the identification of β-catenin target genes important for EMT and tumor progression. These data may help identifying new therapeutic targets in breast cancer tumor progression and metastasis formation.

2.2 Introduction

2.2.1 Breast cancer

2.2.1.1 Breast development

Over the lifetime, the breast tissue undergoes many changes from birth to puberty and pregnancy until the menopause. The mammary glands are complex secretory organs composed of various different cell types. In brief, they are composed of epithelial cells that grow from the nipple into a fat pad formed by adipocytes that is infiltrated by vascular endothelial cells, fibroblasts and immune cells. Most information on breast development has been obtained from studies in rodents, however there are some architectural and hormonal differences between rodents and humans. Morphogenesis of the mouse mammary gland starts on embryonic day 10.5 (E10.5) with the ventral formation of two mammary lines called milk lines. At E11.5, five pairs of placodes are formed by those cells which are multilayered ectodermal structures. In contrast, human mammary glands comprise only a single pair of placodes. [9] Subsequently, the murine mammary placodes expand and form buds of epithelial cells that descend into the underlying mesenchyme, where the cells start to extent and sprout from the buds. Once these cells reach the fat pat they start branching and give rise to a rudimental ductal tree which is formed without hormonal input. During E16-18, the lumen is formed, before the invading epithelium becomes a more solid structure. During puberty, the hormones promote the expansion of the ductal tree throughout the mammary fat pads with proliferation structures located at the tips of the growing ducts called terminal end buds (TEBs). [10, 11] The growth is driven by a single layer of cells at the tip of the TEB called cap cells that have been found to differentiate into myoepithelial cells [12]. Later on, the proliferating TEBs are replaced by terminal end-ducts (TEDs) and alveolar end buds which are mitotically quiescent. During pregnancy the number of blood vessels increases and the mammary epithelium expands, estrogen and growth hormones drive this expansion of the ductal network. Furthermore, alveologenesis takes place which is mainly orchestrated by progesterone and prolactin. The alveolar end buds become mature alveoli which are small cavities for milk production and storage. The functional units for milk production and storage are called terminal ductal lobular units (TDLUs) and show a comparable structure to the TEBs in murine breast tissue (Fig. 1A). [13-16] During weaning, the lacking milk demand initiates the process

of involution, compromising apoptosis of the milk-producing cells which is followed by tissue transformation and widespread apoptotic remodeling of the epithelial tree to a state similar to a virgin adult mouse [17]. The mammary epithelium is composed of a double-layer originating form adult mammary stem cells (MaSCs) comprising an inner layer of luminal epithelial cells and an outer layer of contractile myoepithelial/basal epithelial cells secreting and lying on the basement membrane (Fig. 1B) [18]. These cell types can be distinguished using a number of cytokeratins, intermediate filament proteins that can act as lineage markers in the mammary epithelium. For example, K4 and K18 mark luminal cells, whereas K5 and K14 identify basal/myoepithelial cells [19-21].

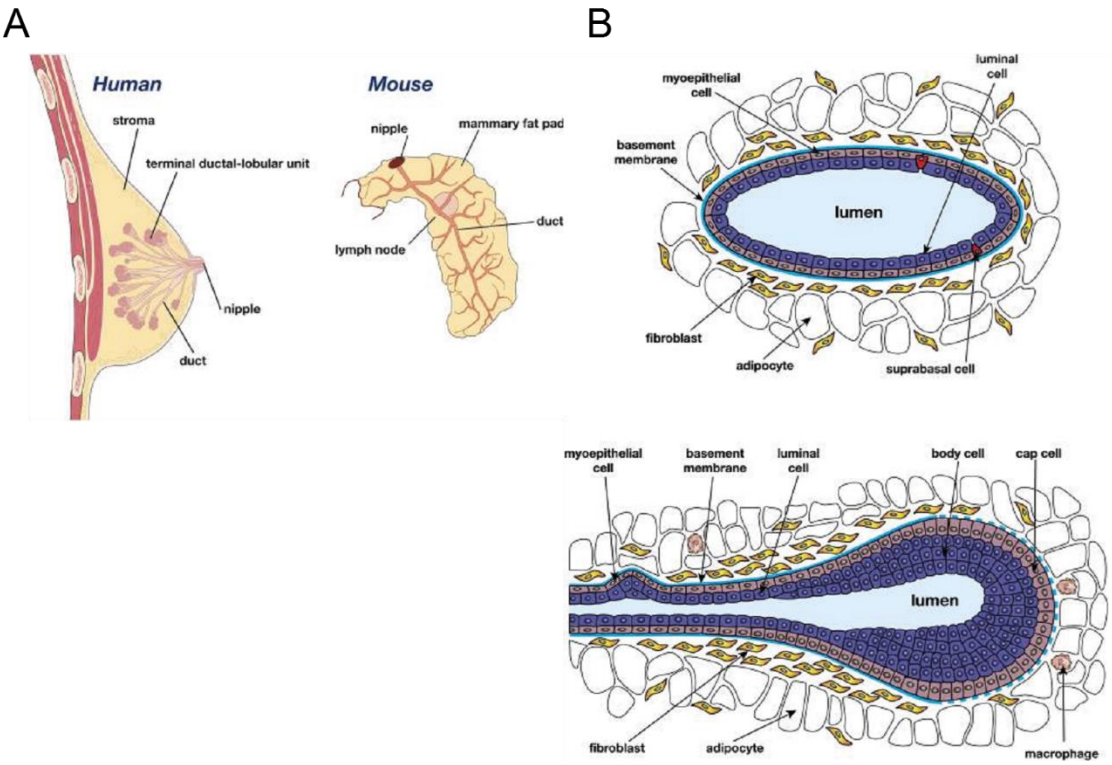

Figure 1. The mammary gland. (A) Schematic representation of the human and mouse mammary gland. **(B)** Schematic representation of a duct (top) and a terminal end bud (TEB) (bottom). The mammary gland epithelium is composed out of two layers, the inner layer of luminal cells line and the basal myoepithelial cells which are surrounded by the basement membrane [21].

2.2.1.2 Breast cancer

Breast cancer is a malignant disease caused by an uncontrolled growth of cells in the breast tissue. It is the most common cancer type in women and the second leading

cause for cancer-related death in women after lung cancer in the United States [6, 22]. Several risk factors have been associated with the development of breast cancer which include inherent factors such as age, sex, race, genetic predisposition but also extrinsic factors like the lifestyle, diet or long-term medical interventions. Furthermore, it has been shown that an earlier age at menarche, a higher age at first pregnancy as well as a late menopause may increase the risk of breast cancer development [22-25]. A rather small portion of breast cancers has been shown to be caused by hereditary germline mutations in susceptibility genes (5-10%). Among the most frequently mutated genes predisposing to hereditary breast are the tumor suppressor genes *BRCA1 (BRCA1, DNA repair associated)* and *BRCA2 (BRCA2, DNA repair associated)* which are both involved in DNA damage response [26-30]. Meanwhile, many other genes have been found that are involved in increasing the risk to develop breast cancer, including *CHEK2 (checkpoint kinase 2), PTEN (phosphatase and tensin homolog), TP53 (tumor protein p53), CDH1 (cadherin 1)* and *STK11 (serine/threonine kinase 11).* Mutations in these genes confer an increased risk to develop breast cancer [31].

Human breast cancer is a heterogenous group of neoplasms originating from the epithelial cells lining the milk ducts of the mammary gland. There appears to be an intra- as well as inter-tumoral heterogeneity as well as a high degree of diversity among patients [32]. To deal with this complexity and to provide the best possible treatment for patients, classification in clinically relevant subtypes is applied. This is achieved by characterization of the histopathological and immunological features as well as gene expression profiles. The combination of classical immunohistochemistry (IHC) markers such as ER (estrogen receptor), PR (progesterone receptor) and HER2 (human epidermal growth factor receptor 2), together with the patients anamneses (age of development, family history, etc.), clinicopathological variables including tumor size, tumor grade and nodal involvement are conventionally used for patient prognosis and management. Classical pathology has classified breast tumors according to their morphology and structural organisation into invasive ductal carcinoma (IDC), the most common type, invasive lobular carcinoma (ILC) and the remaining types, which are summed up as tumors of special type [33, 34].

Analysis of gene expression profiling lead to the identification of different subtypes according to transcriptional signatures. For the use in clinics a classification has been

adopted which correlates with the expression of biomarkers that has been performed already before but adds another level of differentiation to it. Immunohistochemical (IHC) characterization of the ER, PR and HER2 expression combined with a Ki-67 labeling index are used for the clinicopathological classification of mammary cancer tissue into subtypes. These include normal-breast-like, claudin-low, basal-like, luminal A or B, and HER2/ERBB2-overexpressing subtypes [35-39]. This characterization is important, since the expression or loss of these receptors can sensitize or de-sensitize the tumors for specific chemotherapeutics. The majority of diagnosed breast tumors are ER-positive and generally more responsive to anti-estrogen therapy. Thus, patients benefit from treatment using ER antagonists or aromatase inhibitors [40]. HER2-overexpressing tumors can be targeted using monoclonal antibodies, such as trastuzumab or also using Antibody–drug conjugates like trastuzumab emtansine [41, 42]. However, for triple-negative breast cancers (TNB), characterized by the expression loss of PR, ER, and HER2, there is no targeted therapy available and they tend to be more aggressive and to show a worse prognosis [43-45].

2.2.2 Wnt signaling pathway

The Wnt signaling pathway is a conserved pathway in metazoan animals and has been identified over 30 years ago by discovering the segment polarity gene *Wingless* in *Drosophila melanogaster*. Flies harboring mutations in this gene were found to not develop wings. Furthermore, embryos of these flies showed impaired epidermis segmentation [46, 47]. Experiments in mice studying the mammary tumor virus (MMTV) which causes mammary tumors in mice, has led to the discovery of the common integration site of MMTV within the promotor of a gene referred to as *int-1* [48, 49]. In 1987, Rijsewijk and collegues isolated the Drosophila homologue of *int-1* and discovered that it is identical to the *wingless* gene and called it *Wnt-1*(*Wnt family member 1*) [50]. The Wnt pathways are generally subdivided into canonical and non-canonical Wnt pathways. Meanwhile, in humans 19 secreted Wnt glycoproteins (Wnts) have been discovered which are able to either induce the canonical β-catenin-dependant or the non-canonical β-catenin-independent cell polarity (PCP) and the calcium/protein kinase C (PKC) Wnt pathway.

Wnts are cysteine-rich glycoproteins which are glycosylated and lipid-modified in the endoplasmic reticulum and were found to be able to act over short and long distance ranges. Palmitoylation by the acetyltransferase porcupine has been found to be essential for Wnt activity, whereas glycosylation seems to be rather important for proper folding and secretion [51-53]. Another important factor for the secretion of Wnts is Wntless (WLS), a multipass transmembrane protein localized amongst others in the Golgi apparatus where it binds Wnt and helps to transport it to the plasma membrane to be secreted [54-57]. There are different models proposed how Wnts are transmitted between cells. Wnts may bind to some extracellular proteins, to extracellular vesicles or form multiprotein complexes. Furthermore, extracellular matrix components like heparin sulphate proteoglycans (HSPGs) as well as trafficking via filopodia like protrusions (cytonemes) and the transport by exosomal vesicles are potential ways of spreading Wnts [58, 59]. In the extracellular matrix, several secreted proteins are present that can act as Wnt signaling inhibitors by binding to Wnts and prevent their interaction with cell membrane receptors. Amongst them are DKK (Dickkopf Wnt signaling pathway inhibitor), WIF (Wnt inhibitory factor) and SFRP (secreted frizzled-related protein). There are also factors like R-spondins which can bind to cell membrane receptors LRP5/6 (low density lipoprotein receptor-related protein 5/6) and activate Wnt signaling independent of the Wnt ligands [60-63].

The three best-characterized Wnt signaling pathways are the canonical Wnt/β-catenin signaling pathway, the non-canonical planar cell polarity pathway (PCP) and the non-canonical Wnt/calcium pathway (Wnt/Ca^{2+}). Generally, the Wnt proteins Wnt1/2/3a/8a/8b/10a/10b are thought to belong to the canonical Wnts, whereas Wnt4/5a//6/7a/7b/11 are classified as non-canonical Wnts. [64] However, some of them have been found to be able to activate both the canonical and non-canonical pathways. For example, Wnt5a that has been identified as non-canonical Wnt, was found to be able to also activate the canonical Wnt pathway [65]. Another study has found that Wnt5a can inhibit canonical Wnt/β-catenin signaling or induce it, depending on the receptors context [66, 67]. Several studies suggest that the signaling specificity is dictated by the co-receptors with LRP5/6 being specific for canonical Wnt signaling, whereas PTK7 (PTK7 protein tyrosine kinase 7) and ROR2 (receptor tyrosine kinase-like orphan receptor 2) seem to be specific for the non-canonical pathway [68, 69]. However, it has also been found that there are different affinities between Wnt ligands and Frizzled receptors, hence it is thought that the receptor context induces different

Wnt responses [70, 71]. Moreover, there seems to be a high complexity of cross talk between the canonical- and non-canonical Wnt pathways, as for example, the non-canonical pathway has been found to be able to inhibit canonical signaling [72, 73].

2.2.2.1 Canonical-Wnt signaling

The first step in mediating the intracellular Wnt/β-catenin signaling pathway, also named canonical Wnt signaling pathway is triggered by an extracellular stimulus, namely by binding of a Wnt ligand to the cell membrane receptors. Without Wnt ligand-binding to the transmembrane receptors Frizzled (10 distinct family members FZD1 - FZD10) and the single-pass transmembrane co-receptors LRP5/6, the pathway is in an off state and free cytosolic β-catenin is targeted and phosphorylated by the so called destruction complex. This complex is composed of the scaffold proteins Axin and APC (adenomateous polyposis coli) and the kinases GSK3β (glycogen synthase kinase 3β) and CK1α (casein kinase 1α) which phosphorylate β-catenin at amino-terminal Ser and Thr residues, and protein phosphatase 2A (PP2A) [74-76]. There are two *Axin* genes in vertebrates, namely *Axin1* and *Axin2*. Since *Axin2* is a transcriptional target of the canonical Wnt pathway, it hence constitutes a negative feedback loop [77]. CK1α phosphorylates the serine residue in codon 45 of β-catenin. GSK3β has been found to favour substrates that were primed by phosphorylation by other kinases. Hence, GSK3β phosphorylates threonine 41 serine 33 and serine 37 of β-catenin starting from the C-terminus [78]. Both Axin and APC have been found to be phosphorylated by GSK3β as well which increases their binding capacity to β-catenin [79, 80]. Following its phosphorylation, β-catenin is recognized by the $SCF^{\beta\text{-}TRCP}$ E3 ubiquitin ligase complex via the F box protein β-TrCP1 (Beta-transducin repeat containing E3 ubiquitin protein ligase), following ubiquitination and subsequent degradation by the 26S proteasome [81, 82]. It has furthermore been found that β-catenin is ubiquitylated by the E3 ligase JADE1 (Jade family PHD finger 1). However, β–TrCP1 ubiquitinates only phosphorylated β-catenin, whereas JADE1 is able to act on both, phosphorylated and non-phosphorylated β-catenin with preference for phosphorylated β-catenin [83].

Binding of a canonical Wnt ligand to the transmembrane receptor Frizzled and its co-receptor LRP5/6 results in the destabilization of the destruction complex. Since FZDs can mediate the activation of canonical as well as non-canonical pathways, Liu and colleagues have demonstrated that functional interaction of ligands with LRP5/6

distinguishes activation of canonical versus non-canonical Wnt. This was shown by fusing of Wnt5A, which is known for being a non-canonical Wnt ligand to a fraction of Dickkopf-2 (DKK2) which can interact with LRP5/6. This fusion protein was found to be able to activate the canonical Wnt signaling pathway in comparison to normal Wnt5A which was not [69]. Upon ligand binding, the FZD and LRP5/6 complexes become activated, oligomerize and recruit Dishevelled (DVL) to the receptor complex. Three human homologues *Dvl1* to *Dvl3* have been identified (*Dsh* in *Drosophila melanogaster*). Dsh multimerizes via its DIX domain and has been found to interact with and to recruit Axin, thereby facilitating Axin binding to LRP. Axin has been found to be required for LRP6 phosphorylation by binding GSK3β. Zeng et al. and others have shown that GSK3 phosphorylation seems to be the primary Wnt-inducible event, priming the subsequent phosphorylation by CK1α. Phosphorylated LRP6 provides docking sites and seems thereby to recruit additional Axin-GSK3. Hence upon Wnt stimulation, Axin-GSK3 is recruited to the plasma membrane and disrupts the formation of the destruction complex leading to the stabilization of β-catenin in the cytoplasm [84-86]. Unphosphorylated β-catenin accumulates in the cytoplasm and translocates to the nucleus where it binds to the TCF/LEF family of transcription factors (TCF1, LEF1, TCF3, TCF4). Without binding of β-catenin, TCF/LEF associates with Groucho/Transducin-like Enhancer of split (TLE) acting as transcriptional repressors. β-catenin binding displaces Groucho/TLE and thereby leading to the transcription of specific target genes (Fig. 2) [75, 87-89]. Several nuclear cofactors are known to bind to β-catenin and thereby to modulate and fine-tune transcriptional activity. The target genes during development are stage and tissue-specific and are involved in several processes, such as cell fate, proliferation, migration and cell survival [75]. Wnt signaling itself can promote the expression of several Wnt pathway components, like FZD, TCF7, LEF1 and Axin2. Furthermore, also the Wnt pathway inhibitor *Dkk* is among the target genes, indicating that feedback control is an important feature of Wnt signaling regulation [77, 89-93].

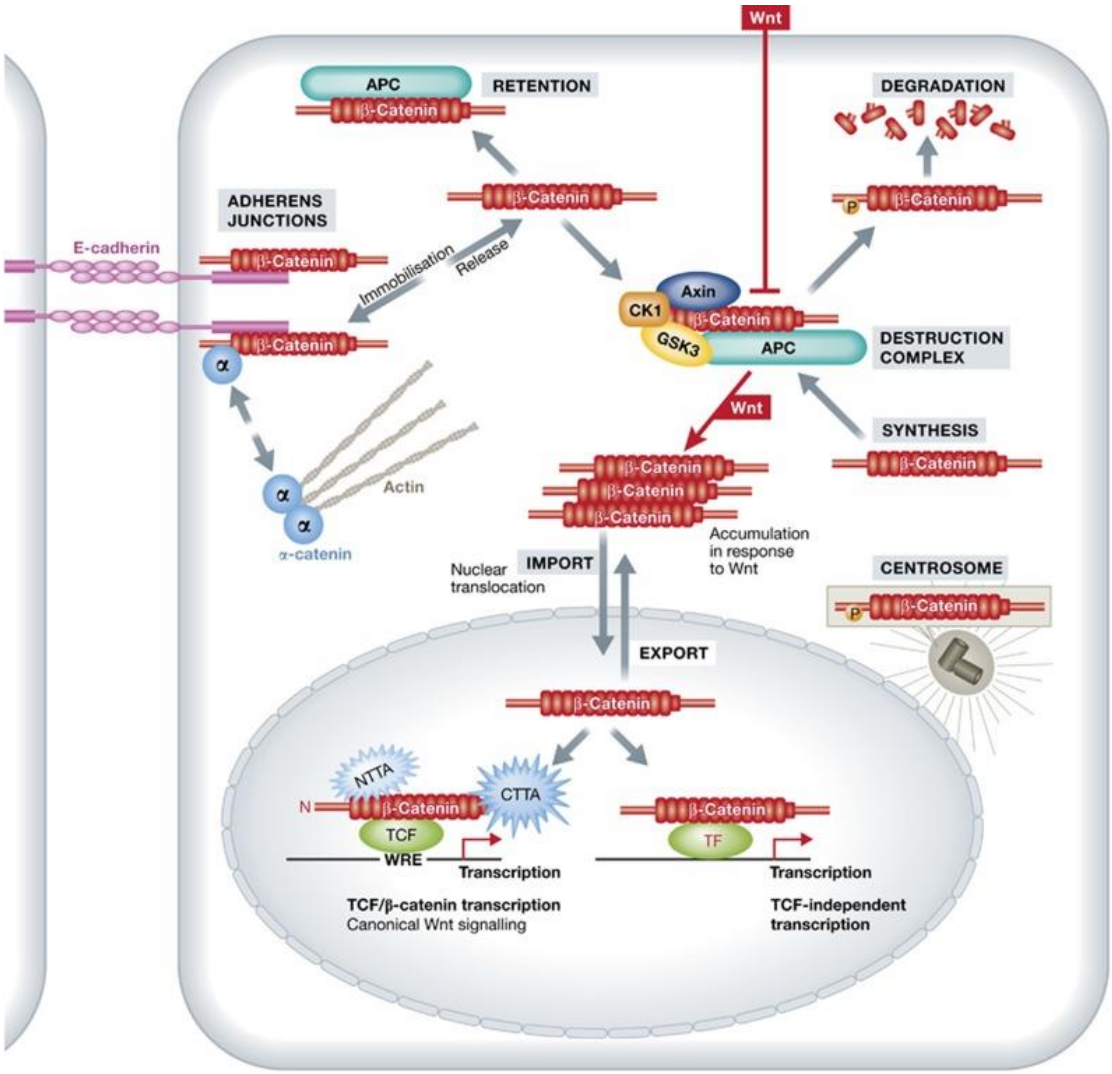

Figure 2. Schematic representation of β-catenin's dual function. β-catenin together with E-cadherin and α-catenin at the cell membrane can form the cell adhesion complex. The immobilised β-catenin at the cell membrane can be released into the cytoplasm upon downregulation of E-cadherin or by the activity of protein kinases. Cytoplasmic β-catenin is either retained in the cytoplasm by binding to APC or immediately degraded by binding to the destruction complex. Wnt ligand binding to cell membrane receptors inhibits the formation of the destruction complex, thus releasing β-catenin in the cytoplasm leading to its accumulation and translocation to the nucleus. There, binding to the TCF/LEF transcription factor leads to the transcription of canonical Wnt target genes. β-catenin was also found to bind to other DNA-binding transcription factors (TF) [75].

2.2.2.2 Non-canonical Wnt signaling

Non-canonical Wnt signaling is also referred to as β-catenin-independent Wnt signaling. The non-canonical pathways can be further subdivided into the Wnt/Ca2+ and planar cell polarity (PCP) pathways. To activate the Wnt/PCP signaling pathway, Wnt ligands bind to Frizzled receptors and to one of the co-receptors like ROR1/2

(receptor tyrosine kinase-like orphan receptor 1 or 2), RYK (ryk receptor-like tyrosine kinase), NRH1 (neurotrophin-receptor-related protein), or PTK7 (protein-tyrosine kinase PTK7) resulting in the recruitment and activation of DVL. This subsequently activates two parallel pathways. On one hand, it activates the Rac GTPase which stimulates JNK (c-jun kinase). On the other hand, DVL forms a complex with DAAM1 (dishevelled-associated activator of morphogenesis 1) which leads to the activation of small GTPase RhoA further triggering the activity of Rho kinase (ROCK) (Fig. 3). Thereby this pathway has been found to regulate cytoskeletal rearrangements and AP-1 (Activator protein 1)-dependant gene transcription involved in regulating cell polarity in morphogenetic processes and cell motility [94-99].

In the Wnt–Ca2+ pathway, Wnts trigger FZD-mediated activation of DVL and heterotrimeric G proteins, which in turn activate phospholipase C (PLC). Subsequently, PLC cleaves PIP2 (phosphatidyl-inositol bisphosphate) into DAG (Diacyl-glycerol) and IP3 (inositol triphosphate). IP3 triggers the release of intracellular calcium and thereby calcium-sensitive calcineurin and CAMKII (calcium/calmodulin-dependent protein kinase type II) are activated which in turn activate NFAT (nuclear factor of activated T cells) which acts as a transcription activator. On the other hand, DAG activates PKC (protein kinase C). CAMKII and PKC can activate various regulatory proteins, including NFκB (nuclear factor kappa-B) and CREB1 (cAMP response element-binding protein 1) which act as nuclear transcription factors and transcribe various downstream regulatory genes found to be involved in processes like vertebral axis formation in embryonic development (Fig. 3) [98-100].

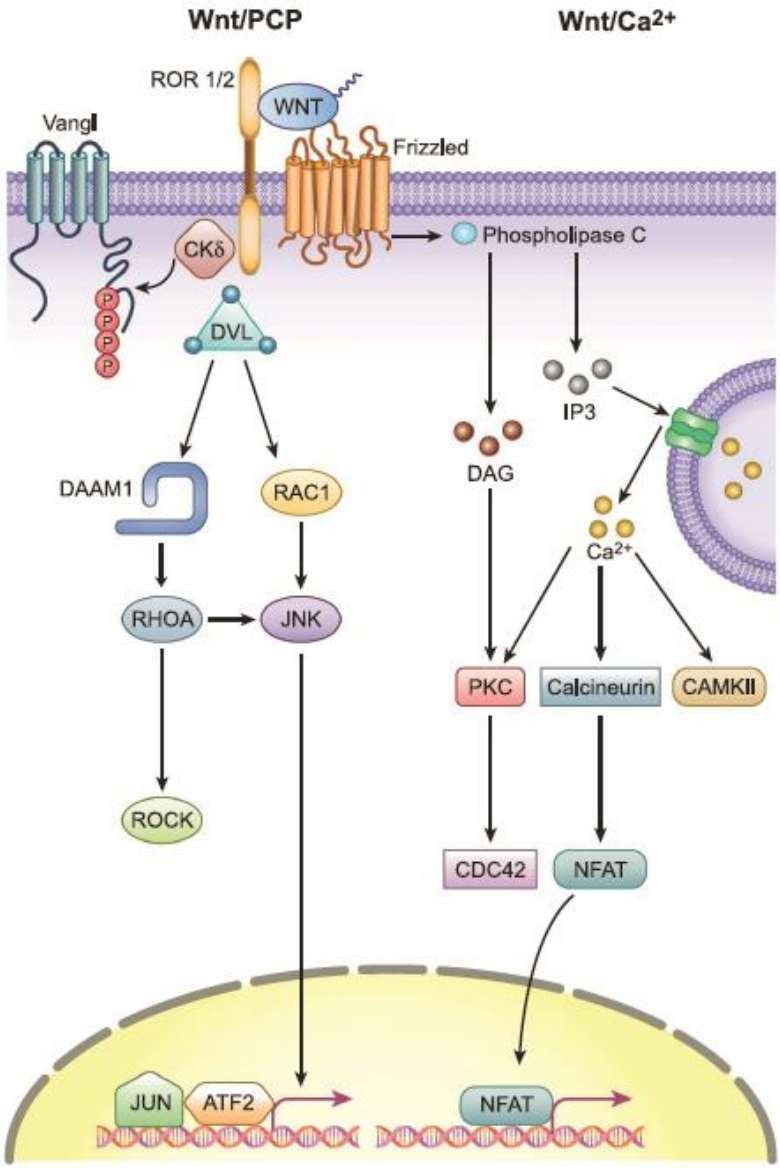

Figure 3. Schematic representation of non-canonical Wnt pathways. Wnt/PCP pathway**:** Binding of Wnt ligands to the cell membrane receptor complex ROR1/2-Fzd, leads to the recruitment of DVL. DVL then activates RAC1 and together with DAAM1 then RHOA. Those in turn mediates the activation of JNK and ROCK. In Wnt/Ca2+pathway, G-protein triggered phospholipase C is activated by binding of Wnt ligand leading to cleavage of PIP2 by PLC into DAG and IP3. The latter induces intracellular calcium release whereas DAG activates PKC. Calcium sensitive enzymes such like CAMKII and calcineurin are thereby activated. This leads to calcium-dependent cytoskeletal and/or transcriptional responses [101].

2.2.2.3 β-catenin

β-catenin has been initially discovered on the basis of its two different functions in signaling and structure. Its first identification has been due to its structural function as part of the adherens junction complex since it was isolated together with α-catenin and

plakoglobin (γ-catenin) associated with E-cadherin (Fig. 2) [102]. Its signaling function has further been revealed in *D. melanogaster*, with the finding of its orthologue Armadillo that was identified in a screen performed to detect genes required in embryonic development for early patterning and morphogenesis [103]. Subsequently, β-catenin was found to be the vertebrate homologue of the *D. melanogaster* segment polarity gene product *Armadillo* [104, 105]. β-catenin has been found to be the key component of the canonical Wnt signaling pathway and being tightly regulated at three hierarchical levels: protein stability, subcellular localization and transcriptional activity. The ***β-catenin*** gene (*Ctnnb1*, catenin beta 1, MGI: 99276; further referred as β-catenin) encodes for a highly conserved protein encoded by 781 amino acids (aa). The protein consists of 12 imperfect Armadillo (ARM) repeats and an N- and C-terminal domain (NTD and CTD respectively). The ARM repeats form a superhelix with a positively charged groove, which is important for the interaction of β-catenin to other proteins. β-catenin has a dual role: it is a crucial component of the E-cadherin-mediated cell adhesion complex as well as the key nuclear effector of the canonical Wnt signaling pathway. With its 12 ARM repeats β-catenin it is able to bind and thus interact with a number of different proteins and distinguish between its function in cell adhesion by binding to E-cadherin at the cell membrane, APC in the cytoplasm or TCF/LEF in the nucleus since all these binding partners have overlapping binding sites within β-catenin [75, 106].

2.2.2.3.1 β-catenin at the membrane

As a component of the cell adherens junction complex, it binds to the intracellular domain of cadherins thereby linking them via the adaptor protein α-catenin to the actin cytoskeleton. Cadherins are Ca^{2+}-dependent single-pass transmembrane proteins named after the tissue they have been found to be most prominently expressed in. By binding to E-cadherin in the endoplasmic reticulum, β-catenin inhibits degradation of E-cadherin, since in covers a PEST motif of E-cadherin. On the other hand, binding of E-cadherin to β-catenin prevents the binding of components of the destruction complex to β-catenin. In addition, β-catenin can also bind to the cytoplasmic domain of all the other catenins [107]. Together, they then move to the cell membrane where other catenin family members α-catenin and P120 (CTNND1) which is important for cadherin stability and the function of the adherens complex. α-catenin can be found in either in

a heterodimeric form (α-catenin/β-catenin heterodimer) or as a homodimer. Since its binding site to β-catenin and its homodimerization domain overlap, it can only bind to β-catenin as a monomer. In its homodimer form it interacts with actin filaments. However, it is thought that α-catenin links the Cadherin/β-catenin complex to the actin cytoskeleton. [108] Moreover, the binding site of α-catenin and BCL9 have been found to be in close proximity. Phosphorylation of β-catenin at tyrosine 142 (Tyr142) affects the binding of α-catenin and rather direct β-catenin into its signaling function. The phosphorylation of this residue is needed for efficient interaction of BCL9-2 with β-catenin [109-111]. Also the phosphorylation at Tyr654 has been observed to have a similar effect by affecting the binding of E-cadherin to β-catenin [112]. Reduction of E-cadherin on the other hand has been found to be connected with increased cytoplasmic levels of β-catenin. Cleavage of E- or N-cadherin by proteases like ADAM10 for example, can direct β-catenin away from its cell adhesion function and into signaling. Since ADAM10 is described as a target of canonical Wnt signaling, it acts in a positive feedback loop [113-115]. In H-Ras-infected immortalized human breast epithelial cells (HMLE), knockdown of E-cadherin has been observed to result in the localization of unphosphorylated and hence active β-catenin in the cytoplasm and nucleus [116]. In colorectal cancer cells, which show constitutive activation of Wnt signaling, knock-down of E-cadherin augmented β-catenin-/TCF-dependent transcription, whereas it had no effect in keratinocytes that do not show Wnt signaling activity [117]. Furthermore, Herzig and colleagues have shown that by loss of E-cadherin expression, canonical Wnt signaling is not induced in the absence of Wnt ligands and β-catenin rather gets degraded [118]. Hence, it seems that the mere loss of E-cadherin does not activate Wnt signaling but might be rather context- and cell type-dependent. Moreover, also in breast cancer cell lines, the absence of E-cadherin was found to have no effect on Wnt signaling activity [119]. Plakoglobin (γ-catenin), a close relative of β-catenin has been found to be able to compensate in some cases the loss of β-catenin at the cell adhesion complex [120]. The loss of E-cadherin is also one of the hallmarks of EMT and several transcriptional repressors of E-cadherin are known, some of them have also been found to be canonical Wnt target genes, amongst them are *Snai2, Zeb1* and *Twist.* Hence, the canonical Wnt pathway fulfills also a role in regulating EMT which will be further discussed below [75].

2.2.2.3.2 β-catenin signaling

In the cytoplasm, if recognized by the destruction complex, β-catenin binds to the scaffolding proteins Axin and APC and is subsequently phosphorylated by CK1α at serine 45 (Ser45) and following by GSK3β at threonine 41 (Thr41), Ser37, and Ser33 marking it for degradation. β-TrCP recognizes phosphorylated β-catenin which is then recruited to the Skp1/Cul1/F-box$^{\beta\text{-TrCP}}$ (SCF$^{\beta\text{-TrCP}}$) E3 ubiquitin ligase and degraded by the 26s proteasome. The phosphorylation of β-catenin has so far been regarded as a progressive process. In recently published studies, it has been suggested that rather sequential phosphorylation takes place and β-catenin is able to dissociate from the destruction complex between the phosphorylation events [75, 121, 122]. Upon activation of the canonical Wnt signaling pathway by ligand binding, β-catenin escapes its degradation and can translocate to the nucleus (Fig. 2). The process of its nuclear translocation is not yet fully understood, since β-catenin's sequence does neither contain a nuclear localization (NLS) nor a nuclear export signal (NES). It has been shown that it can directly interact with nuclear pore complexes which might be a mechanism by which it could pass and localize to the nucleus [75]. Also, BCL9 and Pygopus (PYGO) have been proposed to be important for its nuclear localization [123]. Another hypothesis suggests that it binds to transcription factors containing an NLS, for example FOXM1 (forkhead box M1), which is found to interact with β-catenin and thus might promote its nuclear translocation [124]. In the nucleus, β-catenin displaces Groucho/TLE from TCF/LEF and thereby turns the latter into transcriptional activators [87]. Additionally, a plethora of nuclear transcriptional cofactors are known to bind to β-catenin which can initiate, enhance and alter the transcriptional output. At the C-terminus, of β-catenin several cofactors are found to bind which are not specific to β-catenin only. Among these are CBP (CREB binding protein, CREBBP), EP300 (E1A binding protein p300) and TIP60 (lysin acetyltransferase 5, KAT5) which belong to the chromatin remodeling complexes, SWI/SNF (SWItch/Sucrose Non-Fermentable) and ISWI (imitation Switch) which can affect nucleosome rearrangement or the Mediator complex which connects β-catenin to the transcriptional machinery [57, 75, 125]. Whereas at the N-terminus, the β-catenin-specific cofactor BCL9 (legless in *Drosophila*) binds which in turn recruits Pygopus. Together they have been shown to fine tune the transcriptional activity of β-catenin (Fig. 4). In mammals, there are two paralogues of both, BCL9 namely BCL9 (β-catenin specific cofactor-cell CLL/lymphoma 9) and BCL9l (β-catenin specific cofactor-cell CLL/lymphoma 9-like)

and for Pygopus, Pygopus1 (PYGO1) and Pygopus2 (PYGO2). BCL9 interacts via its homology domain 2 (HD2) with β-catenin and functions as a transcriptional coactivator by recruiting Pygopus and binds to it via its HD1 domain. Pygopus has two distinct domains, an N-terminal homology domain and a C-terminal plant homolog domain. Pygopus binds to BCL9 via the PHD domain [126, 127]. Via the same domain it can also bind methylated histones (H3K4me3) marks and is thereby thought to be involved in chromatin-mediated transcriptional control. However, *Drosophila* Pygopus was found not being able to bind to histones due to a single amino acid in the PHD [128]. BCL9 can also directly interact with some of β-catenin's C-terminal binding cofactors namely CBP/P300, TRRAP (Transformation/transcription domain-associated protein)/GCN5 (lysine acetyltransferase 2A) and enhance their binding (Fig. 4). Similarly, Pygopus has been found to interact with components of the Mediator complex in *Drosophila*. Both, BCL9 and Pygopus are also thought to have β-catenin-independent functions which are under further examination [127, 129-131]. In *Drosophila*, mutants of legless (BCL9) and Pygopus have been found to result in phenotypes similar to that of the wingless (*wg*) mutant [126, 132]. *Pygo1* null mice have been found to be viable and fertile, whereas *Pygo2* null mice died shortly after birth. Thus in mice, loss of *Pygo* was found to lead to rather mild phenotypes in certain tissues like the kidney or in the lung [133, 134]. In mice *Pygo2* has been found being ubiquitously expressed whereas Pygo1 seems to be mainly expressed in heart tissue [135]. Also, BCL9 and BCL9/L seem to be essential during development, since their knockout has been found to result in lethality. Also disrupting the interaction of BCL9/9L with Pygopus or β-catenin results in embryonic lethality enforcing the importance of those interactions during development [131].

β-catenin's dual function in signaling and cell adhesion, made it difficult to specifically study its signaling function. Observed phenotypes by β-catenin knockout could result from the loss of cell adhesion as well as from the loss of Wnt signaling activity. Therefore, to specifically characterize β-catenin's function in Wnt signaling it is required to separate those two functions. In 2011, Valenta et al. generated mutant forms of β-catenin/Armadillo only affecting its transcriptional function by ablating the binding of N-terminal and/or C-terminal cofactors without affecting its binding to E-cadherin or TCF/LEF. The ΔC mutation leads to a truncation of the C-terminus of β-catenin/Arm and thereby prevents the binding of C-terminal transcriptional coactivators. The D164A

mutation in mice or D172A in Drosophila (DA) leads to an amino acid change from aspartic acid to alanine in codon 164 resulting in the abrogation of the binding of Bcl9 and Bcl9L to the N-terminus. Finally, the double-mutant (dm) strain, β-catenin-D164A-ΔC/D172A-ΔC combines both, the D164A mutation and the C-terminal deletion and thereby completely abrogates Wnt signaling. Thereby, they have found that both the N- and the C-terminal cofactors are important for β-catenin-mediated transcription. Amongst other experiments, they were using a TOPflash/FOPflash reporter assay and removed endogenous β-catenin/Arm in mouse embryonic fibroblasts (MEFs) derived from β-catenin conditional knockout mice (β-catenin$^{flox/flox}$) and in Drosophila KC cells. Expression of the β-catenin/Arm mutant forms has revealed, that both the N- and the C- terminal coactivators are important for β-catenin's transcriptional function. In mouse and Drosophila cells, the response to Wnt3a/Wg stimulation was diminished by the expression of the different mutant forms. However, in the murine cells, the transcriptional function was more affected by the loss of the C-terminal cofactors, similar to the effect of the dm mutation, compared to the N-terminal ones, whereas in Drosophila the opposite was found. These observations confirm previous results showing that loss of Pygopus or BCL9 does not entirely phenocopy the ablation of canonical Wnt signaling in mice unlike in *Drosophila* [126, 132, 133, 136]. In both mice and Drosophila, the dm was shown to completely block the Wnt/β-catenin/Arm transcriptional output. Subsequently Valenta and colleagues replaced endogenous β-catenin by knock-in technology with its mutant forms and examined the effect in development. All three mutant forms were shown to be homozygous lethal. The embryos of ΔC mice, similar to β-catenin knockout mice were not able to undergo gastrulation, whereas the D164A mice developed normally until E10, from there on they started to show developmental defects. To further examine β-catenin's signaling function during development, the mutant alleles were combined with a conditional knockout allele and a tissue-specific Cre driver. Crossing the mice with Wnt1-Cre mice showed that the β-catenin$^{dm/fl}$ mice had a milder effect than the complete loss of β-catenin suggesting that this is due to the maintenance of the cell adhesion function. The β-catenin$^{D164A/fl}$ or β-catenin$^{\Delta C/fl}$ mutant had even less severe phenotypes than the dm mutant hence both seem to contribute to the transcriptional β-catenin output. Further examination specifically in the dorsal neural tube have demonstrated ablation of neuronal differentiation in the dorsal neural tube by expression of the dm allele, however no effects on proliferation or apoptosis were observed [137].

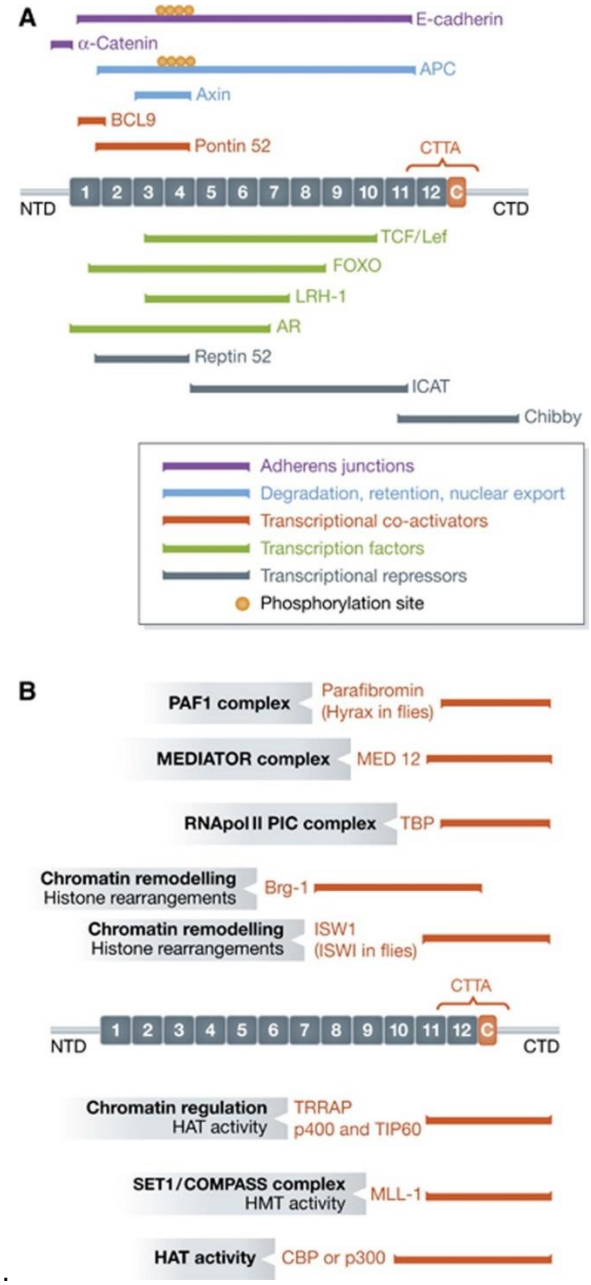

Figure 4. β-catenin interaction partners. (A) Overview of β-catenin interaction partners and their binding sites. β-catenin protein consists of a central region composed of 12 conserved armadillo repeats (numbered boxes) and an amino-terminal domain (NTD) and carboxy-terminal domain (CTD). **(B)** Binding of C-Terminal transcriptional activators (CTTA) to β-catenin. The coloured bars depict experimentally validated binding sites for β-catenin interaction partners (purple: components of adherens junction complex; blue: members of the β-catenin destruction complex; red: transcriptional co-activators; green: transcription factors providing DNA binding; grey: transcriptional inhibitors.

2.2.2.4 Wnt signaling in mammary gland development

Wnt signaling is known to play an important role in the morphogenesis of several organs during development. In mice, disruption of Wnt genes has been found to result in severe developmental defects. Wnt signals have been implicated playing a role of different processes like proliferation, migration, adhesion, tissue patterning and apoptosis. The canonical Wnt signaling pathway has also been found to be important for the development of the mammary gland. In the different stages of development, the expression of several members of the canonical Wnt pathway has been discovered. For example, cells expressing LRP1 (low density lipoprotein receptor-related protein 1) have been found having an increased capability to regenerate the mammary tree when transplanted into cleared mammary fat pad hence increases there stem cell activity, whereas loss of *Lrp5* depleted this capability [138]. Furthermore, treatment of mammary stem cells (MaSCs) with Wnt3a *in vitro* enabled clonal expansion of the cells for several generations and retained their developmental potential *in vivo* [139].The morphogenesis of the mouse mammary gland starts on E10.5. Canonical Wnt signaling defines the cells of the mammary lines and subsequently localizes to the cells that form the placodes. In particular the expression of Wnt10b is found in cells of the mammary line. The five pairs of placodes are formed by those cells. Targeting components of the canonical Wnt pathway, such as *Lrp6*, *Lrp5*, *Lef1* (lymphoid enhancer binding factor 1) and also *Pygo2* has been found to lead to adverse effects resulting in reduced size or loss of the placodes. Stimulation of the canonical Wnt signaling, has been found to result in the opposite: an induction and expansion of the placodes. Also, the ectopic expression of the canonical Wnt inhibitor DKK1 in the surface epithelium inhibited placode formation. At E11.5-12.5 the cells invaginate into the mesenchyme and form buds. In Lef1$^{-/-}$ mice, the buds fail to invaginate [140]. Millar and colleagues have found by RT-PCR and *in-situ* hybridization the expression of several *Wnts*, *Fzds 1-9*, *Tcf1* (*Tcf7*), *Tcf3* (*Tcf7l1*) and *Tcf4* (*Tcf7l2*), *Lef1*, *Dvl1* and *Lrp5/6* in mammary buds [141]. Subsequently, around E15.5-16.5, the cells start to proliferate and sprout into the developing mammary fat pad. Branching is then initiated giving rise to the ductal tree. Also sprouting and branching has been found to be affected in Pygo2$^{-/-}$ and Lrp6$^{-/-}$ mice [142, 143]. The expression of *Wnt1* or *Wnt10b* under the control of the MMTV-promotor has been found to induce hyperbranching of the ductal tree

[144, 145]. During puberty, the ovarian hormones produced lead to the expansion of the ductal tree throughout the mammary fat pads. During this process, enriched expression of *Wnt5a* and *Wnt7b* has been discovered mainly in the terminal end buds (TEBs), which are proliferating structures located at the tips of the growing duct [140].

2.2.2.5 Wnt signaling in cancer

Aberrations in the canonical Wnt signaling pathway have been found to cause a wide range of pathologies in humans. In many different cancer types mutations in at least one of the canonical Wnt signaling components have been found. In colorectal cancer, around 85% loss-of-function mutations in *APC* have been detected resulting in elevated β-catenin levels. Furthermore, mutations in β-catenin have been detected in many different cancer types, stabilizing β-catenin by affecting N-terminal phosphorylation sites. These mutations affect its targeted degradation by the destruction complex [146, 147]. Mutations in *APC* and *β-catenin* have been found to be mutually exclusive. *Axin* loss-of-function mutations are also found in about 5-10% of HCCs (hepatocellular carcinoma cells) which again result in stabilization of β-catenin [148]. Amongst the target genes of the canonical Wnt signaling pathway are *c-Myc* and *Cyclin-D1* (*Ccnd1*) which are important for cell cycle regulation. Association of nuclear β-catenin with upregulated expression of c-MYC and Cyclin-D1 are often found in cancer. In clinical studies, enhanced activity of β-catenin has been found to correlate with a poor prognosis in breast cancer patients [146, 149-151]. Another Wnt target gene, *MMP7* (*matrix metallopeptidase 7*), has also been unveiled being upregulated in different cancer types and, similar to β-catenin, its enhanced expression seems to correlate with poor prognosis. MMP7 is involved in ECM degradation and thereby can promote cancer invasion as well as activate other MMPs, like MMP2 (matrix metallopeptidase 2) and MMP9 (matrix metallopeptidase 9) [152]. The canonical Wnt pathway is also involved in the regulation of EMT (epithelial-to-mesenchymal transition). EMT is a process thought to be important for cells to gain invasive properties and thus contributing to metastasis formation. Wnt target genes, such as *Snai2* (*snail family zinc finger 2*), *Twist1* (*twist basic helix-loop-helix transcription factor 1*) and *Zeb1* (*zinc finger E-box binding homeobox 1*), also function as regulators of the EMT process. [75] The increased expression of *Fibronectin1 (Fn1),* another Wnt target

gene involved in EMT, has also been found to correlate with a worse clinical outcome in patients with invasive breast cancer [153]. *Lgr5 (leucine rich repeat containing G protein-coupled receptor 5)*, another Wnt target gene which has been identified as a stem cell marker in the colon, intestine kidney and mammary gland, is also found to be aberrantly expressed in colon as well as other cancer cells [154-160]. Also, the N-terminal cofactors of β-catenin BCL9/9L and Pygopus have been shown to have implications in cancer formation and progression. BCL9 was found to be aberrantly expressed in human multiple myeloma and colon carcinoma. *Bcl9* overexpression furthermore increased cell proliferation, migration and invasion of tumor cells, knockdown of *Bcl9* on the other hand also seemed to affect the localization of EMT-related markers analyzed (E-cadherin, Vimentin and β-catenin) [161]. In another study, the loss of *Bcl9/9l* resulted in a decreased expression of intestinal stem cell markers and an impaired regeneration of the intestinal epithelium. Additionally, comparing wild type with $Bcl9^{-/-}$/$Bcl9l^{-/-}$ colon tumor cell lines revealed that the loss of *Bcl9/9l* leads to a reduced expression of EMT and stem cell–associated markers [162]. *Pygo2* overexpression has been reported in ovarian, breast, cervical and lung cancers [163]. *Pygo2* knockdown in HCC cell lines has been found to inhibit cell invasion and migration, whereas the opposite has been found upon ectopic expression of *Pygo2*. By binding to the *E-cadherin* promotor, it seemed to increase its methylation properties and thereby downregulate its expression. Additionally, PYGO2 seems to regulate *E-cadherin* expression also indirectly by up-regulating *Zeb2*. Furthermore, *Pygo2* knockdown was able to inhibit HCC metastasis *in vivo* [163]. In lung cancer, *Pygo2* knockdown has been found to result in reduced proliferation *in vitro* and supressed the growth of lung cancer in a xenograft mouse model *in vivo* [164]. Many studies indicate that Wnt signaling also contributes to cancer progression by maintaining cancer stem cells (CSCs), a subset of cancer cells capable of self-renewal and differentiation into heterogeneous tumor cells. Wnt signaling in mammals is known to be involved in the control of maintenance, self-renewal and differentiation of stem cells. Studies in mice have led to the suggestion that aberrant canonical Wnt signaling can increase breast cancer risk by inducing early progenitor and stem cell accumulation. Several developmental pathways like the Notch, Hippo, Hedgehog as well as the Wnt signaling pathway have been found to drive CSC formation. Stem cells in cancer are able to self-renew and are thought to contribute to the initiation, progression, reoccurrence and resistance to drug treatment of tumors [165, 166]. Expression of Wnt1 in human

mammary epithelial cells has been found to lead to an increased self-renewal of stem cells and resistance to apoptosis. MMTV-Wnt1 mice also showed an expanded stem cell population. In line with these observations were also the findings that mice expressing β-catenin or c-MYC driven by the MMTV-promoter showed similar results. In further studies, CSCs with higher activity of the canonical Wnt pathway have been found to be more tumorigenic. Moreover, the inhibition of the pathway decreased the amount of breast cancer metastases. Also, LGR4 (leucine rich repeat containing G protein coupled receptor 4) has been found to play a role in maintaining cancer stem cells in breast cancer and to modulate tumor initiation and metastases formation. The expression of *LGR4* correlated with worse prognosis for breast cancer patients. Also in MMTV- PyMT and Wnt1 mouse models, its deletion inhibited tumor growth and metastases formation [167, 168]. Similarly, LGR5 has been found to be a marker for colorectal CSCs and LGR5 positive cells have been found to have an increased capacity to form colonies, self-renewal and tumorigenicity [169, 170]. Another study has revealed, that silencing of *Lgr5* reduced proliferation, migration and colony formation of colorectal carcinoma cell lines *in vitro* and tumorigenicity *in vivo* [171]. Moreover, Wnt signaling has been shown to be able to promote the CSC phenotype in various cancer cell lines [172]. Hence, several cell surface markers that have been used to enrich for CSC populations relate to Wnt activity or are even canonical Wnt target genes like CD44 (CD44 antigen) and LGR5 [173, 174]. Targeting the Wnt signaling pathway proves to be quite a challenge since it is crucial during both normal embryonic development and throughout the life of the organism. There are only few FDA approved drugs that have been found to inhibit the canonical Wnt pathway, for example niclosamide downregulating DVL-1, sulindac affecting DVL and pyrvinium activating CK1α. These and a few others drugs are already in clinical trials as reviewed in [175, 176].

2.2.2.6 Wnt signaling in breast cancer

Although mutations in the Wnt signaling pathway are observed in many cancer types, mutations in *β-catenin* or other canonical Wnt signaling components like *AXIN* or *APC* are only rarely found in breast cancer. However, there is evidence for aberrant Wnt/β-catenin signaling activation in the majority of breast cancers which results in translocation of β-catenin to the nucleus and the subsequent transcription of its target

genes [2]. Hence by immunohistochemical staining elevated levels of cytoplasmic or nuclear β-catenin can be detected which is linked to reduced overall survival. Consistent with these findings, canonical Wnt target genes like *Cyclin-D1* can be found to be upregulated in the majority of breast cancer patients [149]. This leads to the suggestion that further upstream and/or other pathways that lead to the stabilization of β-catenin are deregulated. Experimental evidence suggests that the Wnt pathway in breast cancer may be changed by the loss of expression of negative pathway regulators or overexpression of individual Wnt ligands. For example, upregulation of W*nt2, Wnt4*, *Wnt7b* and *Wnt10b* has been confirmed in a subset of breast cancers [177, 178]. Epigenetic silencing of negative pathway regulators like *Wnt inhibitory factor 1* (*WIF1*), *secreted frizzled-related protein* (*SFRP*), *Dickkopf 1* and *Dickkopf 3* (*DKK1* and *DKK3*) as well as *APC* (*Adenomatous polyposis coli)* and also *E-cadherin* (*CDH1*) are found to be hypermethylated and their expression to be significantly reduced in human breast cancers [179-183]. Consistently, increased nuclear β-catenin is detected in many breast tumors. The modulation of the receptor activation might be another mechanism resulting in hyperactive Wnt/β-catenin signaling. Aberrant splicing of *Lrp5* affecting the interaction with DKK1, an extracellular antagonist has been discovered. In line with these results the upregulation of the Wnt signaling component *DVL1* in breast cancer as well as the epigenetic silencing of inhibitors of DVL1 have been found [184-186]. Furthermore, nuclear co-factors of β-catenin like *BCL9* and *PYGO2* have been found to be upregulated [187, 188]. In patient samples of ductal carcinoma and invasive ductal carcinoma, BCL9 expression has been shown to correlate with the tumor nuclear grade (grading system according to size and shape of the nucleus in the tumor cells) and ERBB2/HER2 expression [188]. Furthermore, knockdown of *Bcl9* in *in vivo* and *in vitro* experiments showed that the proliferation and the migratory and invasive capability of ductal carcinoma in situ (DCIS) cells was inhibited [189]. Target genes like *c-Myc* and *Cyclin-D1* (*CCND1*) seem to be amplified in many of human breast cancers [149, 190, 191]. The expression of Limb Heart Bud (LBH) embryonic patterning gene has also been found to be upregulated in tumors of MMTV-Wnt1 transgenic mice and in human breast cancers [192]. *Twist1* (*twist basic helix-loop-helix transcription factor 1*), another Wnt target gene, has rather been found to be associated with increased invasion. *Twist1* has been shown to be essential for metastasis formation from the mammary gland to the lung by the knockdown of *Twist*1 in highly metastatic 4T1 cells and their injection into the mammary fat pad of BALB/c

mice, however no effect was observed on primary tumor formation [193]. Consistent with these findings, studies in mouse models have revealed that activated Wnt signaling leads to mammary tumorigenesis [3, 4]. The *Wnt1* oncogene was first identified being activated by MMTV leading to hyperplasia and subsequently to development into mammary carcinomas. From then on, the oncogenic potential of different *Wnts* has been confirmed in the mammary gland. For example, transgenic expression of *Wnt10b* produced similar effects as MMTV-Wnt1 in mice [144]. Meanwhile, the deregulation of several Wnt components has been found to be able to induce tumor formation, for example in transgenic mice expressing stabilized β-catenin, and overexpressed *Lrp* or the loss of *Apc* in the mammary gland also leads to hyperplasia or tumor formation. Furthermore, *Rspo2* expression under the control of the MMTV promotor alone or together with the expression of *Wnt1* can also induce mouse mammary tumors [194]. Hence deregulation or ectopic Wnt ligand expression of Wnt ligands or mutations in pathway components like *Axin*, *Apc* or *β-catenin* can induce tumorigenesis [140]. RNA sequencing in a chemically induced as well as in a transgenic (loss of *Apc* and *Kras (Kirsten rat sarcoma viral oncogene homolog)*) mouse model revealed that the ablation of Bcl9/9l abrogated the expression of genes related to EMT, stemness and intestinal Wnt targets [162, 195]. In a study from 2014 of Brembeck and colleagues have found that BCL9/L expression induced premalignant changes in the mammary gland and high ER expression which however seemed to be β-catenin independent. ER-positive breast cancers showed an increased expression of BCL9/L [196]. Also PYGO2 has been found to be upregulated in malignant breast tumors and several breast cancer cell lines and to be important for the proliferation of MF7 and MDA-MB-231 cell lines [197]. In the colon, tumor growth was also affected by *Pygo2* loss in a chemically (AOM and DSS)-induced, *Apc* loss-of-function ($Apc^{lox(ex15)/lox(ex15)}$) and a *Ctnnb1* gain-of-function ($Ctnnb1^{lox(ex3)/+}$) tumor mouse model. *Pygo2* loss was able to reduce the overexpression of Wnt target genes, like *Lef/Tcfs, Axin2, Cyclin-D1, Ascl2* and *Lgr5* in the *Ctnnb1* GOF (gain-of-function) mice. Whereas this was not observed in the more severe *Apc* LOF (loss-of-function) mouse model in which the target genes seemed to be even higher upregulated, suggesting that *Pygo2* loss can reduce the canonical Wnt signaling output to a certain threshold [198]. Also in the MMTV-Wnt1 tumor mouse model, loss of *Pygo2* delays tumor onset [187]. The expression of *CD44*, another direct Wnt target gene, has also been found to identify CSCs in primary and metastatic breast cancer [174]. The same is true for *Epcr (Protein*

C Receptor, *Procr)*, a direct Wnt target that has been found to function as a mammary gland specific stem cell marker. Hypomorphic PyMT-EPCR$^{Low/Low}$ mice showed a reduced overall tumor burden as compared to controls. Moreover, using antibodies blocking the EPCR receptor revealed that blocking attenuates tumor initiation and growth when cells were injected into the mammary fat pad [199]. High *Epcr* levels have also been found to correlate with adverse clinical outcome in breast cancer patients [200].

2.2.3 Epithelial-to-mesenchymal transition

Epithelial-to-mesenchymal transition (EMT) is a process of cell remodelling critical during embryonic development and organogenesis. Epithelial cells are tightly packed in a highly organized tissue. The cells are connected by adhesion junctions, tight junctions, desmosomes and gap junctions [201]. During an EMT, the cells undergo morphological and functional changes: the epithelial cells lose the cell-cell connections by delocalization or degradation of the cell-cell junctions and also lose their apical-basal polarity. Furthermore, ECM remodelling and changes in cell-matrix interactions take place as well as cytoskeleton rearrangements, thereby the epithelial cells convert to mesenchymal cells. These changes result in an elongated cell shape and an increased migratory and invasive capability. [202, 203] A hallmark of EMT is the loss of E-cadherin, a component of the adherens junction complex, which is subsequently replaced by N-cadherin. This process is also termed “cadherin switch” [204-206]. EMT is a plastic process and thus mesenchymal cells are able to convert back into epithelial cells by the so called mesenchymal-to-epithelial transition (MET) (Fig. 5)[201].

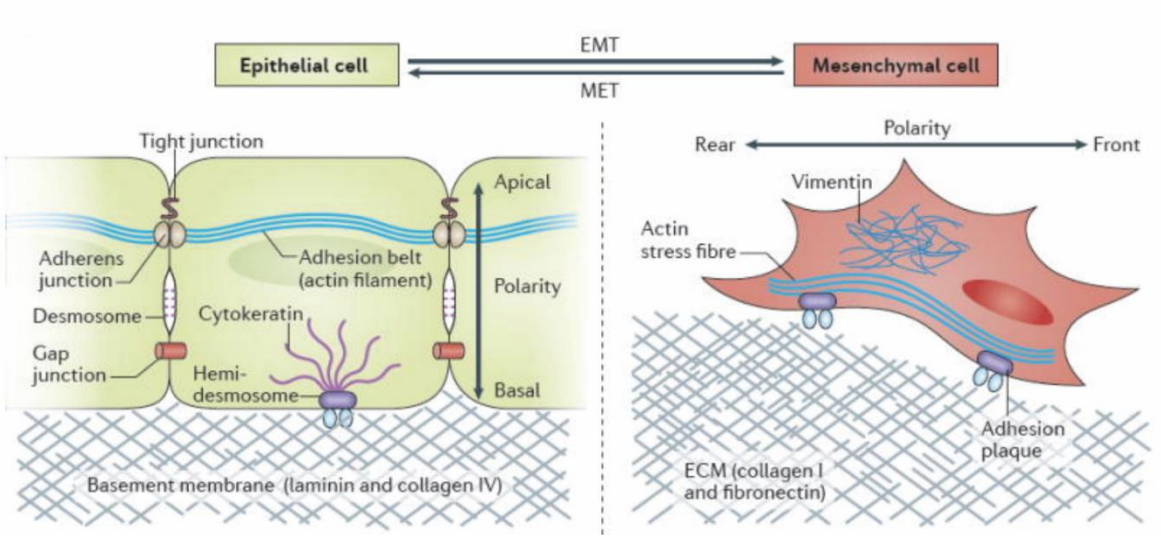

Figure 5. Schematic representation of structural and functional changes associated with EMT. Epithelial cells are connected via cell-cell junctions (desmosomes, adherens junctions and gap junctions) which are disassembled and lost during EMT. The apical-basal polarity of epithelial cells changes into a front-rear polarity and changes in ECM interactions are induced. Moreover, cortical F-Actin is reorganized to actin stress fibres and ECM remodelling is induced facilitating migration and invasion. Cells are also able to revert from a mesenchymal to an epithelial state (MET) [207].

EMT is classified into three different subgroups based on the biological context. Type 1 Developmental EMT, Type 2 EMT involved in physiological and pathological context like wound healing, tissue remodelling and fibrosis and Type 3 oncogenic EMT [208]. During embryonic development, cells of the primitive streak undergo an EMT at the gastrulation stage to form the mesoderm and endoderm, the cells remaining in the epiblast become ectodermal and thereby form the three germ layers. Furthermore, EMT plays a crucial role during neural crest formation, heart valve formation and myogenesis. During embryonic development, several rounds of EMT and MET were found to take place. EMT is also induced by tissue injury or by inflammation. Keratinocytes, the skin epithelial cells are able to undergo an EMT and then migrate to reconstruct and repair the tissue. Also, chronic inflammation can lead to a sustained activation of EMT, leading to fibrosis by the increased production of ECM by the mesenchymal cells, finally resulting in organ failure. Oncogenic EMT describes the process observed in cancer cells. [203, 208, 209] Oncogenic EMT is thought to promote dissemination of cancer cells and the formation of metastasis. In order to establish a metastasis in a different organ it is thought that epithelial cells have to gain motile properties thereby EMT might contribute to the metastatic cascade. It is proposed that EMT provides cancer cells with the ability to intravasate into the blood

circulation, extravasation into distant organs where MET takes place for metastatic colonisation. Additionally, EMT is also implicated in anoikis resistance, evasion of immune surveillance, acquisition of stem-cell like properties and resistance to chemotherapy (Fig. 5) [203, 210, 211]. There are two prominent models of metastasis formation which are still debated. The linear model states that metastasis formation occurs at rather late stages of tumor progression, whereas in the parallel model it is thought that metastasis formation already occurs during earlier stages [212]. Due to EMT being a transient process, a full EMT is rarely observed in patients, and the involvement of EMT in metastasis formation is still under debate with some reports even questioning a pivotal role of EMT in metastasis formation. However, there are many observations demonstrating and supporting EMT/MET plasticity occurring in tumor cells and promoting metastasis formation. *In vitro* and *in vivo* studies have demonstrated that EMT promotes migration and invasion of tumor cells, whereas inhibition has been found to reduce metastasis formation [203, 210, 213]. Circulating tumor cells (CTCs) of patients have also been found to express rather mesenchymal markers as compared to the primary tumor tissue and show an increase in expression of stem cell markers [214-216]. Also, loss of E-cadherin correlates with a worse prognosis in several cancer types [217]. E-cadherin expression or membrane localization is for example lost in most lobular breast cancers [218]. However, it is often observed that tumor cells show a co-expression of epithelial and mesenchymal markers. Therefore, it is thought that rather a partial EMT might take place. It was for example shown, that CTCs co-express epithelial as well as mesenchymal markers [215]. Furthermore, the co-expression of epithelial and mesenchymal signatures has been found to correlate with enrichment of stem-like cells and a poor survival in luminal and basal breast cancer patients [219].

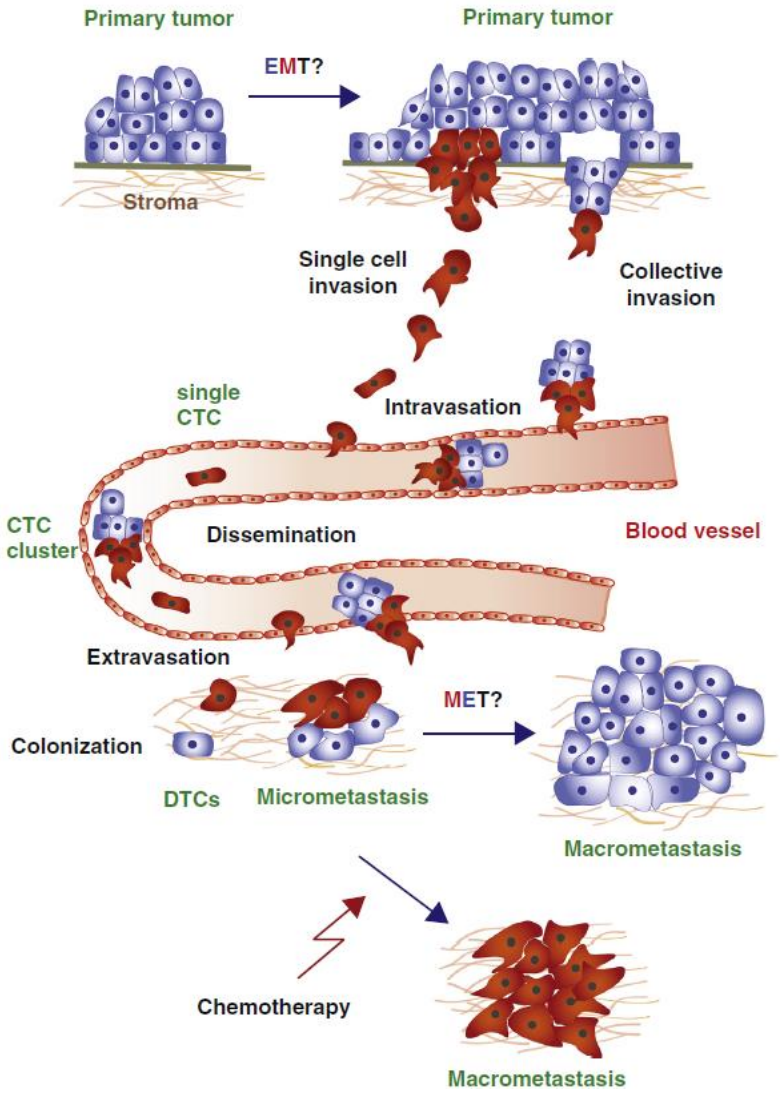

Figure 6. Schematic representation of the dissemination of cancer cells into distant organs. Cells from the primary tumor are thought to undergo EMT and thereby either as single cells or as clusters they invade the surrounding tissue, intravasate into the blood circulation, extravasate at a distant site and form micrometastasis. Those then undergo MET and establish macrometastasis. However by chemotherapy it might also be selected for cells that underwent EMT since they appear to be more drug resistant [213].

2.2.3.1 Wnt in EMT

The canonical Wnt pathway is one of the pathways known to be able to regulate EMT. Several of its transcriptional downstream targets are involved in EMT and play a crucial role. One of the hallmarks of EMT is the downregulation of the cell-adhesion molecule E-cadherin and its loss at the cell membrane, thereby β-catenin can accumulate in the cytoplasm which can induce transcription of Wnt targets. Hence, E-cadherin by binding to β-catenin can compete with β-catenins transcriptional activity. Amongst the

canonical Wnt signaling target genes are *Zeb1, Twist*, *Fibronectin* and the transcriptional repressors *Snai2 (Slug*) and *Snai1*. *Snai2* has been found being a direct target of the canonical Wnt pathway whereas *Snai1* has been shown being regulated indirectly via GSK3β. GSK3β has been found being able to phosphorylate SNAI1 resulting ultimately in its degradation. Hence, upon activation of the canonical Wnt pathway, GSK3β activity is inhibited resulting in an increased expression of *Snai1* [220, 221]. Transcription factor *zinc-finger E-box bonding homeobox 1* (*Zeb1*), another Wnt target gene, is also able to repress *E-cadherin* expression but was furthermore found to induce the expression of mesenchymal genes [222]. Transcription factor, Twist can also transcriptionally repress *E-cadherin* but also downregulates other epithelial markers like *claudins* and *occludins*. Furthermore, Twist is able to upregulate the expression of the mesenchymal markers N-cadherin, Vimentin, MMPs, and Fibronectin [193, 223, 224]. Notably, *Fibronectin* and *Mmp7* themselves are direct targets of canonical Wnt signaling. Matrix metalloproteases (MMPs) degrade the ECM and cell-cell contacts thereby facilitating the detachment and migration of cells [225, 226]. Other target genes, which however might be indirectly regulated are enzymes involved in regulating cell adhesion stability, like *Tiam1,* and some are components of cell junctions, such as *L1cam* and *Nr-cam*, whereby the latter has been found to be a direct Wnt target gene [227]. Also *Vimentin* has been identified as a target of the canonical Wnt pathway in human breast cancer cell lines. Hence, many of the canonical Wnt target genes are involved in EMT and abrogating the canonical Wnt pathway has been found to affect EMT [162, 228-231]. However, even though the canonical Wnt pathways seems to be necessary to induce EMT in at least a subset of cells, it does not seem to be sufficient [232].

2.2.4 Mouse models of metastatic breast cancer

Mouse models enabled and significantly contributed to testing and elucidating mechanisms and genes involved in tumor progression and metastatic spread. Furthermore, they provide means to test novel therapeutic strategies. The ease of breeding them and maintaining them as well as the high level of molecular, genetic, cellular and physiological conservation between vertebrates make them a powerful tool for cancer research. However, mice also often respond differently than humans.

Carcinogens in mice are not *per se* carcinogenic for humans, and they can also respond distinctly to treatments. Furthermore, mimicking human genetic diseases in mice might results in different phenotypes. Hence, one has to make use of the similarities and to consider the present and known differences. Researchers now have access to a plethora of mouse models, each with its own advantages and limitations. This also true for mouse models for breast cancer [233, 234]. Tumor xenografts can be performed to investigate tumor growth and metastasis formation of human cell lines or patient material (PDX) *in vivo*. However, for such experiments immunocompromised or humanized mice have to be used. Further transplantation methods can be used as cancer cells can also be transplanted from one mouse to another genetically identical or closely related allowing the investigation of the contribution of an intact immune system (syngeneic transplantation). Furthermore, allotransplantation is the transplantation of mouse cells, tissues or organs in immunoproficient mice with the same genetic background. The site of injection or implantation also plays a crucial role in the outgrowth of the tumors or tumor cells and metastasis formation. Another possibility for studying human cancer is the use of genetically engineered mouse models (GEMM). In transgenic mice, cloned oncogenes can be expressed or the expression of specific genes can be ablated in knockout mice or modified in knock-in mice. Furthermore, different promotors can be used to drive the expression of oncogenes and transgenes [234, 235]. There are also different promotors driving the expression specifically or mainly in the mammary gland and hence can be used to examine breast carcinogenesis in mice. One of those promotors is the mammary tumor virus long terminal repeat (MMTV LTR) leading to the expression mainly in the mammary epithelium, but also to low levels in other tissues as the ovaries and salivary glands [235, 236]. In this study we used the MMTV-PyMT mouse model, in which the expression of the oncoprotein polyoma middle T antigen (PyMT), is under the control of the MMTV LTR. Polyoma middle T antigen activates different signaling transduction pathways, including Src, Ras and PI3K. These pathways were also detected to be activated in human cancers. In this mouse model, multiple tumor foci can be found in all mammary glands. The progression from a premalignant to malignant stages is well recapitulated in these mice. At around 4 weeks of age, tumor growth is induced by steroid hormones during lactation. At the beginning, one primary focus around the main duct and sometimes some adjacent foci develop. The initially hyperplastic lesions are composed of lobules formed on the duct. Around 8 to 9 weeks of age, the progression

to the adenoma stage is visible by an increased proliferation of the epithelial cells with a still intact basement membrane and the cells start to fill the lumen. A transition to the malignant early carcinoma stage can be detected around 8 to12 weeks of age. Around 10 weeks of age, in half of the mice, a progression to the late carcinoma stage can be found were no acinar structures are visible anymore and the tumors are composed of solid epithelial sheets. As the tumors progress through the different stages, expression of ER and PR is gradually lost, while an increase in the expression of ERBB2/HER2 as well as Cyclin-D1 is observed. Furthermore, β-integrin expression, which has a role in cell proliferation, apoptosis and differentiation, is found being altered during tumor progression in this mouse model (Fig. 6). Hence this model shows many similarities to observations found in the progression of human breast cancer, in morphology but also with regard to biomarker expression and metastasis formation. Furthermore, this model shows a high penetrance, short latency and the formation of lung metastases, thereby it provides a tool to examine tumor progression as well as metastasis formation in breast cancer [237, 238].

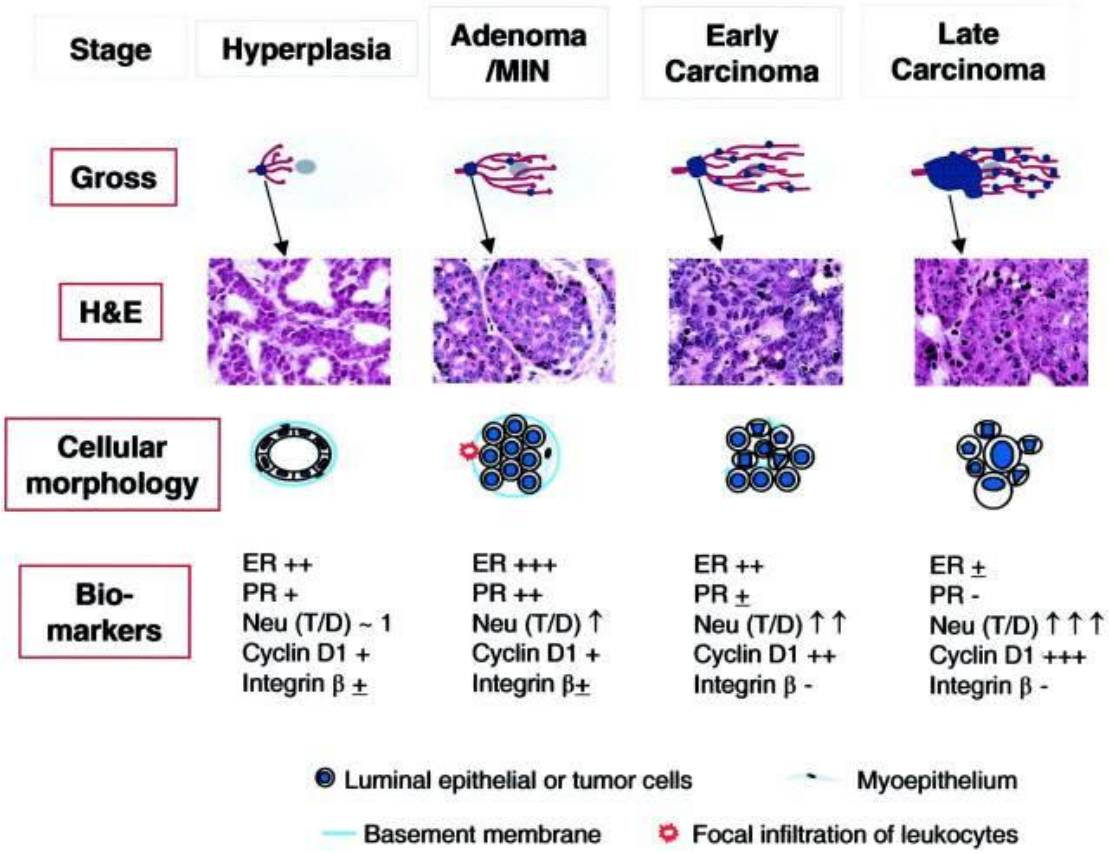

Figure 6. MMTV-PyMT tumor mouse model, tumor progression and biomarker expression. Four tumor stages are observed in the MMTV-PyMT breast cancer mouse model. The earliest stage (hyperplasia) starts around 4 weeks of age, further progressing via the adenoma stage with a visibly increased proliferation of the epithelial cells to an early- and then late carcinoma stage where the tumors are composed of solid epithelial sheets. Gross shows the development of the lesions in the mammary glands. H&E depicts the corresponding histology at the different stages of tumor progression. The cellular morphology panel schematically illustrates changes in the cytology and the integrity of the basement membrane. The Biomarkers panel depicts the changes in the biomarkers during tumor progression in the MMTV-PyMT mouse model [238].

2.3 Aim of the study

The canonical Wnt signaling pathway is often found to be aberrantly activated in human breast cancer and the expression of several components of the pathway is changed. Furthermore, nuclear β-catenin was found to correlate clinically in breast cancer patients. Therefore, in this project we aimed to examine the contribution of β-catenin signaling in mammary tumor progression and metastasis formation. In order to delineate the contribution of β-catenin and its interaction domains, β-catenin knockin mutant strains established by Valenta and colleagues, were used and examined [137]. The β-catenin-D164A mutation abrogates the binding of the N-terminal cofactors BCL9/9L to β-catenin whereas the β-catenin-ΔC mutant abrogates the binding of a plethora of coactivators binding to the C-terminus of β-catenin. The β-catenin-D164A-ΔC strain combines both mutations which prevents the binding of N- and C-terminal coactivators and thereby should inhibit the canonical Wnt singling output. Those mutant forms do not abrogate the binding of E-cadherin and hence do not affect β-catenin's function in cell adhesion. Next to those mutant forms, conditional knockout mice carrying β-catenin floxed (fl) alleles were analyzed. Recombination in the mammary gland mediated by Cre under the control of the mouse mammary tumor virus (MMTV) long terminal repeat (LTR), allowed the examination of the loss of both of β-catenin's functions, in signaling as well as cell adhesion on mammary tumor profession and metastasis formation. Thereby we aimed to dissect the requirement of β-catenin for cell adhesion as compared to its transcriptional function. In order to delineate the effect of these modulations in breast carcinogenesis and metastasis formation a MMTV-PyMT transgenic mouse model was used. Female mice were examined at 12 weeks of age and the weight of the tumors, the number of lung metastasis as well as tumor progression by quantification of the different tumor stages in the mouse models used, has been determined. Furthermore, for the mice carrying mutant forms of β-catenin tumor cell proliferation and apoptosis was examined by immunofluorescence staining to determine the causes for alterations in tumor weight. From the tumors of the various genotypes, cell lines have been established to further examine the observed changes *in vivo*. Using the established cell lines, we aimed to assess β-catenin's transcriptional activities using a reporter assay to find out if the mutant forms are able to activate the canonical Wnt pathway to the same extent as the wild type cells upon Wnt3a treatment. Moreover, by treatment with transforming growth factor β

(TGFβ) and subsequent analysis we attempted to examine if altering the canonical Wnt output affects EMT, which might contribute to changes observed in metastasis formation. Additionally, by performing RNA sequencing we aimed to elucidate which target genes and signaling pathways are affected by the specific modulations of nuclear Wnt signaling upon activation of the pathway by Wnt3a and during EMT induced by TGFβ. By comparing the gene expression of wild type cells and the different β-catenin mutant forms we wanted to identify expression patterns and target genes specifically affected by the loss of N- and/or C-terminal coactivators. Thereby we wanted to distinguish target genes that are no more regulated in cell lines expressing the mutant forms of β-catenin and the target genes specifically regulated by N- or C-terminal coactivators which might contribute to observed differences. Moreover, we sought to examine the effect of the complete abrogation of the canonical Wnt output using the dm form of β-catenin. Additionally, ChIP sequencing was performed to be able to generate a list of direct Wnt targets affected by the different mutations as compared to the wild type. Combining RNA and ChIP sequencing data will allow the detection of gene signatures or specific target genes affected by canonical Wnt signaling which might constitute promising novel therapeutic targets.

2.4 Results

β-catenin signaling function vs. adhesion: Role in epithelial-mesenchymal transition (EMT) and malignant mammary tumor progression

Buechel, David[1]; Saxena, Meera[1]; Kalathur, Ravi Kiran Reddy[1]; Rubinstein, Natalia[2]; Valenta, Tomas[3]; Hausmann, George[3]; Cantù, Claudio[4]; Basler, Konrad[3]; Christofori, Gerhard[1]

[1]Department of Biomedicine, University of Basel, Basel, Switzerland

[2]Departamento de Fisiología, Biología Molecular y Celular, Facultad de Ciencias Exactas y Naturales, Universidad de Buenos Aires, Buenos Aires, Argentina

[3]Institute of Molecular Life Sciences, University of Zürich, Zürich, Switzerland

[4]Department of Clinical and Experimental Medicine (IKE), Faculty of Health Sciences, Wallenberg Center for Molecular Medicine (WCMM), Linköping University, Linköping, Sweden

- in preparation -

2.4.1 Abstract

Aberrations in the Wnt signaling pathway have been found in correlation with poor prognosis in breast cancer patients. Although mutations in β-catenin and other canonical Wnt signaling components are only rarely found in breast cancer, there is evidence for aberrant Wnt signaling and β-catenin stabilization. However its role in breast cancer remains poorly defined. β-catenin exerts a dual role, it is the key nuclear effector of canonical Wnt signaling and is as well a crucial component of the E-cadherin mediated cell-cell adhesion complex. To provide a better understanding of β-catenin's function in breast tumor progression and metastasis formation, functional *in vivo* analyses in a MMTV-PyMT mouse model were performed. The effect of a conditional β-catenin conditional knockout was analyzed and to further dissect the requirement of β-catenin for cell adhesion as compared to its transcriptional function, we used mice expressing mutant forms of β-catenin which retain its function in cell adhesion but lack the N- and/or C-terminal transcriptional outputs. Assessment of the tumor mass and number of lung metastases revealed a reduction in tumor mass in mice expressing mutant forms of β-catenin. The number of lung metastases was significantly reduced in the mutant strains in which the binding of N-terminal coactivators BCL9//9L is abrogated. Complementary *in vitro* experiments showed a significant reduction in canonical Wnt activity and the inability to bind to BCL9/9L affected EMT *in vitro*. RNA sequencing analyses of tumor-derived cell lines identified candidate genes, which seem to be either regulated by N- and C-terminal or specifically by N- or C-terminal coactivators upon Wnt3a or during EMT induced by TGFβ treatment. Furthermore, abrogating the binding of N- and C- terminal coactivators to β-catenin resulted in the almost complete abrogation of the canonical Wnt pathway output, showing only minor changes in some known Wnt target genes as well as pathway components. In conclusion, we show that abrogating the binding of N- and/or C-terminal β-catenin coactivators without affecting β-catenin's function in cell adhesion, affects tumor growth *in vivo*, proliferation and alters the transcriptional output. On the other hand, β-catenin knockout and thereby the complete loss of β-catenin's signaling and adhesion function leads to apoptosis in mammary tumor cells *in vitro* and *in vivo*, which suggests a key role of its adhesion function in cell survival. Furthermore, the observations indicate that the inability of β-catenin to bind BCL9/9L are critical for a subset of Wnt target genes involved in EMT.

2.4.2 Introduction

The canonical Wnt/β-catenin pathway is known to be important for several processes during the development, amongst them are stem cell maintenance, differentiation, homeostatic self-renewal and regulation of growth. Aberrations in this pathway have been found to cause a wide range of pathologies in humans [1]. Though, mutations affecting members of the Wnt signaling pathway are observed in many different cancer types, mutations in β-catenin or other canonical Wnt signaling components are only rarely found in breast cancer. However, aberrant activation of the Wnt/β-catenin signaling pathway resulting in translocation of β-catenin to the nucleus and the subsequent transcription of its target genes is found in the majority of breast cancers. Several components of the Wnt signaling pathway have been found to be differentially expressed in breast cancer [2-6]. Consistent with these findings *Wnt1* was the first oncogene identified [7, 8]. The oncogenic potential of Wnts and other canonical Wnt pathway components has from then on been confirmed in the mammary gland [5]. For example, expression of stabilized *β-catenin*, overexpression of *Lrp (low density lipoprotein receptor-related protein 5/6*) or loss of *Apc (adenomatous polyposis coli)* in the mammary gland of transgenic mice have been shown to lead to hyperplasia or tumor formation [9-12]. Experimental evidence in patients suggests, that the Wnt pathway in breast cancer may be changed by the loss of expression of negative pathway regulators or overexpression of individual Wnt ligands. Negative pathway regulators like *Wnt inhibitory factor 1* (*WIF1*), *secreted frizzled-related protein* (*SFRP*), *Dickkopf 1* (*DKK1*) as well as *APC*, *AXIN1* and *AXIN2* have been found to be hypermethylated and their expression to be significantly reduced in breast cancer [13-17]. Consistently, increased nuclear β-catenin can be detected in many breast tumors [5, 6]. β-catenin itself has a dual function: it is a crucial component of the E-cadherin mediated cell-cell adhesion complex needed for structural integrity and functional polarization of epithelia as well as the key nuclear effector of the canonical Wnt signaling pathway. Without Wnt ligand binding to the transmembrane receptors Frizzled (Fzd) and the single-pass transmembrane co-receptors LRP5/6, the pathway is in an off state and free cytosolic β-catenin is targeted and phosphorylated by the so-called destruction complex. This complex is composed out of the scaffold proteins AXIN and APC and the kinases GSK3β (glycogen synthase kinase 3β), CK1α (casein kinase 1α) which phosphorylate β-catenin at amino-terminal serine and threonine

residues. Subsequently, β-catenin is degraded by the ubiquitin proteasome pathway. Whereas the binding of a canonical Wnt ligand to the transmembrane receptor Frizzled and its co-receptor LRP5/6 ultimately results in the destabilization of the destruction complex. Unphosphorylated β-catenin can accumulate in the cytoplasm and translocate to the nucleus where it binds to the TCF/LEF transcription factors [18, 19]. Different coactivators binding to β-catenin can modulate the transcriptional activity. At the C-terminus of β-catenin several coactivators have been found to bind which are not β-catenin specific. Amongst them are CBP (CREB binding protein, CREBBP), p300 (E1A binding protein P300) and TIP60 (lysin acetyltransferase 5, KAT5) which can affect chomatin structure (chromatin remodeling complexes), SWI/SNF (SWItch/Sucrose Non-Fermentable) and ISWI (imitation Switch) which can affect nucleosome rearrangement or the Mediator complex which connects β-catenin to the transcriptional machinery. Whereas, at the N-terminus, the β-catenin specific cofactor BCL9/9L binds which in turn recruit Pygopus [19-22]. β-catenin's dual function made it difficult to specifically study its signaling function and effect on tumor progression and metastasis formation. Therefore, to specifically characterize β-catenin's role in Wnt signalling, it is required to separate those two functions. Valenta and colleagues have generated specific β-catenin mutant forms that only affect the transcriptional Wnt signaling activity of β-catenin but not its cell adhesion function. The D164A mutation abrogates the binding of the N-terminal β-catenin specific cofactor BCL9/9L, the ΔC mutation leads to a truncation of the C-terminus of β-catenin and thereby prevents the binding of C-terminal transcriptional cofactors involved in chromatin remodeling and transcriptional activation. The double-mutant (dm) combines both those mutations and thereby completely abrogates Wnt/ β-catenin signaling but preserves β-catenin's function in cell adhesion [20]. Those mutant forms were compared to conditional knockout mice carrying β-catenin floxed (fl) alleles by which its function in cell adhesion and signaling are lost. In this study we exploit the functional role of β-catenin and its nuclear N- and C- terminal co-factors in breast tumor growth and metastasis formation in a MMTV-PyMT tumor mouse model *in vivo* and during EMT in cell culture assays *in vitro*. We show that loss of β-catenin and thereby its adhesion as well as signalling function, results in apoptosis *in vitro* and *in vivo*. Whereas, selective abrogation of the N- and/or C-terminal transcriptional output of β-catenin affects tumor progression and tumor cell proliferation. Lack of the N-terminal transcriptional output only or the complete abrogation of Wnt signaling activity in the double-mutant form of β-catenin

also affects metastasis formation *in vivo* and an epithelial-to-mesenchymal transition (EMT) *in vitro*. The results show that, as compared to the β-catenin knockout cells, cell deprived of only β-catenin's transcriptional activity were viable, suggesting a key role of β-catenin's adhesion function in cell survival. Additionally, the β-catenin mutant forms displayed a dominant-negative effect. Moreover, we wished to assess whether the nuclear Wnt signaling and some of its target genes could serve as potential diagnostic factors *in vivo* and as potential therapeutic targets for the specific ablation of Wnt signaling in metastatic cancer. RNA sequencing performed by using tumor-derived cell lines showed that the different mutant forms of β-catenin alter the transcriptional output and target genes were identified which seem to be regulated either by N- and C-terminal or specifically by N- or C-terminal coactivators of β-catenin upon Wnt3a or during EMT induced by TGFβ treatment. Furthermore, abrogating the binding of coactivators to β-catenin in the double-mutant cell line resulted in almost complete abrogation of the canonical Wnt pathway output.

2.4.3 Knockout of β-catenin leads to apoptosis *in vitro* and *in vivo*

To evaluate the role of β-catenin in tumor progression and metastasis formation, β-catenin$^{fl/fl}$; MMTV-PymT; MMTV-Cre conditional knockout mice were generated. β-catenin$^{fl/fl}$; MMTV-PyMT; MMTV-Cre mice did not show significant differences in tumor weight, the number of lung metastases, the metastasis index or the different tumor stages comparing twelve-week-old Cre^{+} to Cre^{-} control mice (Supplementary Fig. 1A, 1B). Immunofluorescence (IF) staining of tumor sections revealed that β-catenin was still present in tumors of β-catenin$^{fl/fl}$; MMTV-PyMT; MMTV-Cre conditional knockout mice (Supplementary Fig. 1C). Also genotyping of the tumors demonstrated an incomplete deletion of the *β-catenin* gene in tumors (Supplementary Fig. 1D). The ability of Cre to delete *β-catenin* was also examined using GFP-reporter mice. Quantifying the recombination in 5- and 12-week-old mice revealed an incomplete and similar recombination efficiency between wild-type and *β-catenin* knockout mice at 5 weeks of age. At 12 weeks of age the percentage of GFP-positive cells per tumor was reduced in β-catenin knockout mice whereas similar levels were observed in the wild type mice (Supplementary Fig. 1F). This revealed an incomplete deletion and suggests an outgrowth of GFP-positive wild-type cells, whereas GFP-positive β-catenin

knockout cells are eliminated. However, exogenous addition of Adenovirus-Cre-IRES-GFP on primary tumor cell lines derived from β-catenin$^{fl/fl}$; MMTV-PyMT tumors eliminated the β-catenin gene as assessed by genotyping and led to an increase in the amount of cleaved caspase-3 positive cells compared to the cells transduced with a control Adenovirus-IRES-GFP or to β-catenin$^{wt/wt}$; MMTV-PyMT cells (Fig. 1A, 1B, Supplementary Fig. 1E). These results indicate that the presence of β-catenin is essential for tumor cell survival and that loss of its signaling as well as its adhesion function leads to cell death *in vitro*. Increased cleaved caspase-3 staining was also found *in vivo*, in tumor sections of β-catenin conditional knockout mice (5 weeks old, just after Cre activation) compared to β-catenin wild-type mice (Fig. 1C). These results suggest that there is a selection pressure during tumor progression, favoring the outgrowth of β-catenin-positive cells and reveal that β-catenin is required for mammary tumor cell survival.

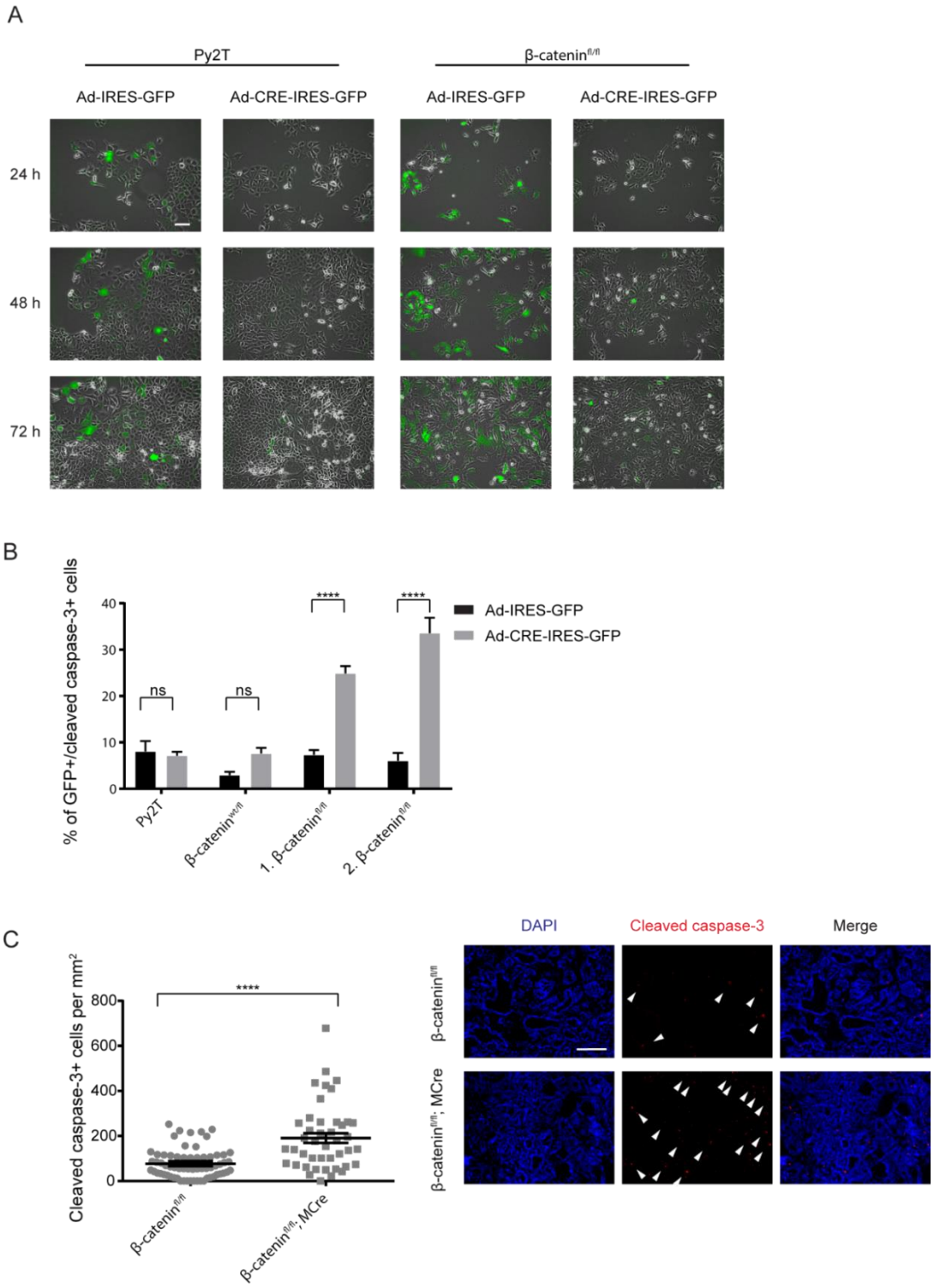

Figure 1. Knockout of β-catenin leads to apoptosis *in vitro* and *in vivo*. (A) Infection of β-catenin$^{wt/wt}$ (Py2T) and β-catenin$^{fl/fl}$ cells with either Adeno-CRE-IRES-GFP or Adeno-IRES-GFP. GFP positive cells were lost only in β-catenin$^{fl/fl}$ cells upon infection with the Adeno-CRE-IRES-GFP virus. Scale bar: 100 µm. **(B)** β-catenin$^{wt/wt}$ (Py2T), β-catenin$^{wt/fl}$ and β-catenin$^{fl/fl}$ cells were infected with either Adeno-CRE-IRES-GFP or Adeno-IRES-GFP. The number of infected (GFP positive) and apoptotic (Cleaved Caspase 3 positive) cells revealed a significant increase in the amount of apoptotic cells upon knockout of β-catenin. Data are displayed as mean ± SEM. The results represent four independent experiments. Statistical analysis was performed using ordinary one-way ANOVA multiple comparison test: **** P <

0.0001. **(C)** Cleaved Caspase-3 quantification in vivo in mice at 5 weeks of age demonstrated a significant increase in the amount of apoptotic cells upon β-catenin knockout. White arrows indicate cleaved caspase-3 positive cells. DAPI was used to visualize nuclei. Scale bar: 100 µm. Data are displayed as mean ± SEM. n=5. Statistical analysis was performed using Mann-Whitney U test; **** P < 0.0001.

2.4.4 Abrogating the binding of BCL9/9L to β-catenin affects tumor growth and metastasis formation

To assess the importance of the binding of BCL9/9L, the β-catenin-specific cofactors for malignant breast tumor progression and metastasis formation, we examined the tumor growth and metastasis formation of mice harboring the D164A mutant form of β-catenin. This point mutation leads to the abrogation of the binding of BCL9/9L to β-catenin (Fig. 2A). Composite transgenic β-catenin$^{D164A/fl}$; MMTV-PyMT as well as β-catenin$^{D164A/fl}$; MMTV-PyMT; MMTV-Cre 12-week-old mice showed a significantly lower tumor mass, less lung metastases as well as a decrease in the metastasis index compared to age-matched control mice (β-catenin $^{fl/fl}$; MMTV-PyMT) (Fig. 2B). Quantification of cleaved caspase-3 (apoptosis) and phospho-histone H3 (pH3, proliferation) IF staining on tumor sections revealed that the differences in tumor growth between mice expressing the D164A mutant allele and control mice seemed to be due to less proliferation (Fig. 2C), whereas no alteration in cleaved caspase-3 expression was found (Supplementary Fig. 2A). When analyzing different stages of tumor progression of the PyMT tumor model (hyperplasia, adenoma and carcinoma) [238] it became apparent that mice with the D164A mutation have a lower carcinoma burden compared to control mice, suggesting a delay in tumor progression (Fig. 2D). Co-staining for E-cadherin and β-catenin showed co-localization at the cell membrane in mice expressing the D164A mutant β-catenin protein (Fig. 2E). This suggests that β-catenin D164A still maintains its function in the cell adhesion complex. Taken together these results show that binding of BCL9/9L to β-catenin is important for tumor cell proliferation, tumor progression as well as metastasis formation. Furthermore, the D164A mutation appears to exert a dominant negative effect, thereby reducing the tumor weight, metastasis formation and proliferation *in vivo*.

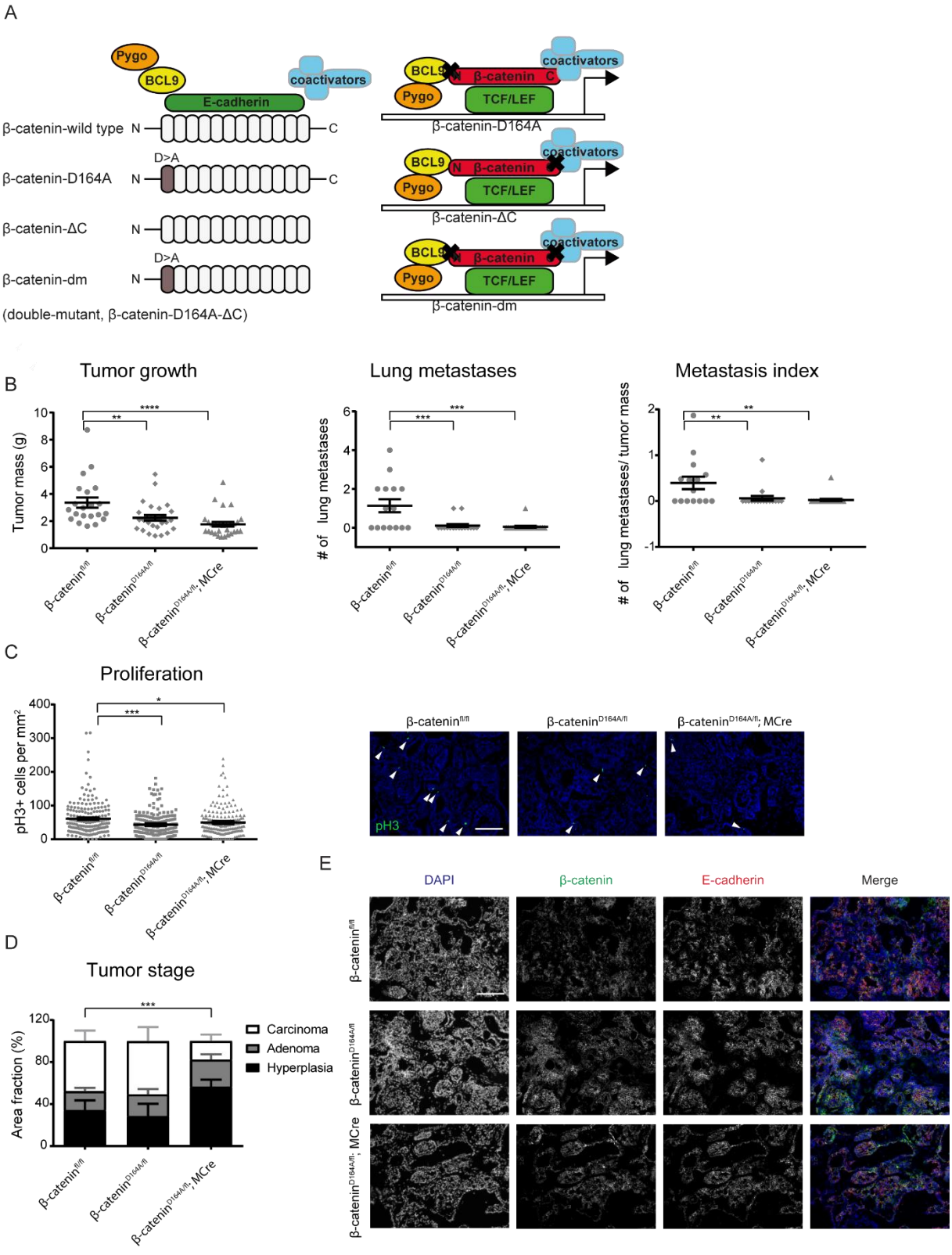

Figure 2. The β-catenin D164A mutation affects tumor growth, progression and metastasis formation. (A) Schematic representation of wild-type and mutant versions of β-catenin (left) used in this study and the abrogation of the binding of coactivators (right). Wild-type β-catenin can be divided into three distinct domains: an N-terminal region, which binds BCL9; a central Armadillo (Arm) repeat region (ovals), which binds TCF/LEF and E-cadherin; and a C-terminal region that binds several transcriptional coactivators. The D164A mutation (D>A) in the first Arm repeat leads to an amino acid change from

aspartic acid to alanine resulting in the abrogation of the binding of BCL9 (β-catenin specific cofactor-cell CLL/lymphoma 9) and BCL9L (β-catenin specific cofactor-cell CLL/lymphoma 9-like) to the N-terminus. The ΔC mutation leads to a truncation of the C-terminus of β-catenin and thereby prevents the binding of C-terminal transcriptional coactivators. Finally, the double-mutant (dm) strain, β-catenin-D164A-ΔC combines both, the D164A mutation and the C-terminal deletion and thereby completely abrogates Wnt signaling. Black crosses represent the abrogated interactions. The unique and important feature of these mutant forms of β-catenin is that they lack either the N- or C-terminal transcriptional output or both but retain the cell adhesion function of β-catenin. **(B)** The mammary glands and the lungs of twelve week old (Cre+ and Cre-) mice of the D164A mutant mouse strains were dissected and the tumor weight as well as the number of lung metastases were compared to β-catenin$^{fl/fl}$; PyMT (wild type) control mice. The β-catenin D164A mutation causes a reduction in the size of the tumors (β-catenin$^{fl/fl}$ n=21, β-catenin$^{D164A/fl}$ n=27, β-catenin$^{D164A/fl}$; MMTV-Cre (MCre) n=29), the number of lung metastases as well as in the metastasis index. β-catenin$^{fl/fl}$ n=15, β-catenin$^{D164A/fl}$ n=18, β-catenin$^{D164A/fl}$; MCre n=21. **(C)** Immunofluorescent staining and quantification for pH3 to assess proliferation on tumor sections of the different mouse genotypes. White arrows indicate pH3 positive cells. Tumor sections from mice expressing the D164A mutant allele have less proliferating cells (pH3) compared to control mice. DAPI was used to visualize nuclei. Scale bar: 100 μm. n=10. **(D)** Quantification of tumor stages, mice with the D164A mutation have less carcinoma than the control mice. β-catenin$^{fl/fl}$ n=7, β-catenin$^{D164A/fl}$ n=7, β-catenin$^{D164A/fl}$; MCre n=12. **(E)** Immunofluorescence staining on tumor sections for E-cadherin and β-catenin, showed co-localization at the cell membrane in mice expressing the D164A mutant β-catenin protein. DAPI was used to visualize nuclei. Scale bar: 100 μm. Data are displayed as mean ± SEM. Statistical analysis was performed using ordinary one-way ANOVA multiple comparison test: * P < 0.05, ** P < 0.01, *** P < 0.001, **** P < 0.0001.

2.4.5 Binding of C-terminal coactivators is essential for tumor growth but not for metastasis formation

To evaluate the importance of C-terminal coactivators binding to β-catenin and their effect on tumor growth and metastasis formation, we examined the effect of the ΔC mutant form of β-catenin. This mutation abrogates the interaction with a multitude of coactivators that bind to the C-terminus of β-catenin thereby affecting the canonical Wnt signaling output (Fig. 2A). When analyzing mice with the ΔC mutation, we found that the β-catenin$^{\Delta C/fl}$; MMTV-PyMT and the β-catenin $^{\Delta C/fl}$; MMTV-PyMT; MMTV-Cre mice have significantly smaller tumors compared to the β-catenin $^{fl/fl}$; MMTV-PyMT mice. Hence, the ΔC mutant protein also seems to have a dominant negative effect. Yet surprisingly, no difference was seen comparing the amount of metastases in the lungs or in the metastasis index (Fig. 3A). To examine if the observed differences in

tumor size between the genotypes are due to changes in proliferation and/or apoptosis, pH3 and cleaved caspase-3 immunofluorescence staining were conducted, a significant decrease in proliferation was observed comparing the mice expressing the ΔC mutant allele to the control mice (Fig. 3B, Supplementary Fig. 2B). Moreover, analysis of the different tumor stages did not reveal any significant changes (Fig. 3C). Additionally staining for E-cadherin and β-catenin showed co-localization at the cell membrane in mice expressing the ΔC mutant form of β-catenin (Fig. 3D). In conclusion, these results show that the diverse cofactors of β-catenin binding to the C-terminus are important for tumor growth and proliferation, whereas the target genes of canonical Wnt signaling affected by this mutation do not seem to be important for tumor progression and metastasis formation. Moreover, in regards to proliferation and tumor weight, a dominant negative effect is observed.

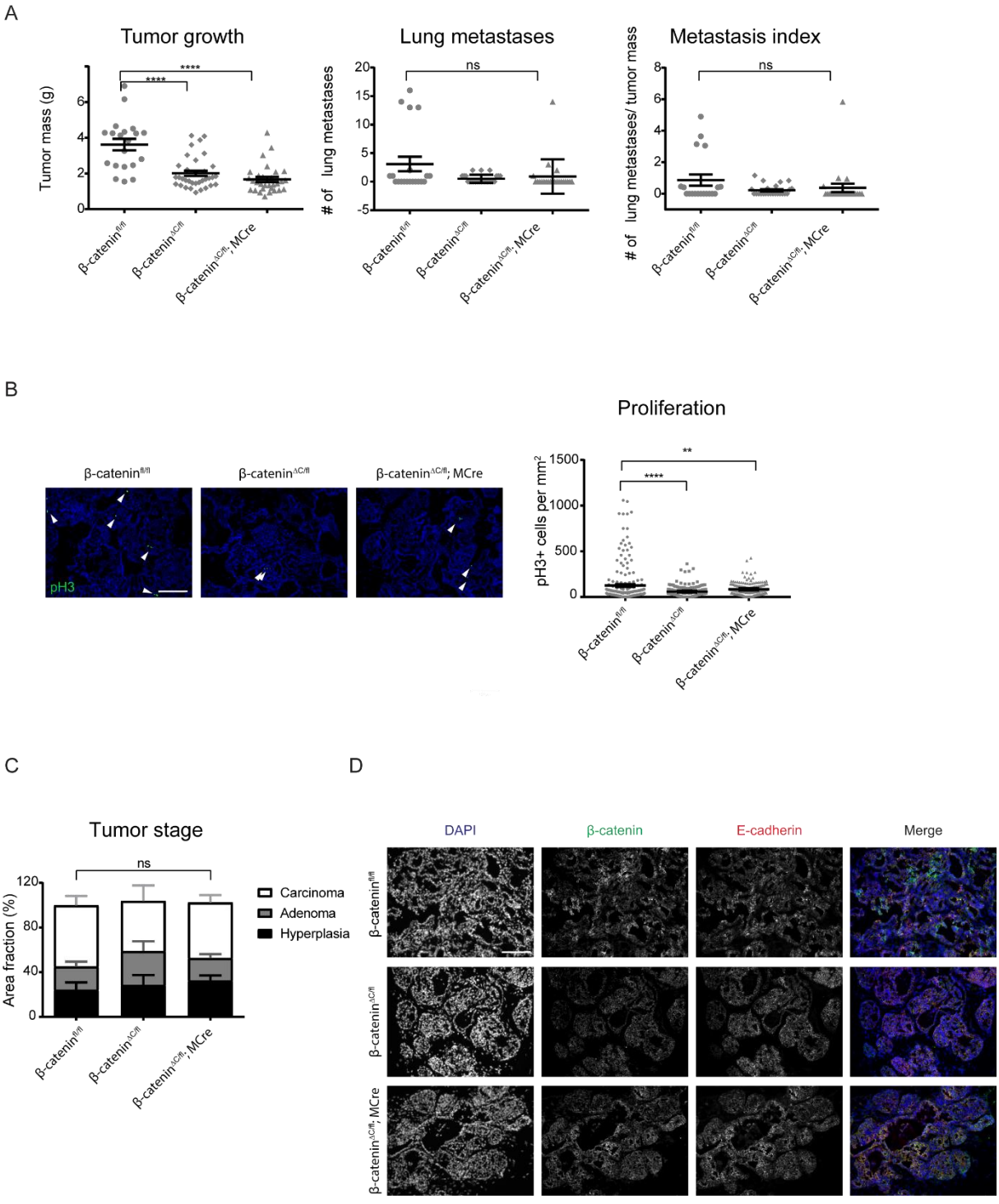

Figure 3. Abrogating the binding of C-terminal coactivators to β-catenin reduces tumor growth. **(A)** The mammary glands and the lungs of twelve week old (Cre+ and Cre-) mice of the ΔC mutant mouse strains were dissected and the tumor weight as well as the number of lung metastases were compared to β-catenin$^{fl/fl}$; PyMT (wild type) control mice. The β-catenin ΔC mutation causes a reduction in the weight of the tumors (β-catenin$^{fl/fl}$ n=20, β-catenin$^{\Delta C/fl}$ n=34, β-catenin$^{\Delta C/fl}$; MMTV-Cre (MCre) n=30) but does not affect metastases formation or the metastasis index. β-catenin$^{fl/fl}$ n=20, β-catenin$^{\Delta C/fl}$ n=24, β-catenin$^{\Delta C/fl}$; MCre n=22. **(B)** The truncated C-terminus results in a reduction of proliferating cells as compared to wild type mice. White arrows indicate pH3 positive cells. DAPI was used to visualize nuclei.

n=10. **(C)** The quantification of tumor stages did not show differences comparing the ΔC and wild type mice. β-catenin$^{fl/fl}$ n=6, β-catenin$^{\Delta C/fl}$ n=7, β-catenin$^{\Delta C/fl}$; MCre n=8. **(D)** Immunofluorescence staining on tumor sections for E-cadherin and β-catenin, showed co-localization at the cell membrane in mice expressing the ΔC mutant β-catenin protein. DAPI was used to visualize nuclei. Scale bar: 100 μm. Data are displayed as mean ± SEM. Statistical analysis was performed using ordinary one-way ANOVA multiple comparison test: ** P < 0.01, **** P < 0.0001.

2.4.6 Block of transcriptional β-catenin output decreases tumor growth and metastasis formation

In order to investigate the effect of complete abrogation of canonical Wnt signaling without affecting β-catenin's function in cell adhesion, we made use of the double-mutant (dm) form of β-catenin (Fig. 2A). In dm mice harboring both mutations (the D164A as well as the ΔC), we also observed smaller tumors, significantly less metastases in the lungs and a decrease in the metastasis index of both, the β-catenin $^{dm/fl}$; MMTV-PyMT; MMTV-Cre and the β-catenin $^{dm/fl}$; MMTV-PyMT mice compared to the β-catenin $^{fl/fl}$; PyMT mice (Fig. 4A). To understand the differences in tumor weight, IF stainings for pH3 and cleaved caspase-3 were conducted. A significant decrease in the amount of pH3-positive cells and a significant increase in the amount of cleaved caspase-3-positive cells was observed in tumors of both β-catenin $^{dm/flox}$; MMTV-PyMT; MMTV-Cre and the β-catenin $^{dm/flox}$; MMTV-PyMT mice compared to the β-catenin $^{fl/fl}$; MMTV-PyMT mice (Fig. 4B, Supplementary Fig. 2C). In addition, analysis of the different tumor stages revealed a trend towards less carcinoma in the mice harboring the dm mutation compared to the control mice (Fig 4C). In addition, also the β-catenin dm mutant form displayed a dominant-negative effect on tumor growth, tumor progression and metastasis formation. Moreover, the double mutation does not seem to affect β-catenin's function at the cell membrane, since it still colocalizes with E-cadherin as assessed by IF staining (Fig. 4D). These results show that a complete abrogation of the canonical Wnt signaling output represses tumor growth by affecting again proliferation but also apoptosis and it reduces metastasis formation and malignant tumor progression.

It should be noted that the mutant versions of β-catenin all seem to exert a dominant-negative effect, since the expression of the mutant forms in the presence of the wild-type allele results in a similar phenotype as the sole expression of the mutant alleles.

The notion of a dominant-negative effect was tested by transient transfection of β-catenin^{wt}, β-catenin^{D164A}, β-catenin$^{\Delta C}$ and β-catenin$^{D164A-\Delta C}$ and a GFP expressing vector construct in a β-catenin wild-type cell line (Py2T). The number of transfected and proliferating cells was quantified by MYC and pH3 staining, which revealed a reduced proliferation of cells transfected with the β-catenin mutant (D164A, ΔC and D164A-ΔC) forms (Supplementary Fig. 2D). This data showed that the mutant forms of β-catenin exert a dominant negative effect on proliferation also *in vitro*.

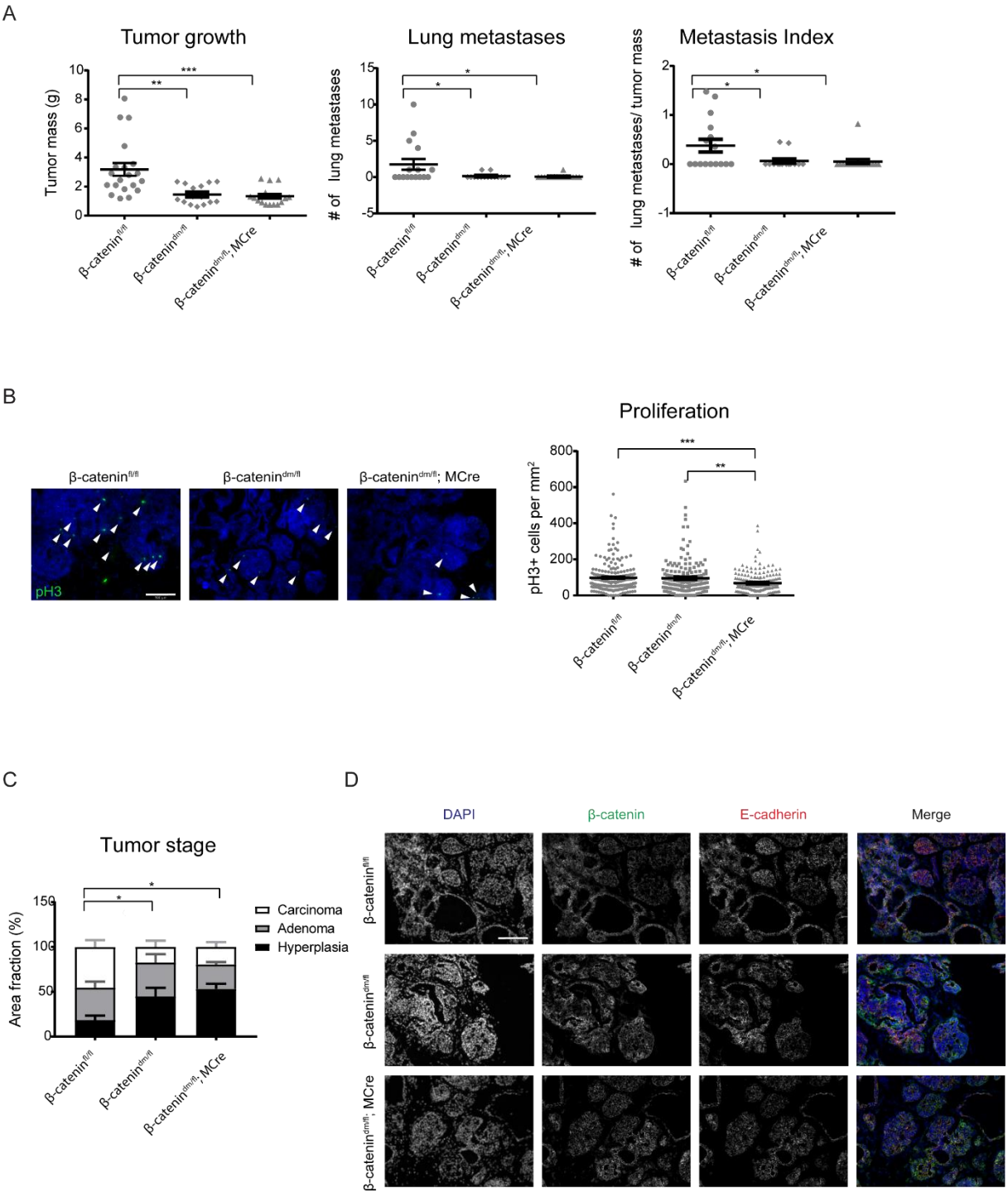

Figure 4. Blocking the canonical Wnt signaling output reduces tumor growth, tumor progression and metastasis formation. (A) The mammary glands and the lungs of twelve week old (Cre+ and Cre-) mice of the dm mutant mouse strains were dissected and the tumor weight as well as the number of lung metastases were compared to β-catenin$^{fl/fl}$; PyMT (wild type) control mice. The β-catenin double mutation causes a reduction in the size of the tumors (β-catenin$^{fl/fl}$ n=20, β-catenin$^{dm/fl}$ n=15, β-catenin$^{dm/fl}$; MMTV-Cre (MCre) n=16), the number of lung metastases and the metastasis index. β-catenin$^{fl/fl}$ n=16, β-catenin$^{dm/fl}$ n=14, β-catenin$^{dm/fl}$; MCre n=16. **(B)** Assessment of the amount of proliferating or apoptotic cells by immunofluorescent staining on tumor sections revealed, that the double mutation causes a reduction in the amount of proliferating cells compared to wild type mice. White arrows indicate pH3

positive cells. DAPI was used to visualize nuclei. n=10. **(C)** A reduction in the amount of carcinoma stage was found in the dm mice as compared to wild type tumor sections. β-catenin$^{fl/fl}$ n=14, β-catenin$^{dm/fl}$ n=12, β-catenin$^{dm/fl}$; MCre n=12. **(D)** Immunofluorescence staining on tumor sections for E-cadherin and β-catenin, showed co-localization at the cell membrane in mice expressing the dm mutant β-catenin protein. DAPI was used to visualize nuclei. Scale bar: 100 µm. Data are displayed as mean ± SEM. Statistical analysis was performed using ordinary one-way ANOVA multiple comparison test: * P < 0.05, ** P < 0.01, *** P < 0.001.

2.4.7 Loss of N- and C-terminal coactivators completely abrogates canonical Wnt activity and the inability of β-catenin to bind BCL9/9L results in an abrogated EMT response

In order to further examine the effects of the different β-catenin mutant forms on canonical Wnt activity and to validate the results in the transgenic mouse models by *in vitro* experimentation, we established cell lines from the different mouse genotypes. Epithelial cell lines were established from the different mutant β-catenin heterozygous tumors and the floxed alleles were removed by infection with Adeno-CRE-IRES-GFP virus and subsequent flow cytometry sorting for GFP-positive cells (Supplementary Fig. 3A, 3B). To determine if the alterations in cell proliferation observed *in vivo* can also be observed *in vitro*, growth curve analysis for the different cell lines established was performed. The results revealed a slower proliferation rate and a higher doubling time of the cells solely expressing the mutant forms of β-catenin compared to a wild-type cell line (Fig. 5A). In the previous study, Valenta and colleagues showed in HEK293T and MEF cells as well as *in vivo* during mouse embryonic development that the binding of N- and C-terminal coactivators are important for proper transcriptional activity of the canonical Wnt pathway and that it can be completely abrogated by expression of the dm protein [137]. To examine the canonical Wnt signaling output *in vitro* in mammary tumor-derived cell lines, the canonical Wnt signaling pathway was induced by addition of Wnt3a. Analysis using the Wnt reporter assay (superTOPflash/superFOPflash) revealed a decreased activation capacity of the canonical Wnt pathway of the cell lines solely expressing the mutant forms of β-catenin compared to wild-type cell lines (Fig. 5B). These results show that the N- and C-terminal coactivators both contribute to the transcriptional output and the dm form blocks β-catenin's signaling function.

Since EMT is regarded a possible mechanism underlying metastatic spread, we assessed whether the loss of β-catenin coactivator binding in the different β-catenin mutant forms might affect EMT. Therefore, a 4-day TGFβ treatment was performed comparing wild-type cells and the cell lines only expressing the mutant alleles for their ability to undergo EMT. Morphological differences were apparent between the cell lines. The β-catenin wild-type cell lines became more mesenchymal upon 4 days of TGFβ treatment and the same was true for the β-catenin$^{\Delta C/-}$ cell line. The morphology of the β-catenin$^{D164A/-}$ cells became more elongated as well, but they still grew as a cluster of cells, whereas the β-catenin$^{dm/-}$ cell line remained in their epithelial clusters and only seemed to form filopodia (Fig. 5C). Also long-term (20d) TGFβ treatment did not further alter the morphology of the β-catenin$^{D164A/-}$ and β-catenin$^{dm/-}$ cell lines (Supplementary Fig. 5C). Further analysis by IF staining for different EMT-related markers after 4 days of TGFβ treatment (E-cadherin, β-catenin, Zonula occludens (ZO-1) and Vimentin) revealed an augmented expression of the mesenchymal marker Vimentin and the reduced expression of the epithelial markers E-cadherin together with β-catenin and ZO-1 at the cell membrane in the wild-type as well as the β-catenin $^{\Delta C/-}$ cell line. In contrast, β-catenin$^{D164A/-}$ and β-catenin$^{dm/-}$ cell lines seem to undergo a partial EMT by retaining the expression of E-cadherin/β-catenin and ZO-1 at the cell membrane, but the β-catenin$^{D164A/-}$ cells were still able to upregulate the expression of Vimentin, whereas the dm cells only showed a mild increase (Fig. 5D, Supplemental Fig. 3D). Moreover, co-immunoprecipitation showed that the interaction of β-catenin with E-cadherin was retained and not affected by the β-catenin mutations (Supplementary Fig. 3E). Those results seem to confirm the observations *in vivo* showing that the D164A as well as the dm form of β-catenin lead to a reduction in metastasis formation, whereas the ΔC mutation did not have a significant effect. Consequently, the results show alteration of the canonical Wnt output by the D164A or ΔC mutation have a mild effect on the Wnt/β-catenin activity, whereas it is completely abrogated by the double mutation. In addition, the D164A and the dm mutant β-catenin-expressing cell lines have a reduced capability to undergo EMT which might account for the reduced metastatic burden observed *in vivo*. Furthermore, since we were able to obtain cell lines only expressing the mutant forms of β-catenin but not cell lines without any β-catenin, we conclude that β-catenin's adhesion function is critically required for mammary tumor cell survival, while its transcriptional output promotes tumor cell proliferation and survival, tumor growth, EMT and metastasis formation.

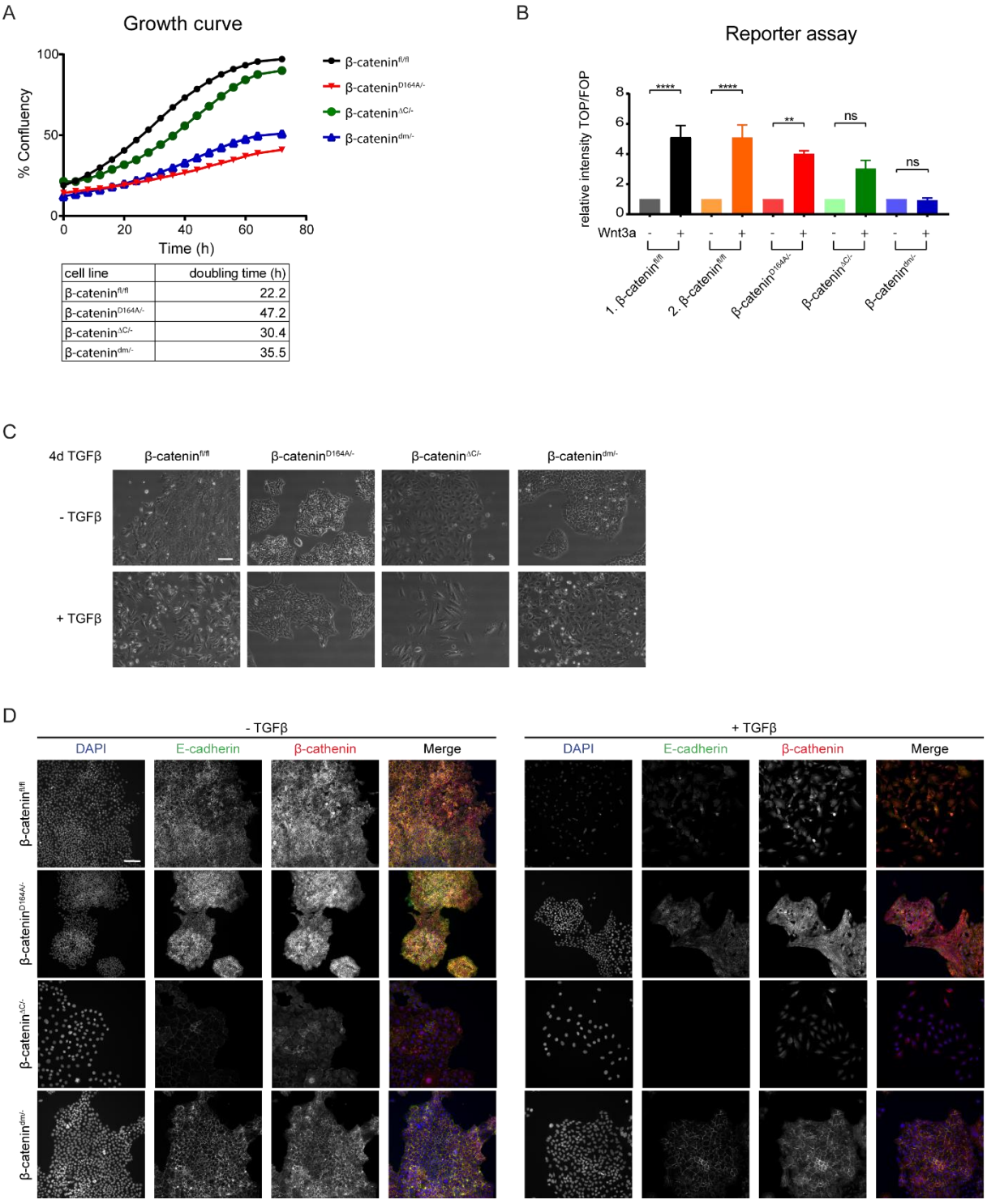

cell line	doubling time (h)
β-catenin$^{fl/fl}$	22.2
β-catenin$^{D164A/-}$	47.2
β-catenin$^{\Delta C/-}$	30.4
β-catenin$^{dm/-}$	35.5

Figure 5. Expression of β-catenin mutant forms results in a reduced growth and capability to activate the canonical Wnt signaling pathway as well as an abrogated EMT response by inhibition of BCL9/9L binding. (A) Comparing the growth curves of β-catenin$^{fl/fl}$, β-catenin$^{D164A/-}$, β-catenin$^{\Delta C/-}$ and β-catenin$^{dm/-}$ cell lines revealed that cell lines expressing mutant forms of β-catenin grow slower and have an higher doubling time. **(B)** Wnt reporter assay (superTOPflash/ superFOPflash). β-catenin mutant forms have a reduced response to TCF/LEF-dependent Wnt signaling upon Wnt3a treatment. The double-mutant (dm) form blocks the transcriptional β-catenin signaling output. The results represent four independent experiments. Data are displayed as mean ± SEM. Statistical analysis

was performed ordinary one-way ANOVA multiple comparison test: ** P < 0.01, **** P < 0.0001. **(C)** The β-catenin wild type cell line shows a mesenchymal morphology upon TGFβ treatment and the same was true for the β-catenin$^{\Delta C/-}$ cell line. The morphology of the β-catenin$^{D164A/-}$ became more elongated as well, but they still grew as a cluster of cells whereas the β-catenin$^{dm/-}$ cell line only seem to form filopodia. Scale bar: 100 µm. **(D)** Further analysis by immunofluorescence stainings for β-catenin and the EMT related marker (E-cadherin) revealed a reduced expression of the epithelial markers E-cadherin at the cell membrane in the wild type as well as β-catenin$^{\Delta C/-}$ cell lines. In contrast, β-catenin$^{D164A/-}$ and β-catenin$^{dm/-}$ cell lines are retaining some expression of E-cadherin and β-catenin at the cell membrane. DAPI was used to visualize nuclei. Scale bar: 100 µm.

2.4.8 β-catenin N- and C- terminal coactivators contribute to the expression of specific Wnt target genes and alter the regulation of Wnt pathway components

In order to better comprehend and examine alterations in the activation of target genes as well as canonical Wnt signaling pathway components affected by the various mutant forms of β-catenin in our breast tumor cell lines, we performed RNA sequencing. This could give more insights on which canonical Wnt target genes might contribute to the observed alterations *in vivo* and *in vitro*. The cells were treated for three or four days with Wnt3a or TGFβ, respectively, to analyze the impact of the β-catenin mutant forms on canonical Wnt signaling and EMT. Thereby, we wanted to examine which canonical Wnt target genes induced by Wnt3a or TGFβ treatment are no more regulated in the mutants and which target genes are specifically regulated by the interaction with N- or C- terminal coactivators. Unsupervised hierarchical clustering of the cell lines according to the top 500 most variable genes revealed, that the cell lines cluster according to the β-catenin mutation but not according to the treatment (Fig. 6A). Moreover, comparative gene expression profiling was performed, and a selected list of direct Wnt target genes (genes with TCF binding sites in their promoter regions) was examined (taken from https://web.stanford.edu/group/nusselab/cgi-bin/wnt/target_genes) and supplemented with known Wnt target genes previously identified in the mammary gland (Fig. 6C, 6D) [140]. Furthermore, the expression of Wnt pathway components was analyzed (*Lrp 5/6, Fzd1-10, Dvl1-3, Axin1/2, Apc, Ck1α, Pp2a, Gsk3β, Ctnnb1, Bcl9/9l, Pygo1/2, Tcfs* and *Lef1* as well as Wnt ligands) (Supplementary Fig. 4A, 4B). For the TGFβ-treated cells, additionally the expression of EMT-related Wnt targets was examined (Fig. 6E). Comparison of untreated (control)

to Wnt3a-treated wild-type cells revealed the upregulation upon Wnt3a treatment of 426 and the downregulation of 1177 genes. In the mutant cell lines, less genes are differentially expressed upon Wnt3a treatment: In the β-catenin$^{D164A/-}$ cell line 306 genes were up- and 179 down-regulated, in the β-catenin$^{\Delta C/-}$ 66 and 404 genes were up- and down-regulated, respectively. In the β-catenin$^{dm/-}$ cells, however, only 33 genes were up- and 24 genes were down-regulated (Fig. 6B). Hence, the Wnt3a treatment resulted only in minor changes in the transcriptional output of the double-mutant cell line. In terms of Wnt target genes, some seemed to be regulated via the N- as well as C-terminal coactivators, since the target genes *Axin2, Tcf7* showed a diminished, but still significant upregulation in the β-catenin$^{D164A/-}$ and β-catenin$^{\Delta C/-}$ cell line. Thus, the C-terminal as well as the N-terminal coactivators seemed to contribute to their expression. However, some genes appeared to be specifically regulated by the N-terminal (*Procr*) or C-terminal coactivators (*Lbh, Notum*), since the upregulation of these genes was lost in the β-catenin$^{D164A/-}$ and β-catenin$^{\Delta C/-}$ cell lines, respectively. In terms of known Wnt target genes the β-catenin$^{dm/-}$ cells showed a significant upregulation of *Tcf7*, *Stra6* (*stimulated by retinoic acid 6*) and *Wisp1*. However, these target genes are not as strongly upregulated as in the wild-type cells. Hence, in the β-catenin$^{dm/-}$ cell line, the regulation of most canonical Wnt targets seems to be prevented (Fig. 6C). Expression changes of canonical Wnt pathway components were observed in all cell lines. Some of these are known to be Wnt target genes as well and thereby constitute possible feedback regulation of the pathway. β-catenin$^{dm/-}$ cells mainly showed a trend towards upregulation of the Wnt cell membrane receptor *Fzd2* and an upregulation of the transcription factors *Tcf7* and *Tcf7l2*. In the β-catenin$^{D164A/-}$ and the β-catenin$^{\Delta C/-}$ cells less genes were differentially regulated as compared to the wild-type cells, they either showed no regulation or only a trend in expression as the wild-type cells (Supplementary Fig. 4A). Taken together, with this approach we were able to identify candidate genes, which seem to be either regulated by N- and C-terminal or specifically by N- or C-terminal coactivators binding to β-catenin. Furthermore, abrogating the binding of coactivators to β-catenin in the β-catenin$^{dm/-}$ cell line results in the almost complete abrogation of the canonical Wnt pathway showing only minor changes in some known Wnt target genes as well as pathway components. A complete list of Wnt target genes upon Wnt3a treatment will be generated from ChIP results and thereby direct target genes lost by the specific β-catenin mutant forms will be identified.

Next, we sought to elucidate the effect of the different mutant forms during EMT upon TGFβ treatment to identify genes that are transcriptionally regulated by β-catenin. Here, also several Wnt target genes showed differential expression upon EMT induction. In this experiment, the target genes *Axin2* and *Notum* showed the completely opposite trend, a downregulation upon TGFβ treatment as compared to the increased expression upon Wnt3a treatment. Furthermore, the significant downregulation of *Notum* seemed to be ablated by the loss of binding of the N-terminal cofactor, whereas a significant regulation of *Axin2* was only observed in the wild-type cells. Interestingly, *Procr* was as well specifically regulated by the N-terminal coactivators upon TGFβ treatment, since it was only up-regulated in wild-type and in β-catenin$^{\Delta C/-}$ cells. *Vegfa* showed a significant up-regulation in the wild-type and in β-catenin$^{D164A/-}$ cells, while this was not the case for the β-catenin$^{\Delta C/-}$ and β-catenin$^{dm/-}$cell lines, suggesting a regulation mainly by C-terminal coactivators (Fig. 6D). Examining EMT-related Wnt targets revealed that E-cadherin is only significantly down-regulated in the wild-type cells, whereas mesenchymal markers like *Fn1, Vimentin, Zeb1* and *Zeb2* were up-regulated in all cell lines. Furthermore, *Snai2* expression was up-regulated in the wild-type cells, whereas it showed the opposite trend towards downregulation in the mutant cell lines (Fig. 6E). With regard to the expression of the Wnt components, many more changes were observed upon TGFβ treatment than upon Wnt3a treatment. Differential expression was observed in all cell lines, although the wild-type and β-catenin$^{dm/-}$cell lines showed the most significant differences, for cell membrane receptors *Fzds*, transcription factors *Tcf7, Tcf7l1* and *Tcf72l* and Wnt ligands which included non-canonical Wnt ligands.

These results show, that upon TGFβ treatment we see alterations in Wnt pathway components as well as in Wnt target genes. However, some genes show an opposite expression trend as upon Wnt3a treatment and hence regulation might be context-specific. Moreover, mesenchymal markers, as for example *vimentin* and *fibronectin* as well as EMT-related transcription factors show upregulated expression in both, the mutant forms and wild-type cells, yet for example *Snai2* shows a differential regulation in the mutant cell lines (Fig. 6D, 6E). In conclusion, we see many alterations in the Wnt pathway upon TGFβ treatment. Furthermore, there seems to be a context-specific up or down-regulation of certain Wnt target genes. We detect target genes that seem to be specifically regulated by either the N- or the C- terminal coactivators during EMT.

The mutant forms of β-catenin are able to alter and partially ablate the EMT response as compared to wild-type β-catenin, however, the cell lines are still able to upregulate most of the mesenchymal genes examined. To further explain the morphological differences and the alterations observed by immunofluorescent staining for EMT-related markers, (Fig. 5C, 5D), the direct Wnt target genes detected in the ongoing ChIP experiment will be analyzed which may help to understand the mechanistic role of β-catenin during EMT.

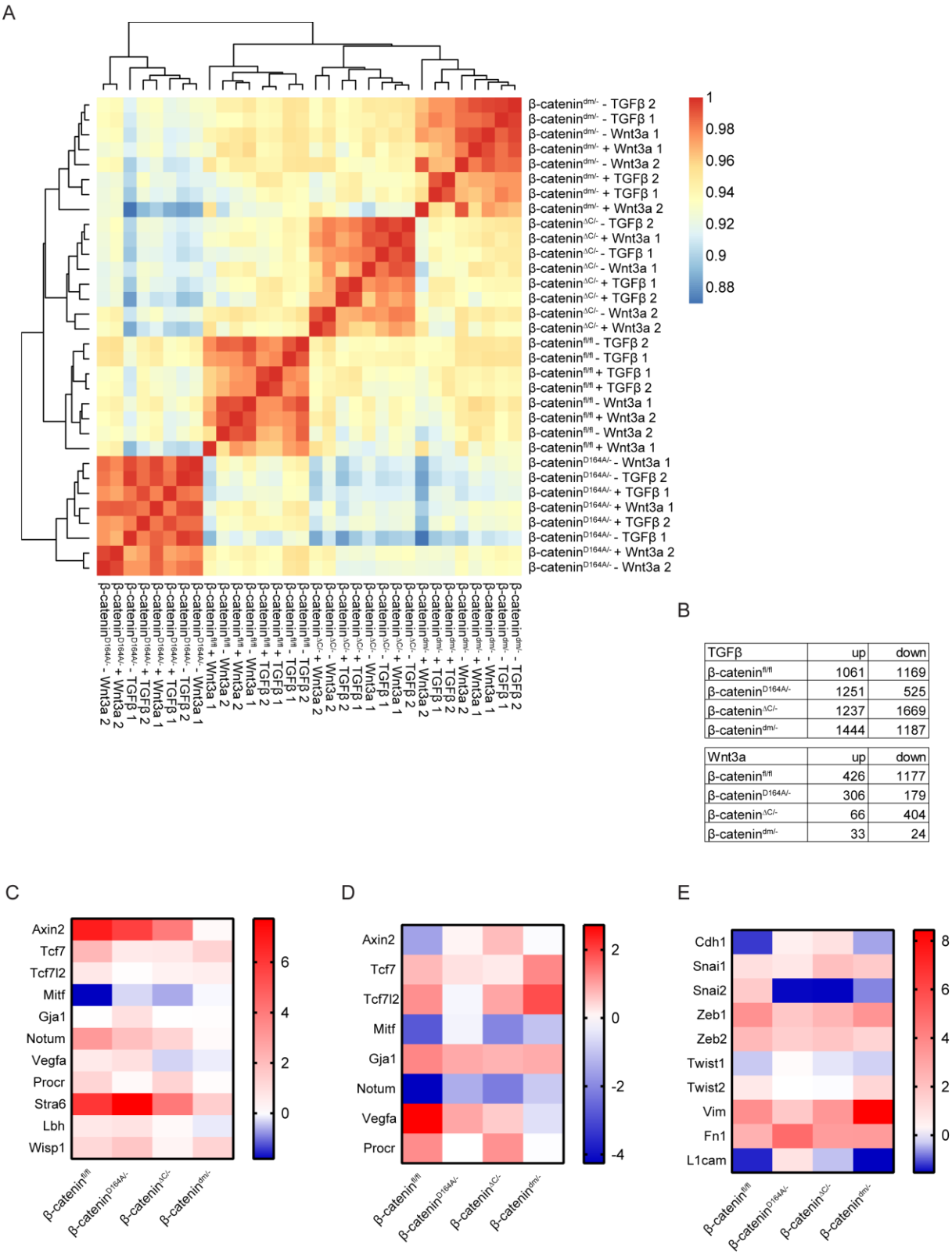

TGFβ	up	down
β-catenin$^{fl/fl}$	1061	1169
β-catenin$^{D164A/-}$	1251	525
β-catenin$^{\Delta C/-}$	1237	1669
β-catenin$^{dm/-}$	1444	1187

Wnt3a	up	down
β-catenin$^{fl/fl}$	426	1177
β-catenin$^{D164A/-}$	306	179
β-catenin$^{\Delta C/-}$	66	404
β-catenin$^{dm/-}$	33	24

Figure 6. Ablating the binding of N- and/or C- terminal coactivators to β-catenin affects the expression of specific Wnt target genes. (A) Dendrogram and heatMap for Unsupervised Hierarchical Clustering of cell lines treated with Wnt3a (+ Wnt3a) or TGFβ (+TGFβ) and their respective untreated controls (- Wnt3a, - TGFβ). Samples cluster into 4 major clusters according to their genotype. The colours indicates the correlation value. **(B)** Number of differentially expressed genes upon Wnt3a or

TGF-β treatment in the different cell lines. Red represents up-regulated expression and blue down-regulated expression. P ≤ 0.05 and fold change ≥ 1.5. **(C)** Heatmap showing the log2 fold changes of examined Wnt target genes,that are significantly differentially expressed in at least one of the cell lines upon Wnt3a treatment. **(D)** Heatmap showing the log2 fold changes of Wnt target genes and **(E)** EMT related Wnt targets examined, being significantly differentially expressed in at least one of the cell lines upon TGFβ treatment. Red represents up-regulated expression and blue down-regulated expression. P ≤ 0.05 and fold change ≥ 1.5.

2.5 Discussion

2.5.1 Effect of β-catenin knockout in mammary tumor cells

The canonical Wnt signaling pathway is often found aberrantly activated in human carcinomas. This is also true in breast cancer were aberrations in the Wnt signaling pathway have been found to correlate with poor prognosis in breast cancer patients. To provide a better understanding of β-catenin's function in breast tumor progression and metastasis formation, in this study we performed functional *in vivo* analyses in the MMTV-PyMT transgenic mouse model of metastatic breast cancer. To further characterize the functional impact of ablating the canonical Wnt signaling output, we used cell lines established from the different genotypes from our mouse model. The examination of the canonical Wnt signaling pathway has several obstacles: the pathway is important for many different mechanisms during development and shows a complexity on different levels. From the 19 Wnt ligands, several are able to activate the canonical Wnt pathway and some of which can also activate the non-canonical Wnt signaling pathways. There are also several Wnt receptors and by distinct receptor-ligand pairings can either activate the canonical or non-canonical pathway [68, 239]. Components of the destruction complex in the cytoplasm like GSK3β have regulatory roles in many other cellular processes. There are also multiple members of the TCF/LEF family which are cell context-dependent and exhibit individual specificities and, without binding of β-catenin, together with Groucho/TLE act as transcriptional repressors [75]. Hence, for all these components different spatial temporal combinations exist. β-catenin is the non-redundant component of the canonical Wnt pathway. However it also plays an important function in the E-cadherin-mediated cell adhesion complex. To be able to specifically dissect its signaling role, Valenta and colleagues have generated β-catenin mutant alleles which retain β-catenin's function in cell adhesion but alter its signaling activity [137]. We first examined the complete loss of β-catenin and its effect on tumor progression and metastasis formation in the MMTV-PyMT mouse model of metastatic breast cancer. Notably, knockout of β-catenin in the mammary epithelium by expression of MMTV-Cre did not affect tumor weight or the number of lung metastasis (Supplementary Fig. 1A). Though, IF staining of tumor sections revealed that β-catenin was still present in the β-catenin conditional knockout mice (Supplementary Fig. 1C). Furthermore, genotyping of the tumors also

demonstrated incomplete deletion which was confirmed in GFP reporter mice (Supplementary Fig. 1D, 1F). However, we found that loss of β-catenin *in vitro* as well as *in vivo* led to mammary tumor cell apoptosis (Fig. 1A, 1B, 1C, Supplementary Fig. 1E). Similar observations have been made in mouse embryonic stem cells where β-catenin loss also lead to increased cell death [228]. Also in head and neck squamous cell carcinomas (HNSCC) and lung cancer cell lines, β-catenin silencing has been found to induce cell death [229, 230]. Hence knockout of β-catenin and with this the loss of its signaling as well as its adhesion function leads to apoptosis.

2.5.2 Wnt signaling in mammary tumor growth, tumor progression and metastasis formation

Ablation of the binding of BCL9/9L resulted in smaller tumors due to less proliferation, less metastasis, a lower metastasis index and a delay in tumor progression (Fig. 2B, 2C, 2D). BCL9 knockdown has been found to result in reduced tumor load and decreased number of metastases in xenograft mouse models using myeloma and colon cancer cell lines [151]. Hence the binding of BCL9/9L seems to be important for MMTV-PyMT tumor growth and metastasis formation. Abrogating the binding of the plethora of cofactors to the C-terminus of β-catenin also resulted in decreased tumor weights due to a decrease in proliferation, but had no effect on tumor progression or metastasis formation (Fig. 3A, 3B, 3C). Inhibition of the binding of CREB to β-catenin has also previously been found to inhibit proliferation in lung cancer cell lines [230]. Together, these results show that ablation of the binding of N- or C- terminal coactivators to β-catenin affects tumor growth and tumor progression differentially. The question remains whether the cofactors enhance the β-catenin transcriptional output in a selective fashion by affecting specific target genes or just by a general enhancement of the output. The complete abrogation of the canonical Wnt activity using the dm mutant form of β-catenin showed an effect on tumor weight, tumor progression, on metastasis formation as well as on the metastasis index (Fig. 4A, 4C). In the dm mutant mice, the tumor weight seemed to be affected again by a decrease in proliferation but a slight increase in the amount of apoptotic cells was observed as well (Fig. 4B, Supplementary Fig. 2C). In conclusion, all the mutant forms of β-catenin have an effect on tumor proliferation whereas only by abrogating the binding of

BCL9/9L in the D164A and the dm mutant have an effect on tumor progression and metastasis formation. Furthermore, all mutant versions of β-catenin exert a dominant-negative effect, this notion has been observed *in vivo* and was then tested *in vitro* (Fig. 2B, 3A, 4A, Supplementary Fig. 2D). By following analyses of the heterozygous cell lines (mutant β-catenin/floxed), which have been included in the RNA sequencing experiment as well, it can be further examined on how the dominant negative effect alters the activation of the canonical Wnt pathway.

2.5.3 The contribution of N- and C-terminal coactivators of β-catenin to Wnt signalig activity and EMT

Further *in vitro* analysis were performed by establishing cell lines from the different tumor genotypes to examine the mechanisms affected in more detail. Examination of the growth of the different cell lines showed a reduced growth of the mutant cell lines compared to a wild-type cell lines (Fig. 5A). This confirmed the results observed *in vivo* that all the β-catenin mutant forms show a proliferation phenotype. Canonical Wnt signaling is known to be able to affect proliferation on different levels: among the targets genes of the canonical Wnt pathway are *Cyclin-D1* and *c-Myc* which contribute to cell cycle progression, furthermore it has been found that specific kinases during G2/M phase can phosphorylate LRP6 to prime the pathway [231-233]. Moreover, it has been found that Wnt signaling not only stabilizes β-catenin but also many other proteins which are found to contain GSK3 phosphorylation sites triggering degradation. Thereby, Wnt signaling can inhibit GSK3 and stabilize other proteins, a mechanism termed Wnt-dependent stabilization of proteins (Wnt/STOP) [234]. β-catenin expression itself varies during the cell cycle. The cytoplasmic and nuclear fraction increase in S phase and peak at G2/M phase while decreasing as the cells re-enter G1. Additionally β-catenin has been found being involved in centrosome regulation and the formation of a bipolar mitotic spindle [235, 236]. Further analysis of the RNA sequencing might reveal which of the functions of the canonical Wnt signaling during mitosis are affected by the β-catenin mutations. Subsequently we wanted to examine how strong the β-catenin mutations affected the canonical Wnt signaling output. A Wnt reporter assay revealed a reduced response to Wnt3a in the D164A and the ΔC mutant cell lines as compared to the wild type cells. The double-mutant (dm) form completely

blocked the transcriptional β-catenin signaling output (Fig. 5B). These observations confirm the results of Valenta and collegues where similar observations have been reported in mouse embryonic fibroblasts (MEFs). In their study they have shown, that in mice the output of the canonical Wnt signaling seems to be more dependent on the presence of the C-terminus than on the binding of BCL9/9L to β-catenin. Also in our cell lines, the ΔC mutation shows a stronger effect. Hence the individual contribution of the N- and C-terminal coactivators to the signalling output seems to differ. In the experiment presented by Valenta and collegues, the double mutation has also completely abrogated canonical Wnt signaling activity [137].

Epithelial-to-Mesenchymal transition (EMT) is a process that plays an important role during embryonic development and is thought to contribute to tumor progression and metastasis formation. Since in our *in vivo* experiments we detected reduced metastasis formation in D164A and dm mutant mice, we proceeded to examine the effect of the β-catenin mutations on EMT *in vitro* which thereby might account for the reduction in metastasis observed *in vivo*. To test this notion, the different cell lines were treated for 4d with TGFβ which is a potent EMT inducing cytokine and several studies have already shown a cross-talk between the TGFβ and Wnt signaling pathways [240-242]. The β-catenin wild-type cell lines became more mesenchymal upon TGFβ treatment and the same was true for the β-catenin$^{\Delta C/-}$ cell line. The morphology of the β-catenin$^{D164A/-}$ cells became more elongated as well, but they still grew as a cell cluster whereas the β-catenin$^{dm/-}$ cell line only seem to form filopodia (Fig. 5C). Those results were confirmed by IF staining for EMT markers showing that the β-catenin$^{D164A/-}$ and β-catenin$^{dm/-}$ cell lines retained the expression of epithelial markers (E-cadherin, ZO-1) (Fig. 5D, Supplementary Fig. 3D). Also long-term treatment (20d) did not further alter the morphology of the cells showing that there is not only a delay but really an ablation of the EMT response due to the loss of the binding of BCL9/9L in the D164A and dm cell lines (Supplementary Fig. 3C). These results correlate with our observations *in vivo*, where we see an effect on metastasis formation in the D164A and dm mice, whereas the ΔC mutation does not seem to have an effect. This findings are in line with a previous study which has shown that *Bcl9* knockdown in myeloma and colon carcinoma cell lines modulated the expression of EMT markers and also reduced their proliferation. Furthermore, it has been demonstrated that *Bcl9* overexpression increased migration of a myeloma cell line, whereas the knockdown reduced the migratory capacity [161]. In conclusion, these results show that especially the binding

of BCL9/9L to β-catenin or the target genes affected by it promote tumor growth and progression as well as metastasis formation and, hence, these target genes may constitute interesting interference points for treatment. On the other hand the β-catenin knockout and hence loss of its adhesion and signaling function affects cell survival *in vitro* as well as *in vivo*. The cell lines expressing the different β-catenin mutant forms however, are able to survive, show an abrogated Wnt signalling output but are still able to bind to E-cadherin (Fig. 5B, Supplementary Fig. 3E). The double-mutant shown to block the transcriptional signalling output indicates that the critical role in cell survival is not the signaling function itself but rather its function in cell adhesion or the loss of both functions combined.

2.5.4 Wnt target genes and pathway components affected by ablation of coactivator binding to β-catenin

To further examine alterations in the expression of target genes after activation of canonical Wnt3a treatment or during EMT, ChIP sequencing and RNA sequencing was performed using the established cell lines expressing wild type β-catenin or its various mutant alleles after treatment with Wnt3a or TGFβ. Unsupervised hierarchical clustering of the cell lines according to the top 500 most variable genes revealed, that the cell lines cluster according to the β-catenin mutation but not according to the treatment (Fig. 6A). This shows that the mutations themselves have a hierarchical higher effect than the treatments. In order to better comprehend and examine the corresponding alterations in the canonical Wnt pathway upon Wnt3a or TGFβ treatment, a preliminary analysis involved the examination of known canonical Wnt targets, canonical Wnt pathway components and Wnt ligands. In the mutant cell lines, especially in the β-catenin$^{dm/-}$ cells, the number of differentially expressed genes upon Wnt3a treatment was dramatically reduced as compared to wild-type cells (Fig. 6B). This confirms the observations made in the luciferase reporter assay, that the β-catenin$^{D164A/-}$ and the β-catenin$^{\Delta C/-}$ cell lines have a reduced response to Wnt3a treatment and that the double-mutant (dm) form blocks the transcriptional β-catenin signaling output (Fig. 5B).

By Wnt3a-mediated induction of the canonical Wnt pathway, some Wnt targets genes seem to be regulated specifically by either N- or C-terminal coactivators (Fig. 6C). This

is consistent with the observations *in vivo* and *in vitro* that specific ablation of N- or C-terminal coactivators can lead to different phenotypes. Additionally, there are some target genes like *Axin2* and *Stra6* where the N- and C-terminal coactivators of β-catenin conjointly contribute to their expression. STRA6 is a cell membrane receptor for retinol-binding protein (RBP) and is able to further activate the JAK/STAT signaling cascade. It has been found to be upregulated in human breast and colon cancer and, together with RBP, it seems to affect proliferation and promote oncogenic properties like migration, invasion and colony formation [243]. Its expression has been reported to be regulated synergistically by Wnt1 and retinoic acid [244]. Among the genes found to be regulated by the C-terminal coactivators are *Notum* and *Lbh*. The transcription cofactor LBH has been found to be deregulated in aggressive human basal breast cancer and to affect differentiation [192]. Notum deacylates Wnt proteins and thereby inhibits the signaling activity and hence acts as a negative feedback loop. In colorectal cancer cell lines, knockdown of *Notum* has been found to inhibit proliferation as well as migration. On the other hand, *Procr* seems to be specifically regulated by the binding of BCL9/9L to β-catenin. This gene is thought to be a stem cell marker and has been found to stimulate several signaling pathways like ERK, PI3K–Akt, and RhoA. Furthermore, its expression is associated with distant metastasis and also cell proliferation [245, 246]. Since the abrogation of the binding of BCL9/9L results in a proliferation phenotype *in vivo* and *in vitro* as well reduces the amount of lung metastasis, PROCR seems to be one of the downstream effectors contributing to these phenotypes. Also in mouse intestinal tumors, a subset of Wnt target genes has been found to be downregulated in $Bcl9^{-/-}$/$Bcl9l^{-/-}$ tumors as compared to wild-type tumors, suggesting an important role for BCL9/9L in regulating canonical Wnt target genes also in other tumor mouse models [162]. In conclusion, our results show that the single mutants retain transcriptional activity affecting specific genes, whereas with the double mutation the regulation of almost all target genes is lost. The upregulation of *Tcf7* and *Stra6* in the β-catenin$^{dm/-}$ cells might also be mediated via other mechanisms. Interestingly, the well-known Wnt target genes *cyclin D1* and *c-Myc* are not regulated in all cell lines upon Wnt3a treatment. However, it is known that they are regulated as well by other pathways [191, 247]. To be able to generate a list of β-catenin target genes in our model and to determine which of those target genes are affected by the different mutations, β-catenin ChIP sequencing was performed. The analysis of this data is still ongoing and the results will then be compared and placed into context with

the RNA sequencing results. So far, the results suggest that the N- and C-terminal coactivators contribute in critical ways to the Wnt signaling output and affect some specific target genes. Also, different alterations in the pathway components in the mutant cell lines as compared to the wild type cell line have been observed. The exclusive upregulation of *Tcf7* and *Fzd1/2* in the β-catenin$^{dm/-}$ could reflect a compensatory effect of the cells trying to maintain/restore canonical Wnt output. Compared to wild-type cell lines, in the β-catenin$^{D164A/-}$ and β-catenin$^{\Delta C/-}$ less pathway components are differentially expressed suggesting a deregulation of the feedback control due to a reduction in activity/output of the pathway (Supplementary Fig. 4A). Feedback loops permit better control of signal amplitude or duration. The extent of those alterations will be determined by first analysing the effect on the canonical Wnt signaling output by identifying the direct target genes using ChIP.

The examination of genes that are transcriptionally regulated by canonical Wnt signaling during the process of EMT showed that many more genes are up- or down-regulated in all cell lines examined as compared to the Wnt3a treatment (Fig. 6B). Also, Wnt target genes are differentially expressed suggesting regulation of those during EMT. The *Gap junction protein alpha 1* (*Gja1*) gene encodes for Connexin43, being important for gap junctions which facilitate cell-cell communication. Its function is still debated, as it has been suggested to act as a tumor suppressor as well as in promoting tumor progression [248]. It is thought to be a direct Wnt target gene but was found to be upregulated upon TGFβ treatment in all cell lines, also in the β-catenin$^{dm/-}$ cell line, suggesting a canonical Wnt-independent upregulation [249]. In wild-type cells, *Axin2* and *Notum* were downregulated upon TGFβ treatment, whereas they were upregulated upon Wnt3a treatment. This suggests a context-specific up- or down-regulation of Wnt target genes. Furthermore, the upregulation of *Notum* via Wnt3a treatment seems to be regulated via C-terminal coactivators, however upon TGFβ treatment the down-regulation of *Notum* seems to be dependent on N-terminal coactivators of β-catenin. Hence the regulation of target genes via N- or C- terminal coactivators might also be context-dependent or also regulated via other mechanisms (Fig. 6D). Furthermore, some EMT-related transcription factors and mesenchymal markers that have been shown to be regulated by canonical Wnt signaling were upregulated in all cell lines upon TGFβ treatment (Fig. 6E) [75, 250]. These results are in line with the results of the IF staining showing that all mutant cell lines are still able to upregulate mesenchymal markers and are able to undergo at least a partial EMT

(Fig. 5D). *Snai2* however, was only upregulated in the wild-type cells showing an opposite trend towards down-regulation in the mutant cell lines. Additionally, *E-cadherin* was only downregulated in the wild type cells even though immunofluorescence staining suggested a downregulation in the β-catenin$^{\Delta C/-}$ cells as well. Nevertheless, not only the expression levels but also the localization of EMT markers like E-cadherin has to be considered. The expression of further epithelial markers might reveal differences observed between the cell lines during EMT. The observation that binding of BCL9/9L might be important for EMT has also been found by Deka and colleagues showing that some EMT-inducing transcription factors were downregulated in Bcl9$^{-/-}$/Bcl9l$^{-/-}$ colon tumors as compared to wild-type tumors [162]. TGFβ also induced changes in the expression of Wnt pathways components, i.e. mainly the expression of Wnt ligands, transcription factors (*Tcf7, Tcf7l1, Tcf7l2* and *Lef1*), and *Fzds* was affected (Supplementary Fig. 4B). Also, non-canonical Wnt ligands were upregulated suggesting an activation of the non-canonical Wnt signaling pathways. Since several of the canonical Wnt target genes are also canonical Wnt pathway components, altering the transcriptional output is also having an effect on the expression of the pathway components, as observed [77, 89-93]. Several studies already have shown the interaction of Wnt and TGFβ signaling, however, which Wnt target genes are affected and what role canonical Wnt signaling plays in EMT and metastasis formation will have to be further examined [208, 251, 252]. Especially target genes affected by abrogating the binding of BCL9/9L to β-catenin will be interesting candidates for further examination, since they seem to contribute to alterations in EMT and reduced metastasis formation.

In ongoing studies, gene set enrichment analysis (GSEA) will be performed to identify significantly enriched gene sets comparing the different cell lines upon Wnt3a and TGFβ treatment most related to the observed effects. Moreover, Integrated System for Motif Activity Response Analysis (ISMARA) will be performed to identify the motifs that are enriched in specific mutant cell lines. A list of canonical Wnt target genes will be generated from ChIP sequencing results to detect target genes which are no more regulated by the different β-catenin mutant forms and will be compared to the RNA sequencing results. This allows the detection of interesting target genes which contribute to the observed phenotypes of reduced tumor growth or effects on metastasis formation and can be examined in patient data available.

In this study we show that abrogating the binding of N- and/or C-terminal β-catenin coactivators without affecting β-catenin's function in cell adhesion, affects tumor growth *in vivo*, proliferation *in vitro* and alters the transcriptional output. Whereas, the complete loss of β-catenin's signaling and adhesion function leads to apoptosis in mammary tumor cells *in vitro* and *in vivo*, suggesting a key role of its adhesion function in cell survival. Furthermore, the observations indicate that the inability of β-catenin to bind BCL9/9L are critical for a subset of Wnt target genes involved in EMT. Canonical Wnt target genes examined so far seem to be either dependent on both, the N- and C-terminal coactivators or specifically dependent on one of those. Nevertheless, the double mutation shows the strongest effects suggesting that coactivators binding to both transactivation domains contribute to the transcriptional output and ablating their binding inhibits the transcriptional output.

2.6 Material and Methods

Antibodies and Reagents

Antibodies:

E-cadherin Monoclonal Antibody (ECCD-2)

(13-1900, Thermo Fisher Scientific, used for immunofluorescence stainings), E-cadherin (610182, Transduction Laboratories, used for immunoblotting), Monoclonal Anti-α-Tubulin antibody mouse (T-9026, Sigma-Aldrich), anti-Fibronectin rabbit (F3648 Sigma-Aldrich), Vimentin (NB300-223, Novus Biologicals), ZO-1 (617300, Thermo Fisher Scientific), Alexa Fluor™ 568 Phalloidin (A12380; Invitrogen), β-catenin (06-734, Cell Signaling Technology, used for immunofluorescent stainings), β-catenin (NBP-32239, Novus Biologicals, used for IP and ChIP), Caspase-3 (Asp 175) (5A1E) (9664, Cell Signaling Technology), Anti-phospho-Histone H3 (Ser10) (06-570, Merck) , Myc-Tag (9B11) Mouse mAb (2276, Cell Signaling Technology), 4′,6-diamidino-2-phenylindole (DAPI, D9542, Sigma-Aldrich).

Reagents:

Recombinant Murine Wnt-3a (315-20, PeproTech), Recombinant Human TGF-beta 1 Protein (240-B, R&D Systems).

Mouse experiments

Mouse colonies were kept at the animal facility of the Department of Biomedicine, University of Basel, Switzerland. All animal experiments were carried out in accordance with the guidelines of the Swiss Federal Veterinary Office (SFVO) and the Cantonal Veterinary Office of Basel-Stadt. To examine conditional knockout of β-catenin in breast cancer, β-catenin$^{fl/wt}$ mice (a kind gift of Konrad Basler, UZH, Zürich, Switzerland) were crossed with MMTV-PyMT (a kind gift of N. Hynes, FMI, Basel, Switzerland) [236, 238] and MMTV-Cre (a kind gift of Lothar Hennighausen, NHI, Bethesda, USA) mice [253]. β-catenin$^{fl/fl}$; MMTV-PyMT, and MMTV-Cre mice obtained were then crossed with the β-catenin knock-in mutant mouse strains (β-catenin$^{D164A/wt}$, β-catenin$^{\Delta C/wt}$ and β-catenin$^{dm/wt}$ lines) (kindly provided by Konrad Basler, backcrossing was performed using speed congenics by Taconic, New York, USA). In the experiments, mice were compared to their littermate controls. To monitor MMTV-Cre mediated recombination, β-catenin$^{fl/fl}$; MPY, MMTV-Cre mice were crossed with GFP-reporter mice (R26-LSL-GFP, kindly provided by Verdon Taylor, DBM, Basel,

Switzerland). Before, the reporter mice were crossed ten generations into the FVB/N background and then used for the experiments. For the quantification of the recombination, the whole tumor section was imaged with a Zeiss Axio Imager Scanning Microscope (10x magnification). The GFP positive area and total tumor area (DAPI positive area) was determined using ImageJ. All experiments were performed on female mice. For analysis of the mammary gland, mice were sacrificed at 5 weeks or 12 weeks of age, before a tumor volume of 1500mm^3 was reached, usually at 12-13 weeks of age.

Tissue histology

For tissue histology, tissues (mammary tumors and lungs) were fixed in 4 % paraformaldehyde overnight at 4 °C followed by ethanol/xylene dehydration and subsequent embedding in paraffin. Paraffin-embedded samples were cut at 5 µm thickness and subjected to Hematoxylin and Eosin (H&E) staining. To determine lung metastases, 9 slides per organ spaced 50 µm were stained with H&E and the number of lung metastases was counted under the microscope with a 10x magnification.

Immonofluorescence on tumor sections

Tumors were fixed at 4 °C in 4 % paraformaldehyde for 2 h followed by cryopreservation overnight in 20 % sucrose/PBS prior to embedding in OCT-Compound freezing medium. The cryosections were cut at 7 µm thickness and air-dried for 15 min prior to rehydration in PBS. Tissue sections were permeabilized with 0.2 % TritonX-100/PBS and blocked for 30 min in 5 % normal goat serum/PBS followed by incubation with the indicated primary antibodies with the appropriate dilution in blocking buffer overnight at 4°C. The next day sections were incubated with fluorophore-coupled secondary antibody (Alexa Fluor, Invitrogen) for 1 h at room temperature in the dark. The cell nuclei were counterstained with DAPI (D5942, Sigma-Aldrich). After staining, the coverslips were mounted in Fluorescence Mounting Medium (S302380-2, Dako) on microscope slides and imaged using a fluorescence microscope (Leica DMI 4000) using 20x magnification.

Cell line derivation

Cells were isolated from breast tumors (mammary gland 2/3) of twelve-week-old MMTV-PyMT transgenic female mice (FVB/N background). A small piece of the tumor was minced and 10 ml of predigestion buffer (10 mM Hepes pH 7.4, 142 mM NaCl, 0.67 mM KCl, 1mM EDTA supplemented with with 50 g/ml gentamycin (Sigma, G1397) and 1X antibiotic-antimycotic (15240062, Thermo Fisher Scientific) were added and incubated for 30 min at 37˚C on a shaker. After washing with PBS the samples were digested using 6 ml digestion buffer (10 mM Hepes pH 7.4, 142 mM NaCl, 0.67 mM KCl, 0.67 mM $CaCl_2$, 20 mM Glucose supplemented with 1 mg/ml Collagenase D (Roche, 11088858001), 50 g/ml gentamycin (Sigma-Aldrich, G1397) and 1x antibiotic-antimycotic (15240062, Thermo Fisher Scientific) and incubated for 30 min at 37°C on a shaker. Subsequently the samples were washed with PBS and then resuspended in growth medium and plated into 10 cm plates. The medium was changed regularly and fibroblasts in culture were removed by differential trypsinization until only epithelial cells remained. The different cell lines were thereof cultured in DMEM supplemented with glutamine, penicillin, streptomycin, and 10% FBS (F7524, Sigma Aldrich). To establish cell lines only expressing the mutant alleles, the established cell lines were seeded into 10 cm plate and on the next day infected either with the Adeno-CRE-IRES-GFP or as a control with the Adeno-IRES-GFP virus using the FuGENE® HD Transfection Reagent (E2311, Promega). On the next day, the medium was changed and after 3 days the cells were sorted for GFP positive cells into 24 well plates using BD FACSAria Flow Cytometer (BD Biosciences). Detachment of the cells was performed using trypsinization followed by two-times washing in 1x PBS and resuspension in 2 % FBS, PBS and syringe filtering (40 µm mesh filter) immediately before FACS sorting into a polystyrene round bottom tube (352054, FALCON) filled with DMEM medium. After centrifugation, the supernatant was discarded and the cells were resuspended and seeded into a 24 well plate. Genotyping by PCR was performed to confirm the removal of the floxed allele. PCR products were run on an agarose gel.

Adenovirus infection

Cells were plated onto 6 cm dishes in duplicates and transfected on the next day with the Adeno-CRE-IRES-GFP or as a control with the Adeno-IRES-GFP virus (1710 and

1761, Vector Biolabs) using Fugene HD transfection reagent (E2311, Promega). The following day, the medium was changed.

Genotyping

To extract genomic DNA, cells from a confluent 10 cm petri dish were trypsinized, washed in PBS and pelleted by centrifugation. The DNA extraction was performed using the GenElute™ Mammalian Genomic DNA Miniprep Kits (G1N70, Sigma-Aldrich) according to the manufacturer's protocol. Standard PCR procedure was then performed. To detect the β-catenin floxed and mutant allele, sense primer RM41 (5- AAG GTA GAG TGA TGA AAG TTG TT -3) and antisense primer RM42 (5- CAC CAT GTC CTC TGT CTA TTC -3) were used, generating 324 bp and 221 bp products from the floxed and mutant alleles, respectively. To detect the deletion of the floxed allele, sense primer RM68 (5- AAT CAC AGG GAC TTC CAT ACC AG -3) and antisense primer RM69 (5- GCC CAG CCT TAG CCC AAC T -3), were used generating a 631 bp product from the deleted allele. [254]

Cell culture

The established cell lines from the different mouse genotypes and the Py2T cells (Waldmeier et al. 2012) were cultured in Dulbecco's modified Eagle's medium (DMEM) (D5671, Sigma-Aldrich) supplemented with 10% Fetal Bovine Serum (FBS 10 % (F7524, Sigma-Aldrich), 2 mM L-Glutamine solution (G7513, Sigma-Aldrich), 100 U penicillin and 0.1 mg/ml streptomycin (P4333, Sigma-Aldrich). All cell lines were grown at 37°C, 5% CO_2, 95% humidity. To activate Wnt/β-catenin mediated transcription, cells were treated with 100 ng/ml Recombinant Murine Wnt3a (315-20, PeproTech) for the indicated time-points. For EMT experiments, cells were treated with 2 ng/ml Recombinant Human TGF-beta 1 Protein (TGFβ) for the time-points indicated every 2^{nd} day.

Transfection with rescue constructs

The retroviral constructs used were kindly provided by Tomas Valenta (University of Zürich, Switzerland). A cDNA encoding EGFP was subcloned from pEGFP-N3 (Clontech) into the retroviral vector pBabe-puro (as described in Jay P.Morgenstern and Hartmut Land, 1990). 4 µg plasmid were used o transfection. Transient

transfection was performed was performed with Lipofectamine 3000 Reagent (L3000-015, Invitrogen) according to the manufacturer's instructions. Medium was changed the day after transfection.

Luciferase reporter assay

To assess Wnt/β-catenin mediated transcription, the firefly luciferase reporter superTOPflash/ superFOPflash (kindly provided by Konrad Basler, UZH Zürich) was used. Cells were plated in duplicates in 24-well plates and transfected the following day with 500 ng of the reporter plasmid reporter and 10 ng of plasmids encoding Renilla luciferase encoding plasmid using Lipofectamine 3000 Reagent (Invitrogen) according to the manufacturer's instructions. The luciferase activity was measured by using the Dual-Luciferase® Reporter Assay System (E1960, Promega). The measured firefly luciferase values were normalized to the Renilla luciferase control values.

Cell IQ

To measure the growth curves and doubling times the cells were seeded into 12 well plates in duplicates. On the next day the medium was changed and the cells were put into the Cell IQ (Model v.2) for 3 days. For the analysis the Cell IQ analysis software was used.

Immunofluorescence of cultured cells

Cells were grown on uncovered glass coverslips (#1, 12 mm round, Menzel–Glaser) and treated for 3 days with Wnt3a or 4 days with TGFβ. Following the cells were washed with PBS and then fixed with 4% paraformaldehyde/PBS for 15 min at room temperature, followed by permeabilization with 0.2 % TritonX-100/PBS for 5 min. Subsequent blocking was performed with 3 % BSA/0.01 % Triton X-100/PBS for 1 h. The indicated primary antibodies were then added in the appropriate dilution with 3 % BSA/ 0.2 % PBS-T for 2 h at room temperature. Afterwards incubation with a fluorophore-coupled secondary antibody (Alexa Fluor, Invitrogen) was performed for 1 h at room temperature in the dark. Cell nuclei were counterstained with DAPI (D5942, Sigma-Aldrich). After staining, the coverslips were mounted in Fluorescence Mounting Medium (S302380-2, Dako) on microscope slides and imaged using a fluorescence microscope (Leica DMI 4000) using a 20x magnification .

Immunoblotting

The cells were lysed in RIPA buffer (R0278, Sigma-Aldrich) supplemented with 1 mM DTT, 1 mM NaF, 2 mM sodium orthovanadate and 1x protease inhibitor cocktail (Sigma-Aldrich) for 30 min on ice followed by scraping into tubes and centrifugation for 10 min at 10,000 rpm at 4 °C. The supernatant was saved and the protein concentration was determined using the Bio-Rad Bradford solution according to the manufacturer's instructions. Equal amounts were prepared, diluted in loading buffer (10 % glycerol, 2 % SDS, 65 mM Tris, 0.01 mg/ml Bromphenolblue, 1% beta-mercaptoethanol) and loaded onto a SDS polyacrylamide gel. Proteins were then transferred onto a nitrocellulose membrane (10600002, Sigma-Aldrich) by wet transfer for 2 h at constant current (0.33 A). Following blocking for 1 h in 5% milk prepared in TBS/0.05 % Tween 20, the membranes were incubated with the indicated primary antibodies overnight at 4 °C. On the next day, the membranes were washed and the blots were incubated with HRP-conjugated secondary antibodies (Jackson Immunoresearch Laboratories and donkey anti goat IgG-HRP, sc-2020, Santa Cruz) for 1 h at room temperature and developed with Immobilon Western Chemiluminescent HRP Substrate (WBKLS0500, Millipore) with a Fusion Fx7 chemoluminescence reader.

Co- Immunoprecipitation

β-catenin$^{fl/fl}$, β-catenin$^{D164A/-}$, β-catenin$^{\Delta C/-}$ and β-catenin$^{dm/-}$ grown in a 15 cm plate were washed with cold PBS, then scraped off in 300 µl IP lysis buffer (20mM Tris pH 7.5, 10 mM NaCl, 10 % glycerol, 1 % NP-40, 2 mM EDTA, 1x PIC (protein inhibitor cocktail)) and collected in an Eppendorf tube. Incubation was performed at 4 °C rotating for 20 min. Subsequently samples were centrifuged at 4 °C (10 min, 16'000 g) and the supernatant was transferred to a new tube. Protein concentration was measured using the Bio-Rad Bradford solution according to the manufacturer's instructions. An input sample was taken and frozen. Per IP, 5 µg anibody or IgG as a control were diluted in 200 µl PBS/0.02 % Tween-20 (PBS-T). Per IP 40 µl DynaMagnetic Beads were prepared by washing 2 two times with 500 µl PBS-T. The beads were collected using a magnetic stand the antibody dilution was added and torated for 15 min at room temperature. The liquid was aspirated on the magnetic stand and the lysate (1 mg) was added and incubated overnight at 4 °C while rotating. The next day, the beads were washed three times with 500 µl IP wash buffer (15mM Tris-

HCl pH 7.8, 100 mM NaCl, 1x PIC). Following beads were diluted in 40 µl 1x SDS-PAGE sample buffer and boiled or 5 min. Empty beads were collected and the supernatant was loaded on an SDS-Gel. Samples were analyzed by SDS-PAGE.

RNA sequencing and analysis

The established cell lines (β-catenin$^{fl/fl}$, β-catenin$^{D164A/fl,}$ β-catenin$^{D164A/-}$, β-catenin$^{\Delta C/fl}$, β-catenin$^{\Delta C/-}$, β-catenin$^{dm/fl}$, β-catenin$^{dm/-}$) were treated either with 100 ng/ml Wnt3a for 2 days or with 2 ng/ml TGFβ for 4 days. Untreated cells served as control. Biological duplicates were prepared for RNA-Sequencing. Total RNA was isolated from the samples using the miRNeasy Mini Kit (Qiagen, 217004) with on-column DNAse digestion according to the manufacturer's instructions. RNA quality control was performed using RNA ScreenTape on the Agilent 4200 TapeStation and the concentration was measured by using the Quanti-iT RiboGreen RNA assay Kit (Life Technologies). RNA-sequencing libraries were prepared from total RNA using poly(A) enrichment with the TruSeq stranded mRNA Sample prep from Illumina using 200 ng input RNA. QC was performed with a fragment analyzer using DNF-473-33-SS NGS Fragment 1-6000bp kit. The RNA-sequence libraries were sequenced on a NextSeq 500 using 75 cycles kit High Output (Illumina). Obtained single-end RNA-seq reads were mapped to the mouse genome assembly, version mm10, with RNA-STAR (PMID:23104886), with default parameters except for allowing only unique hits to genome (outFilterMultimapNmax=1) and filtering reads without evidence in spliced junction table (outFilterType="BySJout"). Using RefSeq mRNA coordinates from UCSC (genome.ucsc.edu, downloaded in December 2015) and the qCount function from QuasR package (version 3.12.1) (PMID:25417205) we quantified gene expression as the number of reads that started within any annotated exon of a gene. The differentially expressed genes were identified using the edgeR package (version 1.10.1) (PMID:19910308). Genes with fdr ≤ 0.05 and minimum log2 fold change of +/- 1.0 were considered statistically significant and used these genes for downstream functional analysis.

Functional enrichment analysis

Functional enrichment analysis of differentially expressed genes for biological processes for pathways was performed in R using several publically available

Bioconductor resources including GO.db (version 3.4.1), GOstats (version 2.42.0) (PMID: 17098774), KEGG.db (version 3.2.3) and ReactomePA (version 1.20.2) (PMID: 26661513). The significance of each biological processes or pathways identified was calculated using the hypergeometric test (equivalent to Fisher's exact test) and those with p values ≤0.05 were considered significant.

ChIP

ChIP was performed using an adapted protocol [255]. For the ChIP experiments the established cell lines (β-catenin$^{fl/fl}$, β-catenin$^{D164A/-}$, β-catenin$^{\Delta C/-}$, β-catenin$^{dm/-}$) were seeded into 1 cm plates and treated with 100 ng/ml Wnt3a for 2 days. Untreated cells served as control. Samples were washed with PBS, following PBS was added and crosslinking was performed by addition of 2 mM Ethylene glycol bis (21565, Thermo Fisher) for 30 min at room temperature. After 20 min 4 % formaldehyde (28908, Thermo Fisher) was added for the remaining 10 min. The reaction was quenched using 125 mM Glycin (in DMSO) and incubated for 10 min at 4 ˚C. The cells were rinsed three times with on with pre-cooled PBS, the cells were scraped off and collected. After centrifugation for 5 min at 600 g (4˚C) the supernatant was discarded and the pellet snap-frozen in liquid-nitrogen. For further processing the samples were thawed on ice and resuspended in ChIP lysis buffer I (10 mM HEPES pH 6.5, 10 mM EDTA, 0.5 mM EGTA, 0.25% Triton X-100, 1x PIC) and incubated for 5min on ice. After centrifugation (5 min at 600 g (4˚C)) the pellets were resuspended in ChIP lysis buffer II (10 mM HEPES pH 6.5, 10 mM EDTA, 0.5 mM EGTA, 200 mM NaCl, 1x PIC) and incubated for 5 min. This washing step was repeated a second time. Then the pellet was lysed by resuspending in 400 µl Chip lysis buffer III (50 mM Tris-HCl pH 8.0, 1 mM EDTA, 0.5% Triton X-100, 0.5 % SDS, 1x PIC)and incubation for 10 min on ice. 300 µl aliquots of 400 ng/µl chromatin in lysis buffer III were then sonicated using the Bioruptor sonicator dianode). Samples were centrifuged at 14'000 g for 10 min at 4 ˚C and the supernatant was saved. Proper fractionation was tested by loading samples on an agarose gel. Subsequently, 100 µg chromatin were diluted in 200 µl Dilution buffer 16.7 mM Tris-HCl pH 8.0, 1.2 mM EDTA, 167 mM NaCl, 1.1% Triton X-100, 0.01 % SDS, 1x PIC)and lysis buffer III was added total of 600 µl. 6 µl were saved and frozen as input samples. 2 µg antibody or IgG control were added and incubated o.n. at 4 °C overhead shaking. On the same day the DynaMagnetic Beads (10003D, Thermo Fisher Scientific) were washed twice with 1 ml TE buffer (10 mM Tris-HCL pH 8.0, 1

mM EDTA). Thereafter, the beads were resuspended in 1 ml TE buffer and 100 µl BSA (10 mg/ml) and 50 µl tRNA (10 mg/ml, AM7119, Invitrogen) or preblocking, were added. The beads were then incubated for 2h at 4°C overead shaking and subsequently washed three times with TE buffer before resuspending them in beads volume TE buffer and then kept at 4 °C. The next day 30 µl preblocked breads were added to the samples and incubated for 2 h at 4°C overhead shaking. Following the samples were washed using a magnetic beads stand: once with ChIP wash buffer I (20 mM Tris-HCl pH 8.0, 2 mM EDTA, 150 mM NaCl, 0.1% SDS, 1% Triton X-100, 1 PIC), two times with 500 µl Chip wash buffer II (20 mM Tris-HCl pH 8.0, 2 mM EDTA, 500 mM NaCl, 0.1% SDS, 1% Triton X-100, 1x PIC), two times using ChIP wash buffer III III (10 mM Tris-HCl pH 8.0, 1 mM EDTA, 250 mM LiCl, 1% sodium deoxycholate, 1% NP-40, 1x PIC) and two times using TE buffer. Thereafter, the bound complexes were eluted by two sequential incubations with 200 µl elution buffer (1% SDS, 0.1 M $NaHCO_3$) at 65 °C for 10 min while shaking. The input fractions saved the day before were thawed on ice, resuspended in 400 µl TE buffer and from here on processed together with the other samples. 0.2 mg/ml RNAse A (R6148, Sigma-Aldrich) was added and the samples incubated for 30 min at 37°C on a shaker. Subsequently10 mM EDTA, 40 mM Tris pH 6.5 and 50 µg/ml Proteinase K (03115879001, Thermo Fisher Scientific) were added to each sample and incubated at 55°C for 2.5 h while shaking. Afterwards the temperature was rised to 65°C the samples were incubated overnight without shaking. The next day, the samples were transferred to a 2 ml Eppendorf tube and DNA extraction was performed (adapted from using the QIAquick Gel extraction Kit (28704, Qiagen). 3 volumes of QG buffer and 1 volume of isopropanol were added, followed by heating at 55 °C for 3 minutes. Samples were then loaded onto a QIAquick column and centrifugation for 1 min (13’000 rpm) was perfomed and the low through was discarded. Subsequently 750 µl PE buffer were added and after letting the column stand with the lid open for 2 min at room temperature, the columns were centrifuged, again (1 min, 13’000 rpm). To completely remove the PE buffer, columns were centrifuged for additional 2 min at 13’000 rpm. Elution was then performed twice, once by adding 30 µl buffer EB and a second round by adding 15 µl EB buffer. ChIP libraries were prepared using the APA Hyper Prep Kit from Kapa Biosystems with different amounts of input (from 2ng to 10ng). Samples were sequenced on a NextSeq 500 with using a High Output kit with 75 cycles.

Statistics

Statistical analyses and graphs were generated using GraphPad Prism 7.02 software. All data are presented as mean ± S.E.M.

2.7 Supplementary data

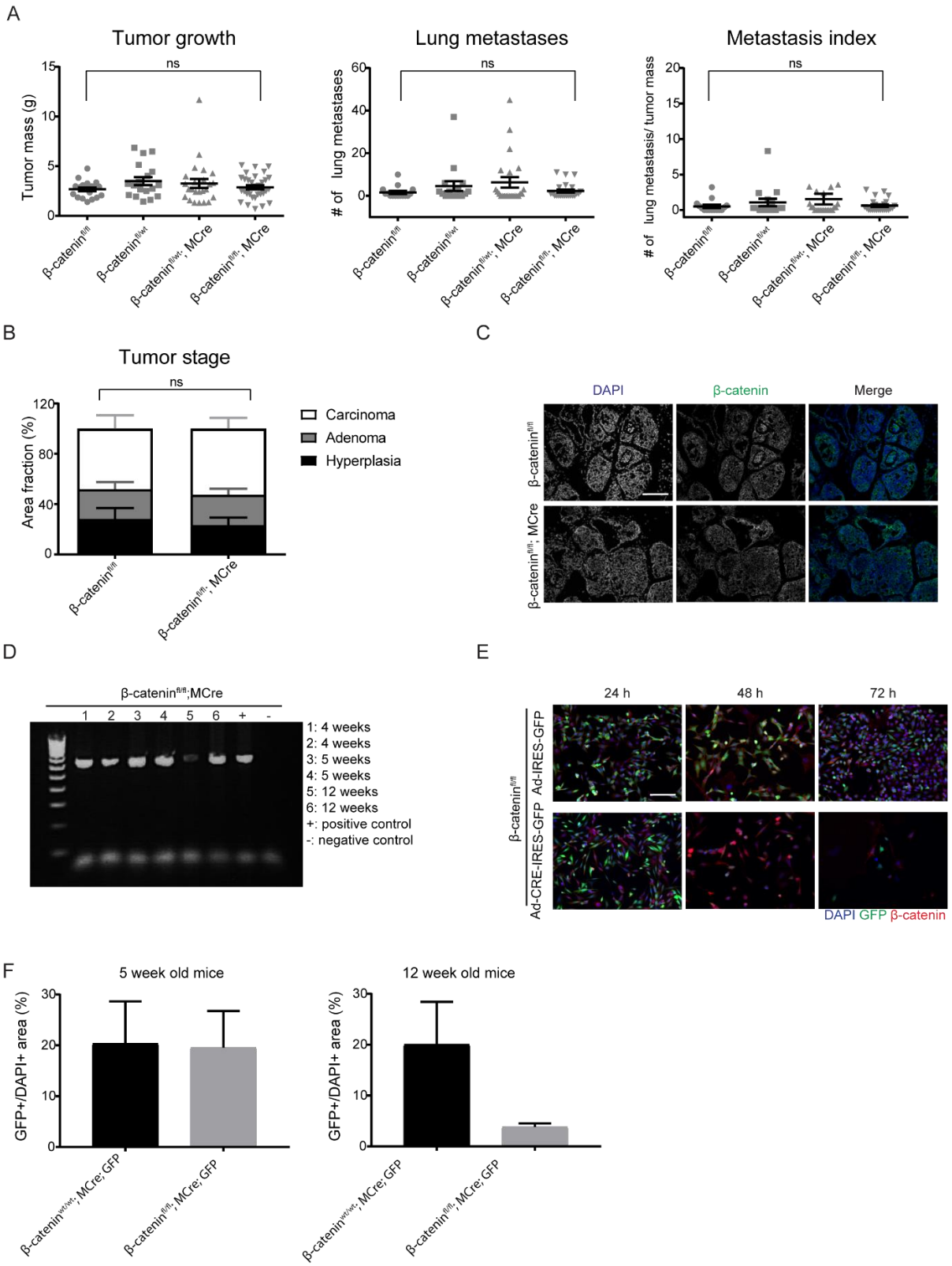

Supplementary Figure 1. Incomplete deletion of β-catenin in murine mammary tumors does not affect tumor growth, metastasis formation or tumor progression. (A) β-catenin conditional knockout (MMTV-Cre, MCre) did not affect PyMT tumor growth (β-catenin$^{fl/fl}$ n=19, β-catenin$^{fl/wt}$ n=18, β-

catenin$^{fl/wt}$; MCre n=24, β-catenin$^{fl/fl}$; MCre n=31), the number of lung metastasis or the metastasis index (β-catenin$^{fl/fl}$ n=15, β-catenin$^{fl/wt}$ n=16, β-catenin$^{fl/wt}$; MCre n=23, β-catenin$^{fl/fl}$; MCre n=24). Data are displayed as mean ± SEM. Statistical analysis was performed using ordinary one-way ANOVA multiple comparison test **(B)** Quantification of the different tumor stages revealed that the knockout of β-catenin does not affect tumor progression compared to β-catenin wt mice. β-catenin$^{fl/fl}$ n=7, β-catenin$^{fl/fl}$; MCre n=11. Data are displayed as mean ± SEM. Statistical analysis was performed using a Mann-Whitney U test. **(C)** Immunofluorescence (IF) staining of tumor sections revealed that β-catenin was still present in the β-catenin$^{fl/fl}$; PyMT; MMTV-Cre conditional knockout mice suggesting an escape phenotype. DAPI was used to visualize nuclei. Scale bar: 100 µm **(D)** Genotyping of the tumors demonstrated an incomplete deletion of the β-catenin gene **(E)** Exogenous addition of Adenovirus-Cre-IRES-GFP on primary tumor cell lines derived from β-catenin$^{fl/fl}$; PyMT tumors resulted in the elimination of the infected cells as compared to cells infected with the control Adeno-IRES-GFP virus. DAPI was used to visualize nuclei. Scale bar: 100 µm. **(F)** Quantification of the recombination efficiency of MMTV–Cre in the mammary gland using GFP reporter mice comparing β-catenin$^{wt/wt}$ PyMT; MMTV-Cre to β-catenin$^{fl/fl}$; PyMT; MMTV-Cre mice at 5 and 12 weeks of age . Scale bar: 100 µm. n=5. Data are displayed as mean ± SEM.

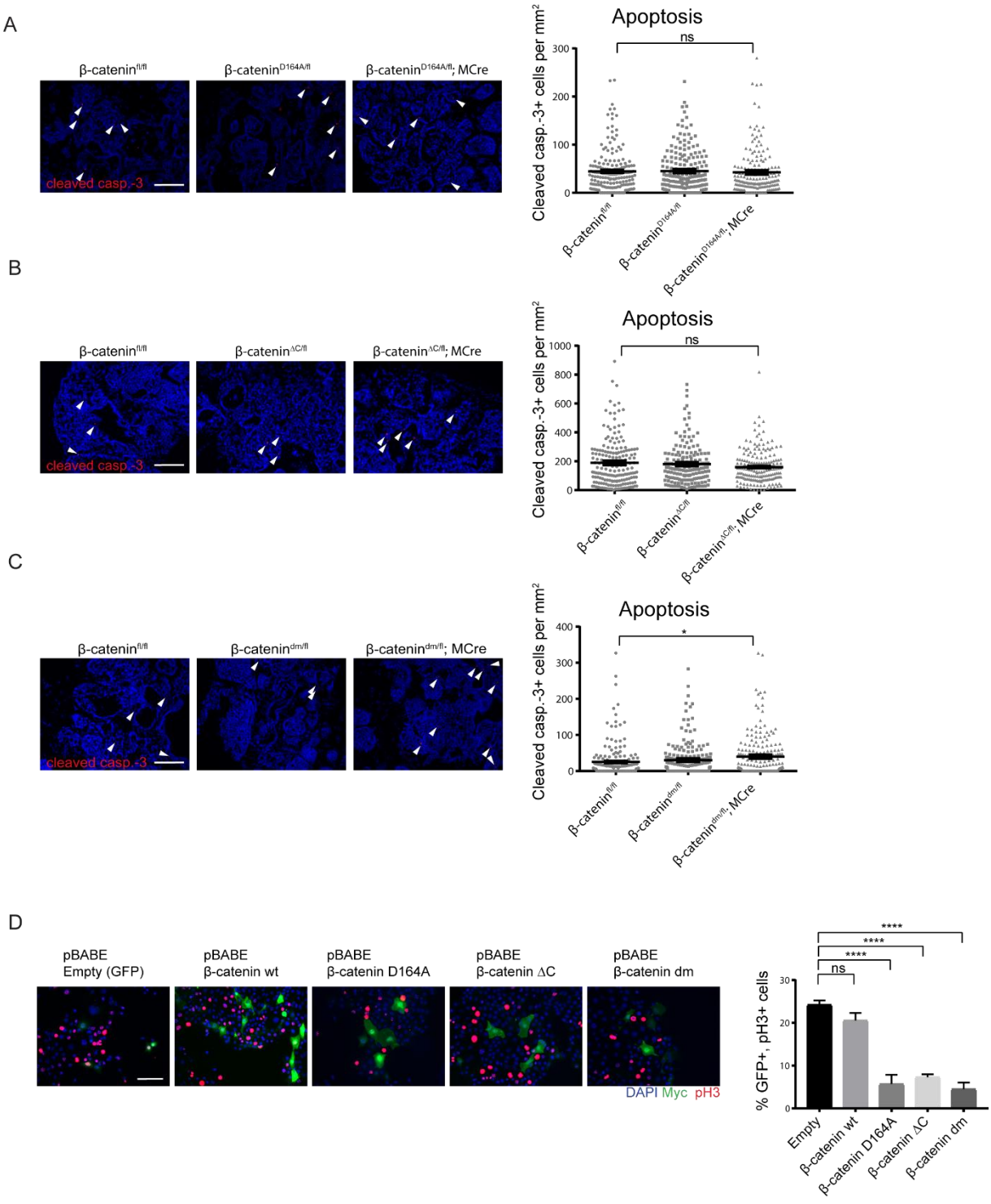

Supplementary Figure 2. Comparison of apoptosis *in vivo* and the dominant-negative effect *in vitro* of the different mutant forms of β-catenin. Immunofluorescence staining and quantification of cleaved caspase 3 to assess apoptosis on tumor sections of the different mouse genotypes. **(A)** On tumor sections from mice expressing the D164A mutant allele the amount of apoptotic (cleaved casp.3) cells is not affected compared to wild type mice. β-catenin$^{fl/fl}$ n=10, β-catenin$^{D164A/fl}$ n=11, β-catenin$^{D164A/fl}$; MCre n=10. **(B)** The truncated C-terminus does not affect apoptosis. β-catenin$^{fl/fl}$ n=10, β-catenin$^{\Delta C/fl}$ n=10, β-catenin$^{\Delta C/fl}$; MCre n=10. **(C)** The doube mutation causes an increase in the amout of apoptotic

cells compared to wild type mice. β-catenin$^{fl/fl}$ n=10, β-catenin$^{dm/fl}$ n=10, β-catenin$^{dm/fl}$; MCre n=10. White arrows indicate cleaved caspase-3 positive cells. DAPI was used to visualize nuclei. Scale bar: 100 µm. Data are displayed as mean ± SEM. Statistical analysis was performed using ordinary one-way ANOVA multiple comparison test: * P < 0.05. **(D)** Transient transfection of MYC-tagged β-catenin^{wt}, β-catenin^{D164A}, β-catenin$^{\Delta C}$ and β-catenin$^{D164A-\Delta C}$ or an empty GFP vector construct in a β-catenin wild type cell line (Py2T). The number of transfected and proliferating cells was quantified by MYC and pH3 staining, which revealed a reduced proliferation of cells transfected with the β-catenin mutant (D164A, ΔC and D164A-ΔC) forms compared to GFP or wild type. Data are displayed as mean ± SEM. n=3. Statistical analysis was performed using ordinary one-way ANOVA multiple comparison test. **** P < 0.0001. Scale bar: 100 µm.

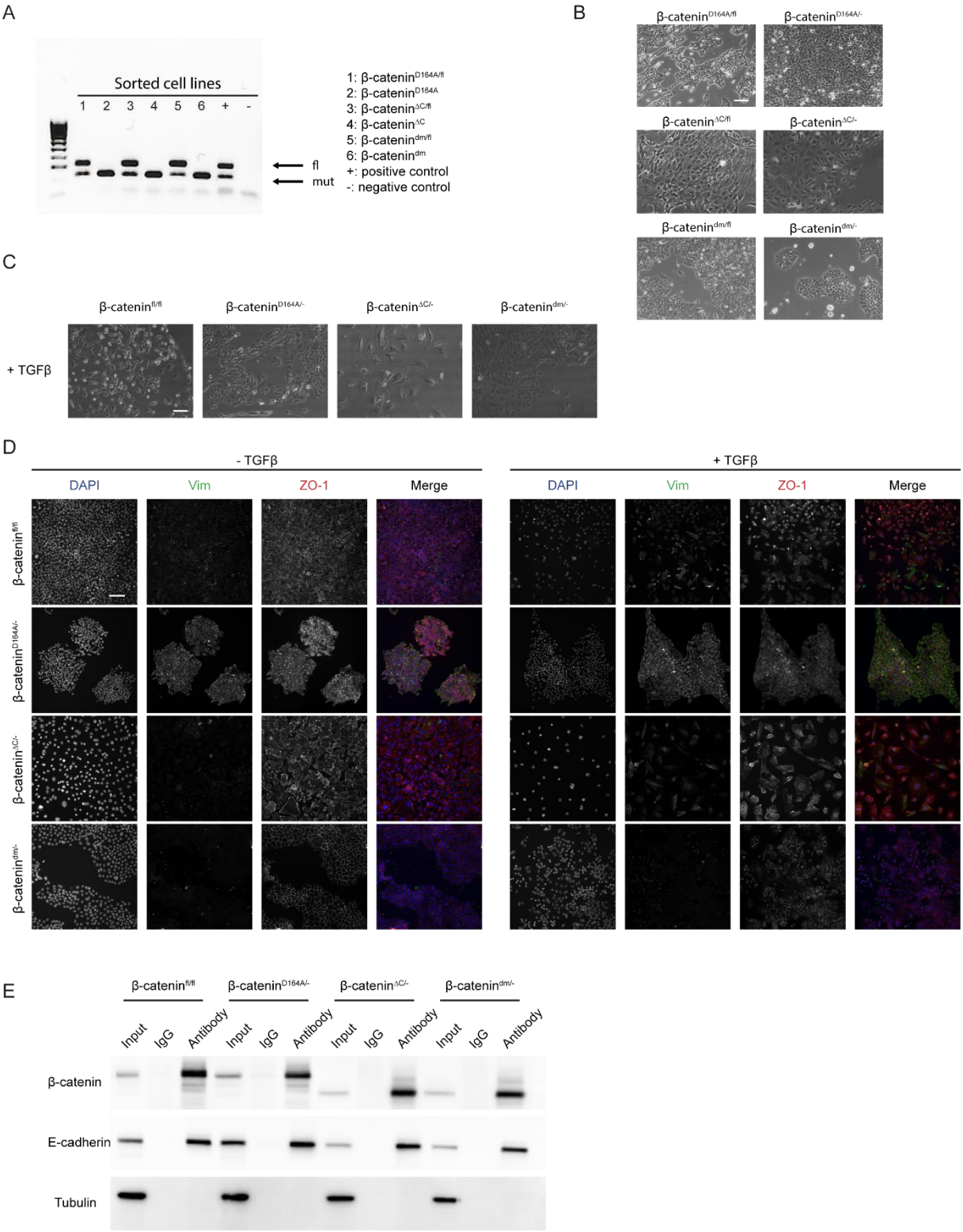

Supplementary Figure 3. Inability of β-catenin to bind BCL9/9L results in an abrogated EMT response. (A) Established cell lines from different dissected tumors. Floxed alleles were removed by infection with the Adeno-Cre-IRES-GFP virus and then FACS sorting for GFP+ cells. **(B)** Epithelial morphology of the established cell lines before and after removal of the floxed allele. Scale bar: 100 µm. **(C)** Morphology of the cell lines after 20 days of TGFβ treatment. The β-catenin wild type cell line still shows a mesenchymal morphology upon TGFβ treatment and the same was true for the β-catenin$^{\Delta C/-}$ cell line. The β-catenin$^{D164A/-}$ cells still grew in clusters but were more elongated. The β-catenin$^{dm/-}$ cell

line did not show a mesenchymal morphology only the formation of some phylopodia. Scale bar: 100 µm. **(D)** Immunofluorescent staining for Vimentin (Vim) and ZO-1 after 4d of TGFβ treatment. β-catenin$^{fl/fl}$ and β-catenin$^{\Delta C/-}$ upregulate the mesenchymal marker Vimentin and lost the expression of ZO-1 at the cell membrane. The β-catenin$^{D164A/-}$ and the β-catenin$^{dm/-}$ cell lines however, still retained ZO-1 expression at the cell membrane. Vimentin signal was increased in the β -catenin$^{D164A/-}$ cell line,whereas the β-catenin$^{dm/-}$ only show a slight increase in Vimentin. DAPI was used to visualize nuclei. Scale bar: 100 µm. **(E)** Co-immunoprecipitation (IP) was performed with an antibody against β-catenin or rabbit IgG as a negative control in the established cell lines. It was determined if β-catenin was pulled down together with E-cadherin by immunoblotting analysis. Tubulin served as a loading control.

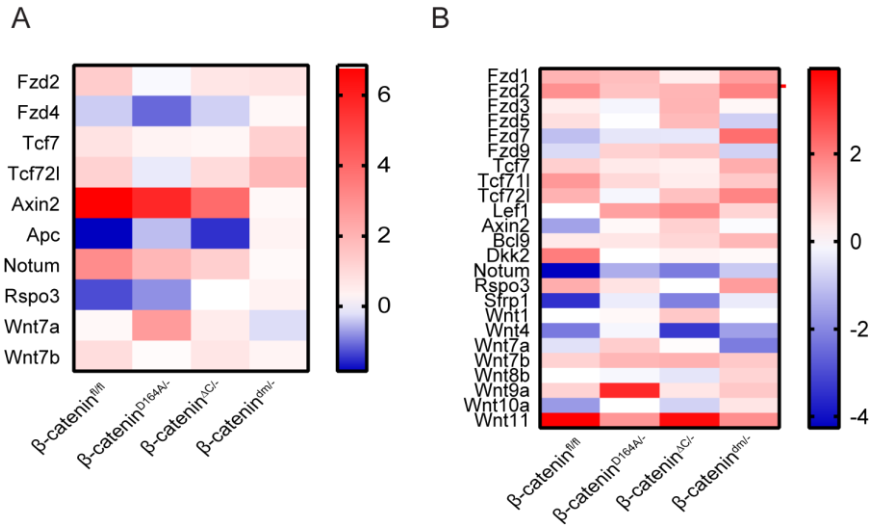

Supplementary Figure 4. The β-catenin mutant cell lines show different alterations in the expression of canonical Wnt pathway components as compared to the wild type cells. (A) Heatmap showin the log2 fold changes of Wnt ligands and canonical Wnt pathway components being significantly differentially expressed in at least one of the cell lines upon Wnt3a or **(B)** TGF-β treatment. Red represents up-regulated expression and blue down-regulated expression. $P \leq 0.05$ and fold change ≥ 1.5.

3. Project II: Mechanisms of evasive resistance to sorafenib in hepatocellular carcinoma

3.1 Summary

Hepatocellular carcinoma (HCC) is the second most common cause for cancer-related death worldwide. There is need for more effective medical therapies, so far the standard treatment for patients with advanced HCC is sorafenib, a multikinase inhibitor which prolongs the time of tumor progression and improves the overall survival of the patients by two to three months. However, the use of Sorafenib is hampered by the occurrence of drug resistance leading to progression of the tumor after initial response to chemotherapy. To examine the escape of such therapies by the activation of compensatory pathways or via other mechanisms was therefore the aim of this study. We aimed to investigate the molecular mechanisms involved in evasive resistance to sorafenib in HCC. Therefore, we determined the IC50 for sorafenib of a number of HCC cell lines. This enabled us to differentiate between more sensitive cell lines and intrinsically drug resistant ones. We established sorafenib-resistant HCC cell lines out of the most susceptible ones, using two different approaches and investigated their changes in morphology, gene expression and migratory capacity. The resistant cells seemed to undergo an EMT since they became more mesenchymal as well as more migratory. Furthermore, they decreased the expression of diagnostic HCC markers and increased the expression of stem cell markers. However, those changes seemed to be epigenetic, since sorafenib withdrawal partially reverted the observed effects. Therefore, treatment with HDAC inhibitors was tested on intrinsically resistant cell lines with a mesenchymal morphology. Initial tests suggested a reversion of the mesenchymal to an epithelial morphology of those cells and a synergistic effect on cell growth of the co-treatment of pan-HDAC inhibitors together with sorafenib. To compare the differences in gene expression between the parental- and the established resistant cell lines and to able to identify pathways or genes contributing to evasive resistance to sorafenib, RNA sequencing has been performed. The results revealed changes in pathways involved in ECM organization and cell surface interactions which are also associated with EMT as well as pathways associated with epigenetic alterations and cell cycle control. Taken together, this study provides a model to examine evasive resistance and preliminary results show overlapping mechanisms between different

cell lines. Sorafenib-resistant cell lines seem to undergo an EMT and become more migratory. This cell model was further used in preliminary experiments to investigate the restoration of the morphology and sensitivity to sorafenib using HDAC inhibitors.

3.2 Introduction

3.2.1 Hepatocellular carcinoma (HCC)

Liver cancer is the second most common cause of cancer-related deaths worldwide. Hepatocellular carcinoma (HCC) is the most frequent type of liver cancer representing around 90% of cases and is more common in men than in women [256]. The main risk factors for the development of HCC are Hepatitis B and C virus (HBV and HCV) infections, alcohol-related liver disease and non-alcoholic fatty liver disease (NAFLD). HCV is an RNA virus that does not integrate into the host genome, whereas HBV as a DNA virus can integrate. HCV can induce pathway alterations caused by viral factors or by the immune response which is mediated by a chronic state of inflammation [257]. HBV on the other hand can directly integrate into the genome and can thereby cause genomic instability and alteration of gene expression. Also, viral proteins HBx and HBs as well as chronic inflammation due to infection can contribute to the carcinogenic process [258]. Alcohol abuse can induce liver damage by oxidative stress and inflammation which might have an effect on pathways promoting development of HCC [259]. NAFLD is the increased storage of fat in the liver due to other reasons than alcohol which represents a broad spectrum of disorders like diabetes and obesity. Thereby liver injury and cancer-promoting mutations can result in the development of HCC [260]. Thus, patients with cirrhotic liver damage are prone to develop HCC, but it can develop also in patients without liver cirrhosis [256, 261, 262]. HBV infection accounts for around 33% of deaths in HCC patients, whereas HCV infection accounts for 16% and alcohol abuse for 30%, respectively [263]. The knowledge of such risk factors also gives the possibility of prevention and surveillance of the development of HCC. Preventions of HCC development include vaccination against HBV infection, reduction of alcohol abuse or save transfusions and injections. Dysregulation of a number of signaling pathways affected by those risk factors have been linked to HCC, including the Wnt/β-catenin pathway, the p53 pathway, and importantly, the growth factor-activated receptor tyrosine kinase pathways PI3K/Akt/mTOR and RAS/MAP kinase [256, 264].

3.2.2 HCC treatment

The clinical symptoms of HCC patients include abdominal pain and swelling, weight loss, fever and early satiety. However, patients at early stages of HCC are mainly asymptomatic and thus mostly diagnosed at later stages [265]. Early diagnosis of HCC has been shown to be an important factor to increase therapeutic success and prolonged patient's survival rate and several imaging techniques are available to detect HCC. Furthermore, laboratory tests are used in HCC screening. A widely used marker is serum alpha-fetoprotein (AFP), a glycoprotein expressed by fetal hepatocytes in HCC cells. Serum AFP levels are often increased during HCC but not in all patients [266, 267]. Upon diagnosis, tumor staging to determine growth, spreading and progression is necessary for specific and optimized treatment. For HCC different staging systems are available for example the Okuda staging system based on presence of ascites, tumor size, albumin and bilirubin levels or the widely used Barcelona clinic liver cancer classification taking into account tumor extension, liver functional reserve, physical status and cancer-related symptoms (Fig. 1) [268, 269].

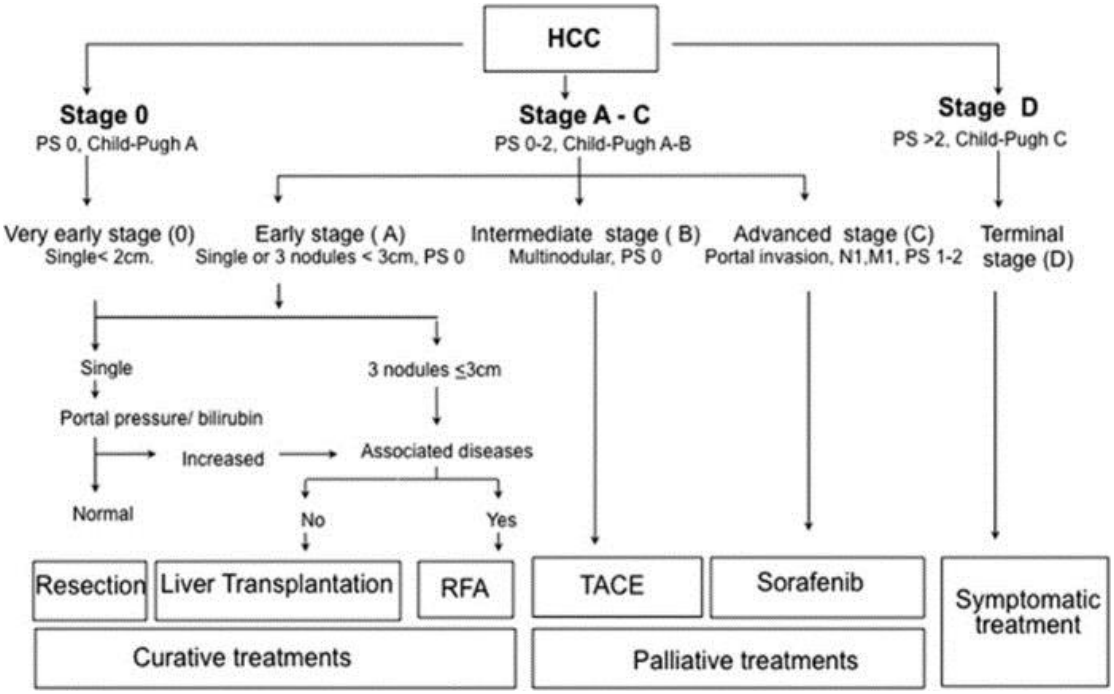

Figure 1. BCLC Barcelona Clinic Liver Cancer staging system for the management of HCC. M, metastasis classification; N, node classification; PS, performance status; Child-Pugh score, liver function score; RFA, radiofrequency ablation; TACE, transarterial chemoembolization [268, 270].

The therapeutic possibilities for HCC are divided into curative and palliative and comprise surgical resection, liver transplantation and the so-called locoregional

therapy encompassing percutaneous ablation and intra-arterial chemoembolo therapy. Surgical resection and liver transplantation are the first line treatment options for early stage HCC. The percutaneous ablation is the direct application of alcohol, heating or freezing to the tumor tissue by needle injection. Intra-arterial chemoembolo therapy constitutes the treatment by chemotherapy or radiation and their application into the hepatic artery supplying the tumor called transcatheter arterial chemoembolization (TACE) or radioembolization (selective internal radiation therapy, SIRT) respectively. Thereby the toxicity for the metabolism and patient is kept as low as possible since it is known that liver tumors draw their blood supply almost exclusively from the hepatic artery. The standard chemotherapeutic treatment and only approved systemic therapy for patients with advanced HCC is sorafenib [271, 272]. This compound is a multi-kinase inhibitor and targets c-Raf, platelet-derived growth factor receptor (PDGFR), epidermal growth factor receptor (EGFR), vascular endothelial growth factor receptor (VEGFR), FMS-like tyrosine kinase-3 (FLT-3) and c-KIT and thereby suppresses angiogenesis and proliferation. The SHARP (Sorafenib HCC Assessment Randomized Protocol) study published in 2008 has shown that sorafenib delays the time of tumor progression and improves the overall survival of the patients by two to three months (Fig. 2) [273, 274].

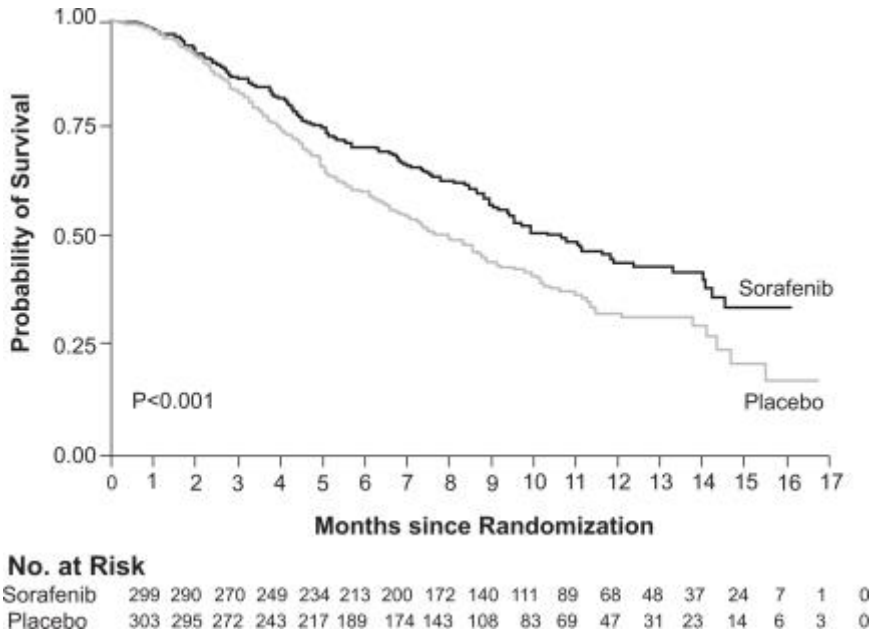

Figure 2. SHARP (Sorafenib HCC Assessment Randomized Protocol) trial including 602 patients. Overall survival study of patients with advanced-stage HCC of whom 299 received sorafenib treatment and 303 placebo. Sorafenib treatment significantly increased the overall survival rate (10.7 months) compared to the control group (7.9 months).

However, the application of sorafenib is hampered by two phenomena: the severe side effects and the development of drug resistance leading to progression of tumor formation after initial response. Side effects found in sorafenib treated patients amongst others are diarrhoea, weight loss, hand-foot skin reaction (HFSR), fatigue, hypertension and rashes [274, 275]. Sorafenib treatment is only beneficial in about 30% of patients and acquired resistance develops within 6 months [274]. Due to primary as well as acquired resistance and also to reduce its adverse effects by applying lower doses, co-treatment with other drugs are being tested.

3.2.3 Drug resistance

Several possible resistance mechanisms have been found and proposed. Cells might be intrinsically resistant (called primary resistance) which can be due to tumor heterogeneity favoring the outgrowth of a subset of cells. The expression levels of several genes have meanwhile been found to potentially predict the sensitivity to sorafenib treatment. Amongst them are EGFR, phosphor-ERK (pERK), JNKs (C-Jun-N-terminal kinases), VEGF (vascular endothelial growth factor A) and Glutamine synthetase (GS). Testing the effect of sorafenib treatment on different cell lines, (Huh7, Hep3B, HepG2, SNU-182, SNU-398 and SNU-449) has revealed, that the cell lines more resistant to sorafenib showed a higher EGFR activity in an antibody array compared to more sensitive ones. Hence, EGFR is proposed as a possible determinant of the sensitivity of HCC cells to sorafenib treatment. Sorafenib and EGFR inhibitors showed a synergistic effect on proliferation inhibition [276, 277]. Supporting this hypothesis, EGFR has also been found to be frequently overexpressed in patient-derived HCC samples. However, also in resistant cells aberrant activation of *EGFR* and its dimerization partner *HER3* (*human epidermal growth factor receptor 3*, HGNC: *ERBB3, erb-b2 receptor tyrosine kinase 3*) as well as overexpression of EGFR ligands have been observed. Silencing *EGFR* together with *HER3* increased the effect of sorafenib on proliferation *in vitro.* Thus this might constitute also an adaptive response to sorafenib [278, 279]. Another study has revealed that the effect of sorafenib on cell proliferation correlated with basal expression levels of pERK. Cells with lower expression levels of pERK were less sensitive to sorafenib treatment [280]. In a phase

II study, the pERK level in pre-treated tumors has been found to correlate with the progression time upon sorafenib treatment [281]. Furthermore, by analyzing the association of JNK activation and the therapeutic response to sorafenib, it has been observed that the progression time and overall survival of patients significantly correlated with low c-Jun expression in samples before treatment [282]. In some human and mouse HCCs genomic *VEGFA* amplification has been discovered. Those tumors showed a higher proliferation, higher vessel density and a higher macrophage content compared to tumors without VEGFA amplification. Since sorafenib also inhibits VEGFRs and BRAF (B-Raf proto-oncogene), treatment reduced tumor growth *in vivo* in *VEGFA*–amplified tumors. Also, in patients the improved survival correlated with VEGFA expression [283]. In the liver, the expression of GS seems to be regulated by canonical Wnt signaling. *β-catenin* mutations and/or aberrant activation of the canonical Wnt signaling pathways have frequently been found in HCC and pathway activation induced by *APC* (*adenomatous polyposis coli*) loss was found to be sufficient to induce hepatocarcinogenesis. Analysis of five different HCC cell lines has shown that cells with high GS expression were more sensitive to sorafenib treatment. Upon silencing *GS* expression, the cells became more resistant. *GS* expression seemed to induce autophagy in HCC cells since silencing reduced and overexpression of *GS* induced autophagic activity. Furthermore, sorafenib treatment increased autophagic activity which was reduced by shRNA mediated silencing of *GS* [284-286].

Otherwise adaptive/evasive resistance can emerge. Thereby cancer cells escape therapeutic treatments by activating compensatory pathways. EMT is one such mechanism by which it is thought that cells can become more resistant to chemotherapeutics. The investigation of serum response factor (SRF) in HCC, known to play a role in carcinogenesis and tumor progression as well as EMT, has shown that its overexpression in HLE cells led to an increased expression of mesenchymal markers and a weaker effect of sorafenib treated cells. In contrast, the inhibition of SRF led to a diminished expression of mesenchymal marker, restored E-cadherin expression and enhanced the apoptotic effect of sorafenib treatment [287]. Even though, sorafenib has also been found to be able to inhibit EMT suggesting that once overcoming this inhibition, EMT might contribute to chemoresistance [288, 289]. For example, sorafenib was found to reverse the changes in histone modifications that occur during EMT. The expression of several HDACs as increased during EMT, also

H3K4me3 and H3K9ac levels within the promoter region of *E-cadherin* were decreased and these changes could be blocked by sorafenib treatment [289]. Another study has demonstrated that established sorafenib-resistant HCC cells by long term treatment, became more mesenchymal, had an increased invasive potential and showed a downregulation of liver-specific markers alpha-fetoprotein and glypican [290]. Long-term treatment of HCC cell lines with sorafenib also resulted in a mesenchymal phenotype and drug resistance of the cells. Furthermore, knockdown of *SNAI1* or *MDR1* in the resistant cells reversed drug resistance. *Snai1* knockdown reversed the EMT phenotype, whereas *MDR1* knockdown did not. Moreover, cells stably expressing SNAI1 also showed a higher expression of EMT-related markers, downregulation of E-cadherin and an increased resistance to sorafenib. Furthermore, the resistance was mediated by the PI3K/AKT signaling pathway, and treatment with the Akt inhibitor MK-2206 lead to a reversion of the EMT [291]. Also Chen and co-workers have found that the activation of PI3K/Akt signaling pathway mediated the acquired resistance to sorafenib in Huh7 HCC cells, and MK-2206 reverted resistance to sorafenib and sensitized the cells to sorafenib-induced apoptosis [292]. In another study, an *in vivo* shRNA screen has identified the activation of Mek-Erk and Atf2 signaling by MAPK14 as a resistance mechanism by which cells react to sorafenib treatment. Accordingly, the pharmacological inhibition of MAPK14 increased sorafenib efficiency *in vitro* and *in vivo* suggesting a possible combinatorial treatment [293].

Changes in gene expression during EMT can lead to numerous phenotypic changes, such as cell morphological changes, loss of adhesion and gain of stem cell features [294]. It is thought that cancer growth is also dependant on a few progenitor cells which show pluripotency and self-renewal properties. Such cancer stem cells (CSCs) are thought to be more resistant to radio/chemotherapy and therefore to contribute and thus being associated with recurrence of cancers [295]. Also in liver cancer, the presence of such stem cells has been proposed [296-298]. Current radio- and chemotherapies destroy the vast majority of cancer cells, but are often not able to eliminate the critical CSCs, which are protected by specific resistance mechanisms. Comparing the response to sorafenib of six different liver cancer cell lines has revealed an increased resistance of cells with a rather mesenchymal phenotype and high expression of CD44 whereas rather epithelial cells expressing EPCAM or CD133 were more sensitive [299]. The expression of the stem cell marker CD44

together with active TGFβ/β-catenin pathways was thereby found to be a marker for predicting the efficiency of sorafenib treatment [299]. Moreover, examining chemoresistance of cells showed that poorly-differentiated CD133(-)/ALDH(low) HLE cells were more resistant to cisplatin, doxorubicin or sorafenib [300]. In another study, two different HCC cell lines that have been established from the same patient have showed differences in the morphology. These cell lines were compared as one was showing an epithelial and the other one a mesenchymal phenotype. The mesenchymal cell line was more migratory and invasive *in vitro* and also more resistant to sorafenib or erlotinib treatment as compared to the mesenchymal phenotype cell line [301].

Adaptation to a hypoxic microenvironment has also been found to contribute to drug resistance which is often mediated by hypoxia inducible factor-1α (Hif-1α). Uncontrolled tumor growth reduces the availability of nutrients and oxygens for some cells needed for growth, function and survival. Adaptation to such stress factors also seem to enhance tolerance to drug treatments [302, 303]. In a study in 2013 by Liu and colleagues, it has been found that sorafenib-resistant HCCs from patients showed increased hypoxia compared with HCCs before treatment or HCCs that were sensitive to sorafenib treatment. Enhanced anti-tumoral effects were achieved by combined sorafenib treatment with additional inhibition of HIF-1α. Similar observations have also been made in *in vitro* and *in vivo* mouse models [304]. Hif1-α stabilization can then also lead to the activation of MDR1 (ATP-binding cassette, subfamily b, member 1; HGNC: ABCB1) which can reduce intracellular drug concentrations and might depict another mechanism of resistance [305]. Furthermore, autophagy as a process by which cells can digest and degrade dysfunctional or damaged components seems to be able to play a protective role against cancer treatments. In HCC cell lines, sorafenib has been found to induce the accumulation of autophagosomes and autophagy and thereby might increase cell survival. Moreover, autophagy inhibition enhanced the effect of sorafenib *in vitro* as well as in xenograft mice *in vivo* [306].

Resistance can also be acquired by enhanced efflux or decreased uptake of drugs that can be achieved by increased expression of drug transporters. Drugs used for treatment of HCC like sorafenib and anthracyclines are found to be substrates for such transporters [307, 308]. Several studies have found altered expression of such transporters in HCC that can confer resistance to treatment [307, 309-311].

Transfection of a renal cell line with *MRP2* (*Multidrug resistance-associated protein 2*; HGNC: *ABCC2, ATP-binding cassette, subfamily C, member 2*) showed significantly decreased sorafenib concentrations and increased the IC50 compared to the control. This suggests that sorafenib is a substrate of MRP2 and its expression can contribute to resistance formation [312]. Also MRP3 (ATP-binding cassette, subfamily c, member 3, also ABCC3) has been found as a possible mediator of sorafenib resistance. Established sorafenib-resistant PLC cells showed an increased expression of MRP3, and its knockdown lead to sensitization [313]. Also the inhibition of ABCG2 (ATP binding cassette subfamily G member 2) resulted in a higher susceptibility of HCC cells to sorafenib treatment [314].

3.2.3.1 Epigenetic regulation involved in drug resistance

Epigenetic regulation of translation works through reversible but heritable states of gene expression due to specific gene silencing by methylation and other non-mutating mechanisms thus causing phenotypic alterations without affecting the genotype. Epigenetic changes act on gene expression by affecting chromatin architecture. Euchromatin where chromatin structure allows accession for gene transcription to happen can be changed to heterochromatin, where transcription is structurally hampered and repressed. Epigenetic alterations leading to aberrant gene expression have also been found to play a pivotal role in cancer. EMT, has as well been found to be regulated by epigenetic modifications and in HCC several epigenetic alterations like histone modifications, DNA methylation and non-coding microRNA patterns have been discovered [315, 316].

DNA methylation

DNA methylation is the covalent attachment of a methyl group predominately to cytosines (5-methyl-C) catalyzed by DNA methyltransferases (DNMTs) in CpG islands [317]. In HCC, promotor hypermethylation has been found being involved in the inactivation of tumor suppressor genes which play an important role in carcinogenesis [318]. With regard to EMT, the promotor hypermethylation of *CDH1 (E-cadherin)* was found in malignant breast and prostate carcinomas [316]. Methylation of estrogen receptor-alpha and E-cadherin promotors was also found to increase during breast tumor progression. [319] Also in HCC, frequent hypermethylation of the *CDH1*

promotor and thereby downregulation of *CDH1* has been reported [320]. Furthermore, a genome wide methylation profiling has found distinctive methylation patterns comparing HCC to adjacent normal liver samples. Another study has found five genes (*APC, cyclin dependent kinase inhibitor 2A (CDKN2A), homeobox A9 (HOXA9), Ras association domain family member 1 (RASSF1)*, and runt related transcription factor (*RUNX*) to be more frequently methylated in malignant tissues than in normal liver tissue [321].

Histone modifications

Histone modifications affect chromatin structure and gene expression. This includes phosphorylation, ubiquitination, methylation and acetylation that occurs on N-terminal domains of histones. These modifications can either activate or repress gene expression. Histone acetylation mediated by histone acetyltransferases (HATs) leads to an active state which is opposed by histone deacetylases (HDACs) [318, 322]. In humans, 18 different HDAC isoforms have been identified which are divided into two families and classified into four classes according to sequence similarities. The classical HDAC family comprises the class I HDACs encompassing HDAC1-3 and HDAC8, as well as the class II HDACs, HDAC4-7, 9 and 10 and the class IV HDAC11. The second family contains the NAD+ dependant sirtuins, SIRT1-7 belonging to class III. [323, 324] Again E-cadherin was a target found to be affected by HBx (hepatitis B virus (HBV)-encoded X antigen) expression leading to aberrant histone acetylation and downregulation of E-cadherin in an HCC cell line. Inhibiting the histone deacetylation using the HDAC inhibitor trichostatin A (TSA) was able to restore E-cadherin expression [325].

Histones can be methylated by histone methyltransferases (HMTs). They are classified according to their substrate specificity by either methylating lysine (lysine methyltransferases) or arginine (arginine methyltransferases). Histone methylation mediated by histone methyltransferases (HMTs) can lead to activation as well as repression and histone demethylation by histone demethylases (HDMs) can revert it [318, 326, 327]. Treatment of rats with 2-acetylaminofluorene (2-AAF), a genotoxic rat liver carcinogen resulted in liver carcinogenesis and subsequent analysis of the histone methylation revealed an increased H3K27 tri-methylation in tumor suppressor gene promoter regions of *Rassf1, Cdkn2a, Socs1(suppressor of cytokine signaling 1)*, *Gjb2*

(*gap junction protein beta 2*; old nomenclature: *Cx26*) and again *Cdh1* [328]. In different cancer types, altered gene expression of cancer-related genes induced by an altered histone modification profile has been found. Examining HCCs also revealed an aberrant expression of HDACs and HMTs. For example, the expression of HDAC1, HDAC2, HDAC3 and HDAC6 as well as SIRT1 were found to be upregulated in HCC [329-332]. The expression of HDACs 1-3 showed a high correlation with upregulation of Ki-67 and the tumor grade. The expression of HDAC2 was found being associated with poor survival in low-grade and early-stage tumors [333]. In another study expression of HDAC1 and 2 were also found to correlate with worse survival of the patients [334].

HDAC inhibitors inhibit the enzymatic activity of HDACs and thereby lead to the transcriptional activation of target genes. They can be grouped according to their structure into four different groups: hydroxamates, cyclic peptides, short chain fatty acids and benzamides. Up to date four HDACis are FDA approved: vorinostat (SAHA) and romidepsin (FK228) and belisostat (PXD101) have been approved for treating CTCl (Cutaneous T-Cell lymphoma) patients. Panobinostat (LBH589) has been approved for treatment of multiple myeloma. Those inhibitors as well as others are currently also tested for treatment of HCC [335]. SAHA was found to inhibit proliferation of HepG2.2.15 cells and to induce apoptosis [336]. Romidepsin treatment was found to induce cell cycle arrest and apoptosis in Huh7 HCC cell line mediated by the activation of the MAPK/ERK pathways and JNK/MAPK pathways. Furthermore, it reduced tumor growth in mouse xenografts [337]. Moreover, also combinatory treatments of HDACis and several chemotherapeutic drugs are being tested. Synergistic effects have been observed. In a recent study, sorafenib has been found to have inhibitory activities on HDACs in HCC, HepG2 and PLC/PRF/5 (PLC5) cell lines. It seemed to reduce the expression of HDAC 2, and in HEPG2 cells and of HDAC3 and HDAC4 in PLC5 cells. Liu and colleagues also have shown that patients with high expression of HDAC1 or HDAC2 had a shorter overall survival. Therefore is was thought that amplification the inhibitory effects of sorafenib on HCCs could enhance its effects [334]. Treatment of Huh7, Hep3B and HepG2 cells with panobinostat had an effect on cell viability and proliferation. Co-treatment with sorafenib showed an additive effect on viability of the HEPG2 and Hep3B cells. Besides panobinostat also seemed to induce autophagy in Huh7 cells. Also *in vivo*, using HCC xenografts it was shown that panobinostat alone or together with sorafenib

reduced respectively additively reduced tumor volume and increased survival *in vivo* [338]. Also combinatorial treatment of sorafenib together with vorinostat resulted in additive effects on eliminating hepatic, renal and pancreatic adenocarcinoma cells [339]. Furthermore, resminostat was found to induce apoptosis in HCC cell lines and the cytotoxic effect of sorafenib was enhanced by the co-treatment with resminostat [340]. In a preclinical study, it has been observed that the treatment with resminostat was effective alone or together with sorafenib in patients that showed progression under first-line treatment with sorafenib [341]. Furthermore, a synergistic effect of sorafenib and resminostat was found in mesenchymal HCC cell lines rather insensitive to sorafenib treatment. Moreover, resminostat treatment decreased expression of mesenchymal markers in those cells and increased the expression of epithelial markers, furthermore their stemness and invasive properties were decreased [342].

3.3 Aim of the study

Hepatocellular carcinoma (HCC) is the second most common cause for cancer-related death worldwide. The standard treatment for patients with advanced HCC is sorafenib, which is a multikinase inhibitor and was found to prolong the time of tumor progression and improved the overall survival of the patients by two to three months. However, the use of Sorafenib was found to be hampered by two phenomena, by severe side effects and by the development of drug resistance leading to progression of the tumor after initial response to chemotherapy. Several observations suggested activation of compensatory pathways upon drug treatment leading to the so-called evasive resistance. Therefore, in this project, we wanted to examine how cancer cells respond to sorafenib and to delineate the mechanism of evasive resistance to sorafenib in HCC. These results might shed light on improving the efficacy of sorafenib in HCC patients and additionally on overcoming the development of evasive resistance to sorafenib therapy. Therefore, we made use of available cultured cell lines derived from HCC patients. In a first attempt, we wanted to determine the IC50 for sorafenib of a number of HCC cell lines. This enabled us to differentiate between the more sensitive cell lines and intrinsically drug resistant ones. We then sought to establish sorafenib resistant cell lines out of the most susceptible ones by treating the cells either with constant high or slowly increasing sorafenib concentrations. Following, we wanted to characterize them using different cellular assays, qRT-PCRs and immunofluorescent staining. However, the main goal was to identify genes and pathways altered which contribute to and might mediate evasive resistance to sorafenib. Therefore, we performed RNA sequencing comparing the established resistant to control cells. This allowed the identification of pathways and genes involved in evasive resistance to sorafenib and which might function as predictive biomarkers. Those will be further analyzed and functional tested in cellular assays *in vitro* and in transplantation experiments *in vivo*.

3.4 Results

3.4.1 Development of sorafenib-resistant cell lines

In order to examine evasive resistance mechanisms to sorafenib, in this project we set out to establish sorafenib-resistant cell lines. In a first step, the growth curves and the corresponding IC50 values for sorafenib treatment of several HCC cell lines were determined, in order to differentiate more sensitive cell lines from intrinsically drug-resistant ones (Fig. 1A, 1B). The four most treatment-susceptible cell lines, Huh7, Huh6, HepG2 and Hep3B, were treated with either stepwise increasing concentrations (called I.R.) of sorafenib or constant high concentrations (called C.R.) to establish resistant cell lines. We were successful in establishing sorafenib-resistant Huh7 and Hep3B cell lines with both approaches (Fig. 1C, 1D). With the I.R. approach, the IC50 of the Huh7 cell line was raised from initial 1.9 µM to 10.7 µM and for the Hep3B cell line from 3.1 µM to 6.8 µM. Using the C.R. approach IC50 levels were raised to 10.8 µM and 6.6 µM for the Huh7 and Hep3B cell line, respectively, resulting in constant 7 µM and 5 µM sorafenib applied to Huh7 and Hep3B cells, respectively (Fig. 1D). These IC50 concentrations are close to the clinically relevant concentration of approximately 10 µM [343]. Additionally, the Huh1 cell line was made resistant by treating them with increasing sorafenib concentrations (I.R.) resulting in an increase of the IC50 from 3.9 µM to 7.6 µM (Fig. 1D).

A

Cell line	Derivation
HLE	HCC
Huh1	HCC
Huh6	Hepatoblastoma
Huh7	HCC
HEPG2	HCC
Hep3B	HCC
SNU-182	HCC grade III/IV
SNU-449	HCC grade III/IV
SNU-387	HCC grade IV/V
SNU-398	HCC
SNU-423	HCC grade III/IV
SNU-475	HCC grade II-IV/V
PLC/PRF/5	HCC

B

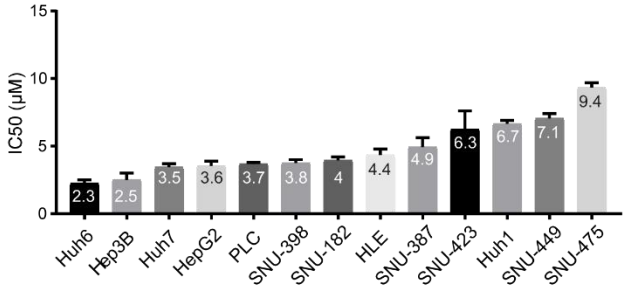

C

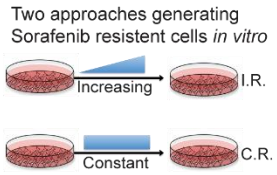

IC50 of control and resistant cells

Cell lines	IC50 (μM)
Huh7 DMSO	1.9
Huh7 I.R.	10.7
Huh7 C.R.	10.8
Hep3B DMSO	3.2
Hep3B I.R.	6.8
Hep3B C.R.	6.6

D

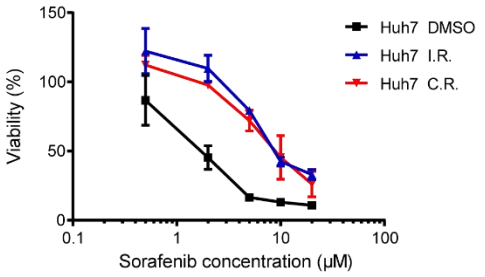

E

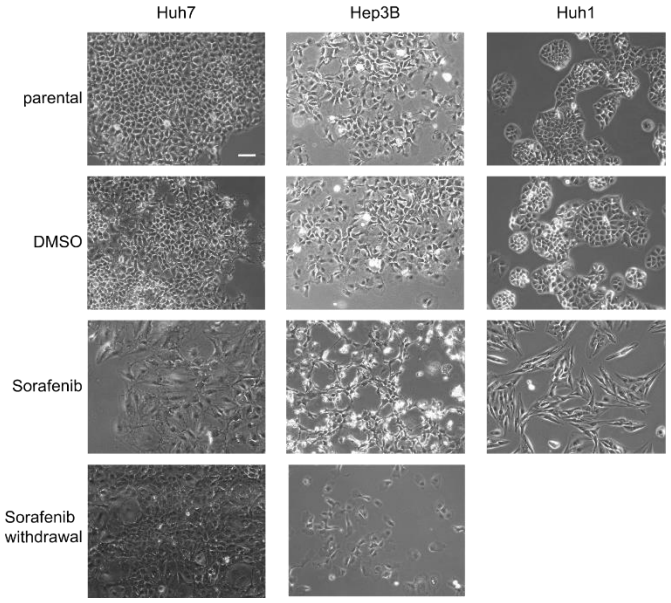

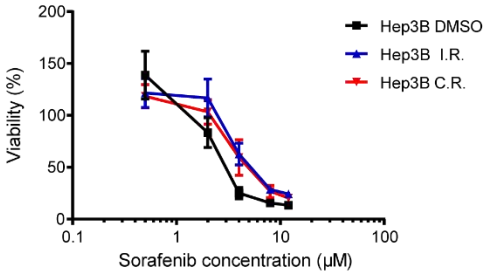

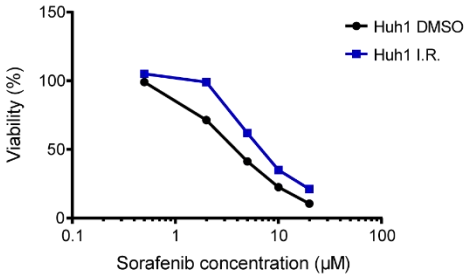

Figure 1. Establishment of sorafenib-resistant cell lines. (A) List of HCC cell lines used in this study. **(B)** Summary of IC50s measured for sorafenib treatment. **(C)** Approaches used to establish sorafenib cell lines. Increasing (I.R) or constant high (C.R.) sorafenib concentrations were applied to the cells resulting in an increase of the IC50. Table with IC50 values of the Huh7 and Hep3B resistant cell lines that were developed and the values for their corresponding control lines determined in three independent experiments. **(D)** Dose response curve and IC50 determination for sorafenib of Huh7 (n=4, for Huh7 C.R. n=3), Hep3B (n=3) and Huh1 (n=1) cells. **(E)** Morphological changes induced in the established sorafenib-resistant cell lines. Phase contrast microscopic image of Hep3B, Huh7, Huh1

parental, control (DMSO) and established resistant (I.R.) cells as well as Hep3B and Huh7 I.R. after three weeks of sorafenib withdrawal. Scale bar: 100 µm.

3.4.2 Characterization of the resistant cell lines

Compared to the parental and control (DMSO) cells, the resistant cell lines had a more mesenchymal morphology (Fig. 1E) and tend to detach easier from the plate surface upon trypsinization and grew much slower. However, after three weeks of sorafenib withdrawal the Huh7 I.R. cell line changed back to a more epithelial morphology and the IC50 was decreased to 7 µM. Moreover, the morphology of the Hep3B cell line reverted as well upon withdrawal (Fig. 1E). Since the resistant cells depicted a more mesenchymal morphology, immunofluorescence (IF) staining for EMT-related markers (E-cadherin, Vimentin, Zonula Occludens-1 (ZO-1) and F-actin) were performed. In the Huh7 I.R. cells, it revealed the expression of mesenchymal features compared to the vehicle-treated control and parental cells that appeared to be rather epithelial. The expression of E-cadherin and ZO-1 was lost at the cell membrane and Vimentin was found to be upregulated in the resistant cells. Furthermore, in the control cells cortical actin fibers, whereas in the resistant cells actin stress fibers were found (Fig. 2A). These results were further confirmed by quantitative RT-PCR which showed an upregulation of mesenchymal markers (N-cadherin, *Vimentin, Snail2, Fibronectin, Zeb1* and *Twist*) and a downregulation of *E-cadherin* compared to the vehicle-treated control (Fig. 2B). In line with these results, Huh7 I.R. cells revealed an approximately three-fold increase in migratory capacity in a scratch wound as well as in a transwell migration assay (Fig. 2C, 2D). Upon removal of sorafenib for three weeks the migratory capacity decreased again. Furthermore, the Huh7 and Hep3B resistant cell lines showed a reduced expression of the differentiation and diagnostic HCC marker *alpha-fetoprotein* (*AFP*) as well as for two other diagnostic HCC markers, *Glypican-3* (*GPC3*) and *heat shock protein 70* (*HSP70*). *Albumin*, a hepatocyte marker was found to be downregulated as well. Upon withdrawal of sorafenib, the expression of *HSP70* was found to be again similar to the control cells (Fig. 3A, 3B). Furthermore, *CD44* and *CD133*, well-known stem-cell markers, are upregulated in the Huh7 I.R. and C.R. cell lines (Fig. 3C). In summary, these results show that the resistant cells seem to undergo an EMT-like process and become more migratory. Furthermore, they reduce the expression of diagnostic HCC markers and upregulate stem cell markers which might

hint to the acquisition of stem cell properties rendering the cells more resistant to sorafenib. Moreover, the sorafenib-induced stress seems to result in reversible mechanistic adaptation, indicating that sorafenib-induced resistance in our models is most likely due to epigenetic, transcriptional and/or translational changes rather than genetic mutations.

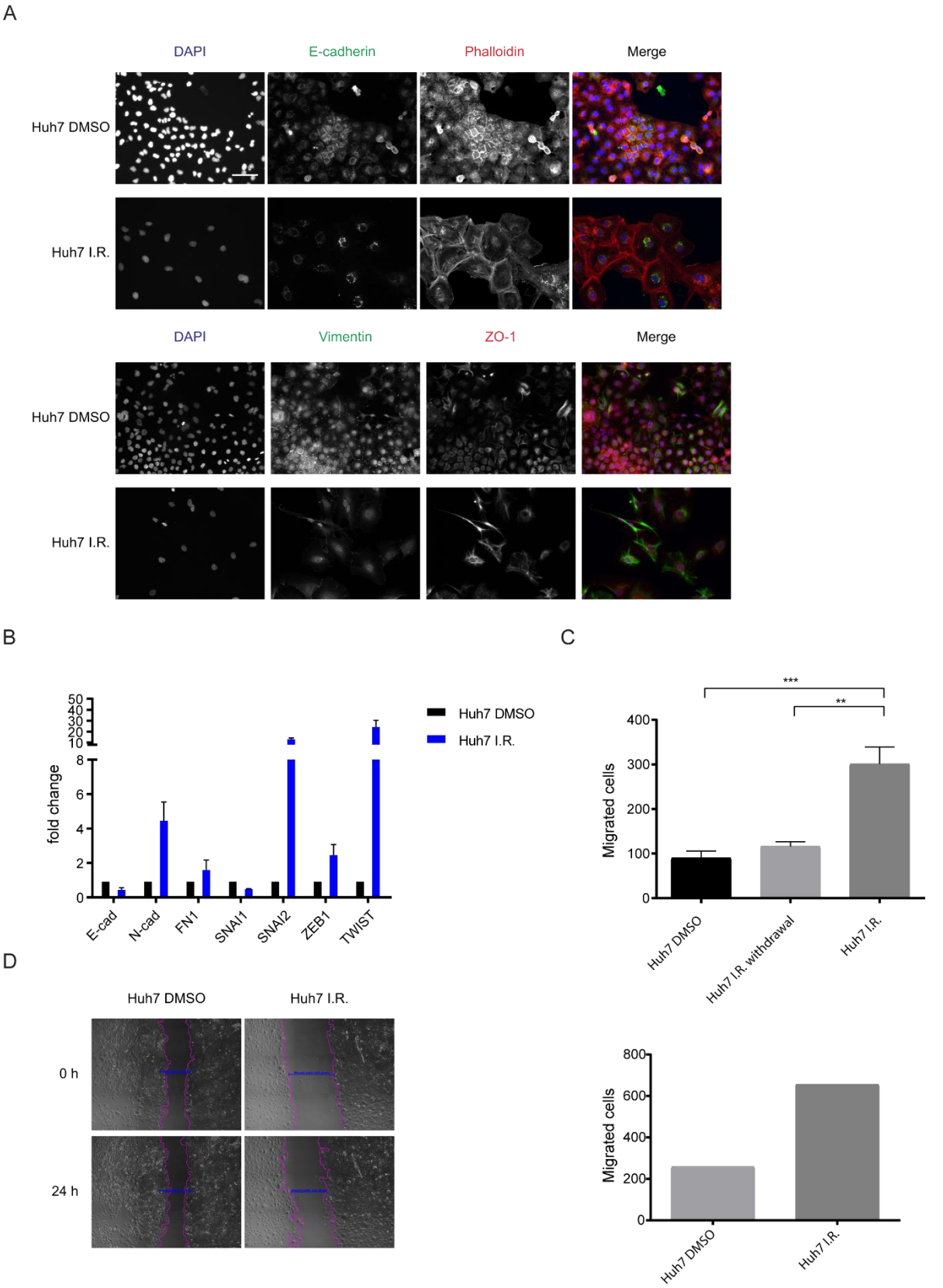

Figure 2. Sorafenib-resistant cells become more mesenchymal. (A) Immunofluorescence staining for EMT-related marker (E-cadherin, F-actin (Phalloidin), Vimentin and ZO-1 comparing Huh7 I.R. to Huh7 control (DMSO) cells. Loss of the epithelial markers at the cell membrane and upregulation of Vimentin were observed as well as changes from cortical actin to actin stress fibres in the resistant cells.

DAPI was used to visualize nuclei. Scale bar: 100 µm. **(B)** qRT-PCR for EMT related markers comparing Huh7 control to established resistant (I.R.) cells. Reduced expression of E-cadherin as well as upregulation of mesenchymal markers N-cadherin, *Fn1*, *Snai2, Zeb1* and *Twist* were found. n=2. Data are displayed as mean ± SEM. **(C)** Migration assay performed comparing Huh7 control DMSO), Huh7 I.R. and Huh7 I.R. after three weeks of sorafenib withdrawal. I.R. cell show an around three-fold increase in the number of migrated cells which is again reduced to the level of the control after sorafenib withdrawal. Data are displayed as mean ± SEM. Statistical analysis was performed using ordinary one-way ANOVA multiple comparison test. n=4; ** P < 0.01, *** P < 0.001. **(D)** Cell IQ images of a scratch wound assay performed to determine the migratory capacity comparing Huh7 control (DMSO) to Huh7 I.R. cells. **(E)** Quantification of the scratch wound assay showing an around three-fold increase in the migratory capacity of the sorafenib-resistant cells. n=1.

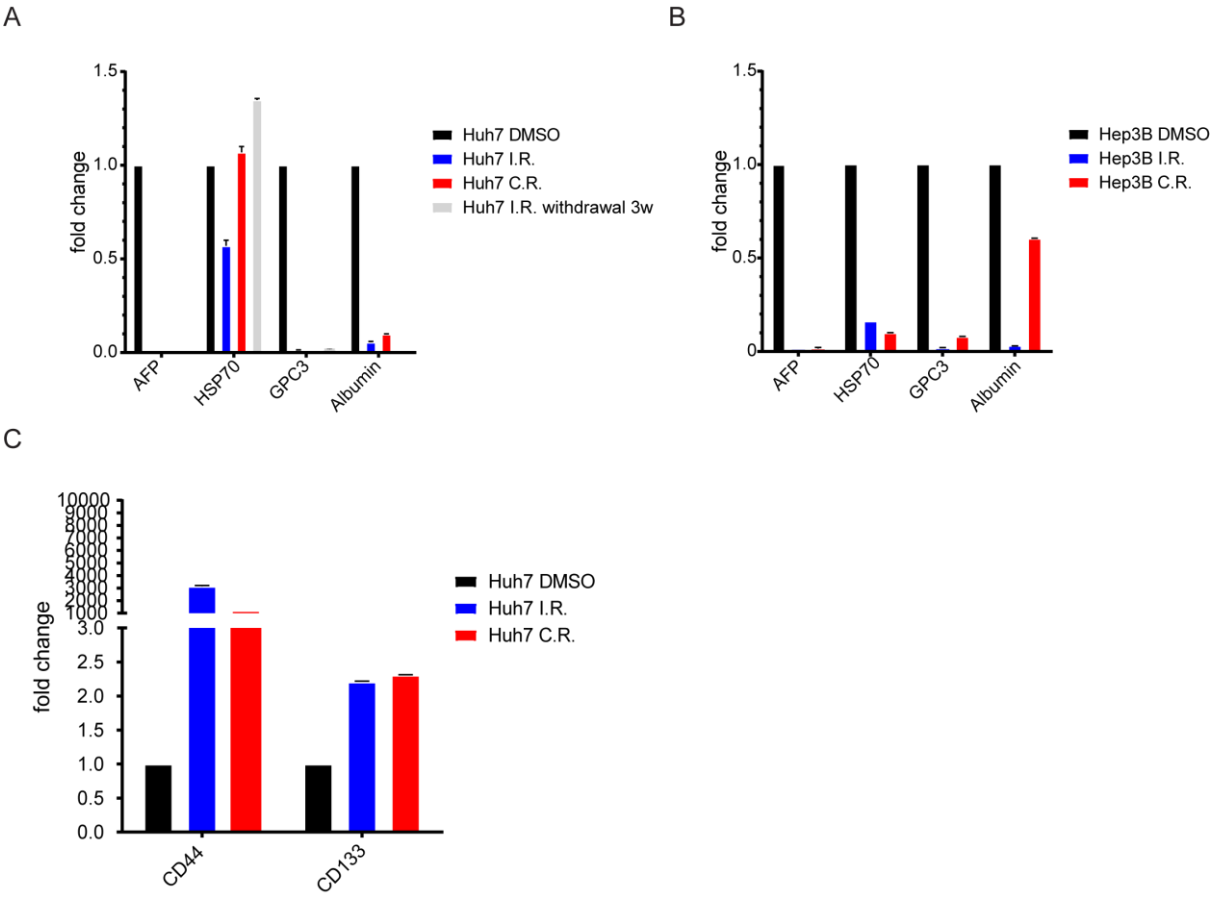

Figure 3. Expression of diagnostic HCC markers and stem cell markers in resistant cell lines. (A) qRT-PCR for hepatocyte and diagnostic HCC marker in Huh7 DMSO, I.R. C.R. and I.R. cells after three weeks of sorafenib withdrawal. n=2. *Albumin* expression has not yet been analysed for the Huh7 I.R. after three weeks of sorafenib withdrawal. A reduced expression of *AFP, GPC* and *Albumin* was found in the established resistant cells as compared to the control. In the I.R. cells also the expression of *HSP70* is reduced which increased again upon sorafenib withdrawal for three weeks. **(B)** qRT-PCR for hepatocyte and diagnostic HCC marker in Hep3B DMSO, I.R. and C.R. cells. The expression of *AFP, Hsp70, GPC3* and *Albumin* is reduced in the established resistant cells as compared to the DMSO treated control. n=2 **(C)** Examination of the expression of stem cell markers *CD44* and *CD133*. Huh7

I.R. and C.R. cells show an upregulation of the expression as compared to the control. n=2. . Data are displayed as mean ± SEM.

3.4.3 HDAC inhibitor treatment reverts the mesenchymal morphology of resistant HCC cells and sensitizes them to sorafenib treatment

EMT also seems to be regulated by epigenetic modifications and also in HCC several epigenetic alterations like histone modifications, DNA methylation and non-coding microRNA patterns have been found [344]. Furthermore, in our laboratory it has already been observed that HDAC inhibition restores the epithelial cell morphology of an established stable mesenchymal cell line (Kilinc et al., submitted for publication). Thus, we wanted to test HDAC inhibitors in HCC to examine if the morphology of the established sorafenib-resistant cells as well as of the intrinsically resistant HCC cell lines might revert from mesenchymal to epithelial and if the cells thereby become more susceptible to sorafenib. Treatment of either sorafenib-sensitive (PLC) as well as intrinsically resistant (SNU-449, SNU-475) cell lines with the pan-HDAC inhibitor pracinostat had an inhibitory effect on proliferation in all cell lines tested (Fig. 4A). Co-treatment of intrinsically resistant HCC cell lines with the pan-HDAC inhibitors trichostatin A (TSA) or pracinostat with sorafenib for three days showed an additive effect on cell growth inhibition and decreased the IC50 for sorafenib (Fig. 4B). The IC50 decreased from 6.8 µM to 2.5 µM with TSA and to 4.5 µM with pracinostat co-treatment in SNU-445 cells. Short treatment (3 days) of SNU-449 cells with TSA had no effect on the morphology or the expression and localisation of EMT related marker as assessed by immunofluorescence staining (data not shown). However, upon long-term (7 days) HDACi treatment with TSA or entinostat (HDAC1 and HDAC3 inhibitor), a subset of cells showed a more epithelial morphology (Fig. 4C). These results show that HDAC inhibitors might be able to increase the sensitivity of the resistant cells to sorafenib and revert them to a more epithelial morphology, indicating that histone acetylation-dependent epigenetic modifications might play an important role in mediating sorafenib resistance.

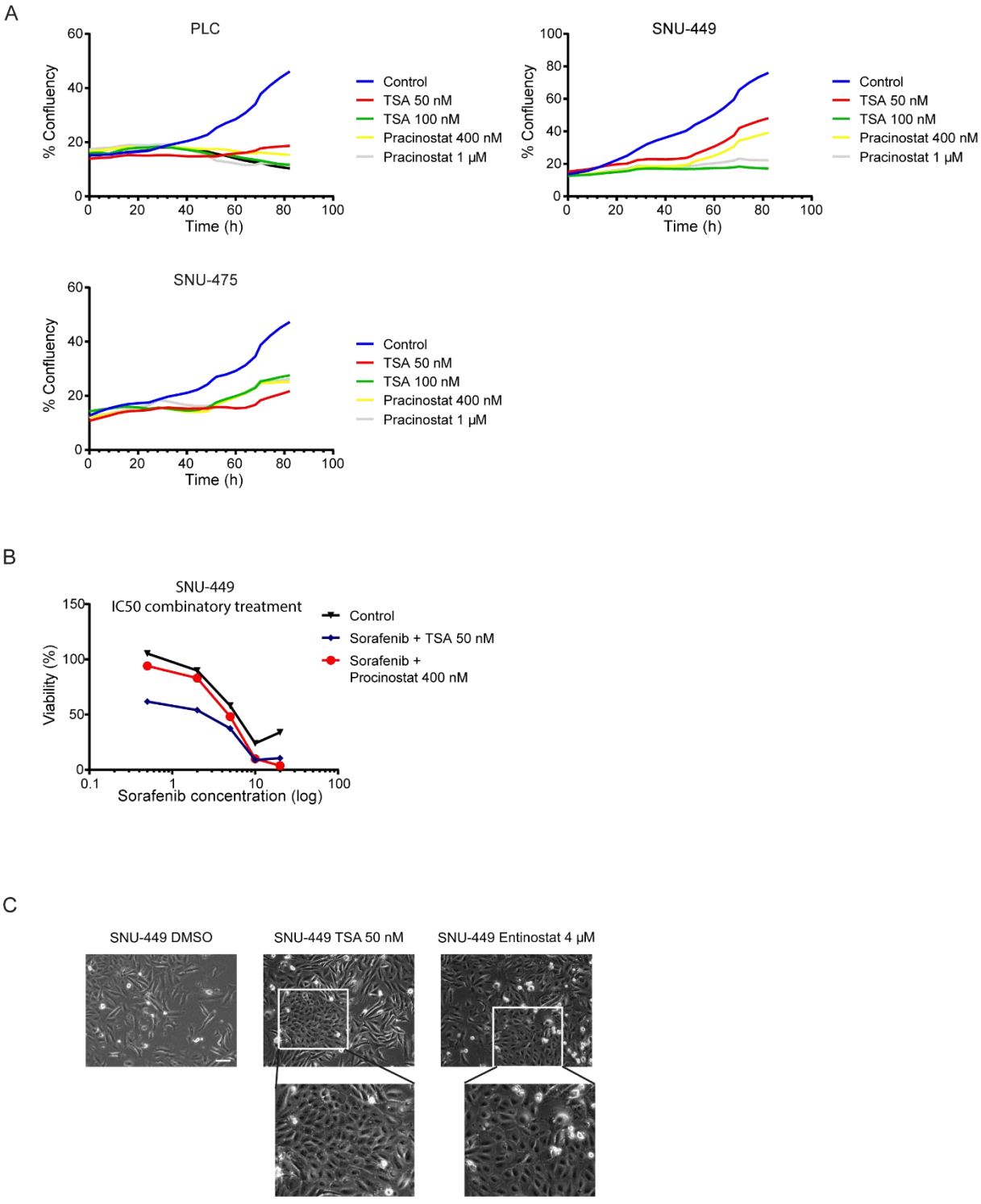

Figure 4. HDACi treatment to sensitize sorafenib-resistant cells. (A) Growth curves of sorafenib-sensitive PLC and intrinsically sorafenib-resistant cell lines SNU-449, SNU-475 upon treatment with pan-HDAC inhibitors TSA and Pracinostat. A growth inhibition was found in all cell lines treated with the HDAC inhibitors. **(B**) Dose response curve and IC50 determination for sorafenib by co-treatment with pan-HDAC inhibitors TSA or pracinostat in intrinsically resistant SNU-449 cells. Synergistic effect of sorafenib with both HDAC inhibitors was found. **(C)** Changes in morphology of SNU-449 cell upon HDACi treatment with TSA or Entinostat. A subset of cells became more epithelial upon HDACi treatment for three days. n=1. Scale bar: 100 µm.

3.4.4 Pathway analysis of differentially expressed genes common to the established resistant cell lines

To determine the differences in gene expression between the control (DMSO)-treated and the established sorafenib-resistant cell lines, gene expression profiles were established by next generation RNA sequencing. Gene expression between the established Huh7 and Hep3B I.R. and C.R. as well as the third established Huh1 I.R. cell line were compared to two intrinsically resistant cell lines (SNU-449, SNU-475) to identify shared genes and pathways between the acquired resistant cell lines and the intrinsically resistant cell lines. Hierarchical clustering distinguishes the Huh7 and Hep3B control (DMSO)-treated samples and the established as well as the intrinsically sorafenib-resistant cell lines from each other. The intrinsically resistant cells cluster together independent of the treatment using DMSO (control) or sorafenib for three days. The established resistant cell lines cluster together irrespectively of their origin (Fig. 5A).

Further analysis investigated commonly affected pathways as well as differentially expressed genes (DEGs) in the established resistant cell lines compared to their controls. There were 191 genes commonly up and 119 genes commonly downregulated in the established resistant cell lines. Subsequently, to better understand the biological function of the DEGs, pathway analysis was performed of the transcriptome data to determine which pathways were most significantly altered between the two groups. Using the Reactome database, of the top 20 significantly enriched upregulated pathways, several were involved in ECM organisation and cell surface interactions which were also associated with EMT. Among the top upregulated were pathways, such as extracellular matrix (ECM) organization, non-integrin membrane-ECM interactions, MET (MET Proto-Oncogene, tyrosine-protein kinase Met) promotes cell motility, signaling by MET, collagen formation, metalloprotease DUBs (deubiquitinating enzymes), interleukin-7 signalling, ECM proteoglycans, laminin interactions and syndecan interactions (Fig. 5B). These results show that in the resistant cells multiple membrane-related signaling events are happening that are related to EMT, suggesting a major role of EMT in sorafenib resistance formation. Downregulated genes belonged mainly to pathways associated with epigenetic alterations, among them are HATs acetylate histones, HDACs deacetylate histones and PRC2 methylates histones, and DNA methylation (Fig. 5C). However, genes

falling into these pathways were mainly histone components, such as *HIST1H2AD, HIST1H2AB, HIST2H2AA3, HIST2H2AC, HIST1H2BL, HIST1H2BN, HIST1H2BC, HIST1H2BO, HIST2H2BE, HIST2H4A, HIST2H4B* and *HIST2H2AA4*. Further pathways significantly affected were associated with cell cycle control: M phase, G2/M checkpoints, cell cycle checkpoints, G2/M DNA damage checkpoints, and meiosis and mitotic prophase. In summary, the RNA sequencing results show so far that the established resistant cells share some alterations and mechanisms. Several pathways are associated with EMT in line with the previous cell culture observations. Furthermore, the reversibility of the resistance by sorafenib withdrawal together with the affected pathways involved in chromatin structure, further confirm the previous results (Fig. 1E) that rather epigenetic changes might be causal for the resistance in or established cell lines than genomic mutations. The RNA sequencing data are currently being further analyzed, and novel pathways and genes which might be involved in mediating evasive resistance to sorafenib will be further examined and functionally tested. Therefore, and to further narrow down genes mediating evasive resistance, a synthetic lethal screen with a genome-wide shRNA library has recently been performed by colleagues in the laboratory and novel genes of interest will be validated and investigated by further *in vitro* experiments.

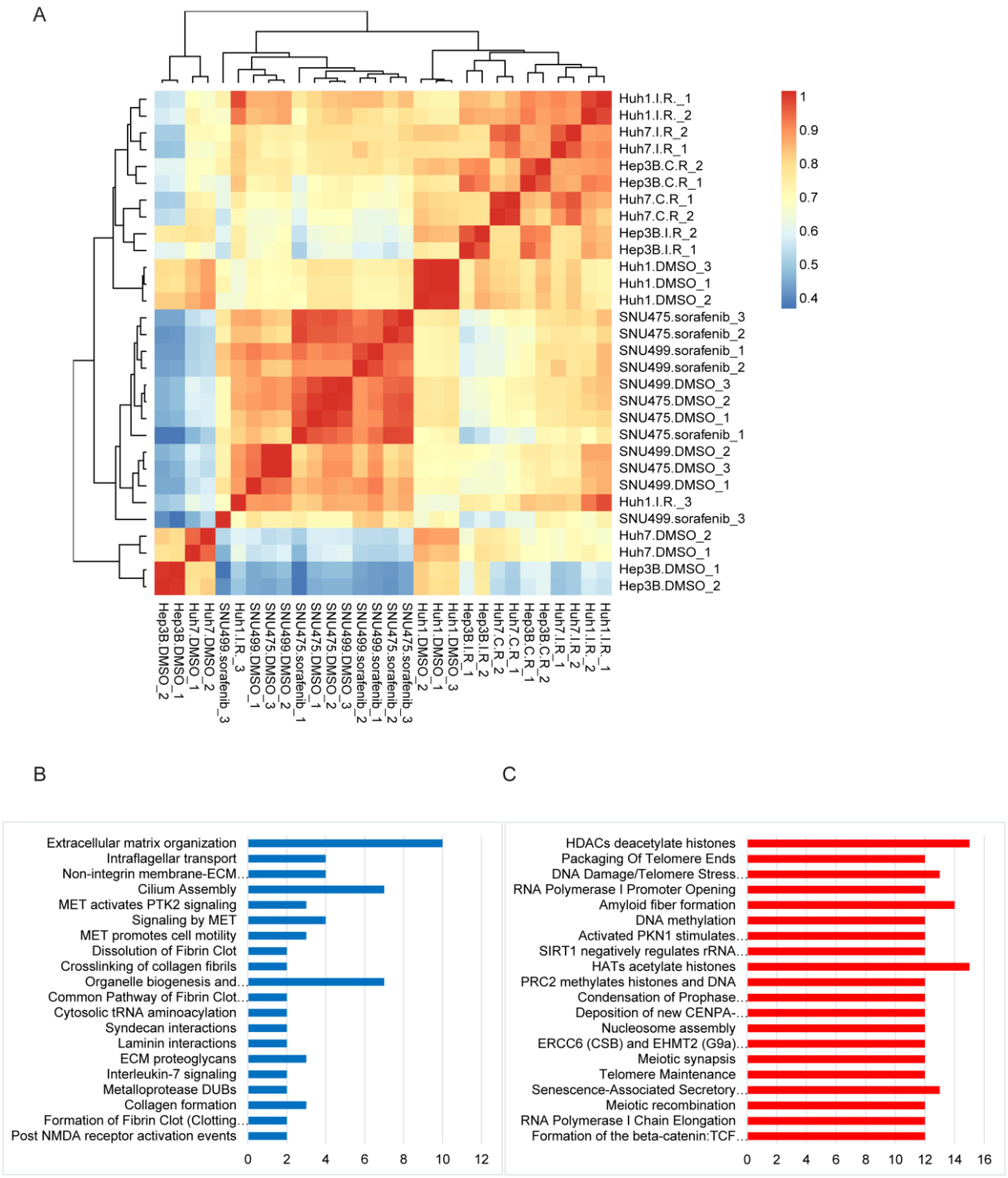

Figure 5. Transcriptome analysis of sorafenib-resistant cells. (A) Unsupervised hierarchical clustering of gene expression profiles of intrinsically resistant SNU-449 and SNU-475 cells treated for three days with sorafenib or vehicle (DMSO), established resistant cell lines Huh1 I.R., Huh7 and Hep3B I.R. and C.R. and their vehicle treated (DMSO) controls. The colours indicates the correlation value. **(B)** DEGS pathway enrichment using Reactome database. Top upregulated 20 REACTOME pathways selected by statistical significance in terms of common DEGs in the established resistant cells as compared to their control. **(C)** DEGS pathway enrichment using Reactome database. Top 20 downregulated REACTOME pathways selected by statistical significance in terms of common DEGs in the established resistant cells as compared to their control. Depicted in blue are up-regulated pathways,

in red down-regulated pathways. The number of DEGs per pathway is depicted.

3.5 Discussion

Sorafenib is the sole systemic treatment for patients with advanced HCC that shows survival benefit. However, sorafenib treatment may cause side effects and patients eventually show progression after initial response due to the development of therapy resistance. Therefore, in this project, we wanted to elucidate these effects by developing sorafenib-resistant cell lines to further delineate the mechanisms which might lead to evasive resistance in those cells. This has been accomplished by two different approaches. By slowly increasing the sorafenib concentrations we have positively selected for intrinsically resistant cells but also allowed stepwise adaptation to the increasing concentration. The treatment with initially high concentration might better represent the situation in patients, those cells might develop different mechanisms of resistance compared to the ones selected via increasing doses.

3.5.1 Sorafenib resistance and EMT

At first, we have observed that the resistant cells adapted a more mesenchymal morphology as compared to the control cells. This has then been confirmed by immunofluorescent stainings and qRT-PCR in Huh7 I.R. cells for EMT markers. In our resistant cells there seems to be an increased expression of *N-cadherin, SNAI2, ZEB1* and *TWIST* and a slight downregulation of *E-cadherin*. *SNAI2, ZEB1* and *TWIST* have been shown to be able to silence *E-cadherin* expression [193, 222, 345]. Similar observations have meanwhile been made for the Huh7 C.R. cell line by a colleague in the laboratory (M. Morini., unpublished results). The Huh7 I.R. resistant cells also became more motile and this notion has to be analyzed further as well for the other cell lines. However, those changes do not seem to be due to genomic mutations, since the Huh7 I.R. and Hep3B I.R. resistant cell lines reverted back into a more epithelial morphology upon sorafenib withdrawal, including a decreased sorafenib IC50, and showed a lower migratory capacity. Sorafenib withdrawal and its effect has also to be analyzed for the other established cell lines. In general, also the intrinsically resistant cell lines show a more mesenchymal morphology compared to the more sensitive cell lines. This suggests an important contribution of EMT to sorafenib resistance. Similar observations for sorafenib resistance have been made in renal cell carcinoma cell lines in which the sorafenib resistance was also reversible [346]. EMT is the mechanism

allowing epithelial cells to gain mesenchymal properties important for example during embryonic development. Epithelial immobile cells show apical-basal polarity and intact cell-cell junctions that connect neighboring cells. Mesenchymal cells are motile cells showing an elongated phenotype. The epithelial marker E-cadherin has been found to be lost in 69% of HCC patients [347]. Moreover, high expression of TWIST, which acts as a negative regulator of E-cadherin has been found in many primary HCCs and metastasis. TWIST expression has also been found to be significantly increased in metastatic HCC cell lines compared to non-metastatic ones [348]. TGFβ is a potent inducer of EMT and TGFβ signatures in patients have been demonstrated to correlate with an invasive phenotype and HCC metastasis. Also a late TGFβ signature which has been established in mouse primary hepatocytes, has been found to correlate with a more aggressive and invasive phenotype of HCC tumors in patients [349]. In HCC, different studies have already shown the potential role of EMT in development of resistance. Sorafenib itself has also been found to influence and alter the cytoskeleton by inhibiting actin polymerisation in Hep3B and PLC cell lines [350]. However, sorafenib has also been found to suppress EMT which has been induced by insufficient radiofrequency ablation (RFA) [351]. In another study, two different HCC cell lines established from one patient have been analysed to examine drug efficacy, one showing an epithelial, the other one a mesenchymal morphology revealing that the mesenchymal cell line was more resistant to sorafenib and erlotinib treatment as compared to the epithelial cell line [301]. In addition to an increase in mesenchymal markers and decrease in epithelial markers, the Huh7 I.R. and Hep3B I.R. resistant cells also showed reduced expression of diagnostic HCC and hepatocyte marker. *HSP70, GPC3, GS* and *Albumin* are commonly used clinical biomarkers for HCC. AFP is a glycoprotein found being expressed by fetal hepatocytes as well as in HCCs and shows an increase in many HCC patients. HSP70, GPC3, and GS are used as biomarkers by immunohistochemistry staining of biopsies to distinguish hepatocellular carcinoma from dysplastic hepatocellular nodules. Albumin can be detected in human plasma and is a marker for hepatocytes. High plasma values have been found to correlate with increased HCC recurrence rates in patients [266, 267, 352-357]. The loss of these markers and the increased expression of stem cell markers (*CD44, CD133*) in Huh7 I.R. and C.R. cells might suggest a dedifferentiation of therapy-resistant cells. Several studies have already shown the connection between an EMT and the acquisition of stem cell properties [165, 223]. Additionally, the expression of

CD44 linked to active TGFβ signalling has been found to confer a lack of response to sorafenib treatment [299]. In summary, these results show that therapy resistance results in EMT and the loss of HCC markers *in vitro.* The loss of diagnostic HCC marker expression hampers the monitoring of patients after initial sorafenib treatment for resistance formation. These notions have to be examined as well in all the established as well as in the intrinsically resistant cell lines to determine if these are common observations in sorafenib-resistant cells. To assess the contribution of EMT to sorafenib resistance, Huh1 cells have been long-term treated with TGFβ resulting in an EMT. These cells became more resistant to sorafenib as well and were included in the transcriptomic analysis (M. Morini, unpublished findings). The comparison of Huh1 control, Huh1 I.R. and the TGFβ long-term treated cells will give further insights into the contribution of an EMT to sorafenib resistance.

3.5.2 HDAC inhibition, EMT and sorafenib resistance

Epigenetic changes such as DNA methylation, changes in histone modification and aberrant expression of mRNAs and long noncoding RNAs have been found to be associated with HCC. Such changes are also thought to play a role in development of resistance and EMT [344]. Since in our cellular models, cell morphology and resistance seem to be reversible upon sorafenib withdrawal, epigenetic changes might contribute to the underlying mechanism. Furthermore, inhibition of dysregulated genes contributing to tumor progression, metastasis formation and evasive resistance to treatment by using drugs affecting epigenetic structures might be an alternative or supplementary treatment approach. Previous studies have already revealed synergistic effects of co-treatments with HDACis and different chemotherapeutic drugs. A pre-clinical study has shown efficacy of treatment with resminostat alone or combined with sorafenib in patients that showed progression under first-line treatment with sorafenib [341]. Furthermore, EMT has been found to be reverted by treatment with HDACis [342]. During EMT several epigenetic changes have been observed, for example the hypermethylation of *miR-200* family promotor was found to result in the increased expression of *ZEB1* and *ZEB2*, correlating with mesenchymal characteristics in cancer cell lines [358]. In terms of histone modifications, acetylation of *SNAI1* by the p300 lysine acetyltransferase has been found to induce EMT in lung

cancer cells. Knockdown of *p300* led to a decrease of *SNAI1* and increase of *E-cadherin* expression [359]. *p300* has furthermore been found highly expressed in 47 % of HCC patient-derived samples and correlated with worse survival, advanced staging and intrahepatic metastasis. The *in vitro* depletion of *p300* resulted in an increased expression of *E-cadherin* together with a downregulation of SNAI1, Twist and HIF-1α and suppressed migration and invasion of the cells [360]. On the other hand, HDAC inhibitors like TSA and SAHA have been shown to induce an EMT phenotype in prostate cancer cells. Moreover, changes in the morphology as well as in the expression of EMT related markers and increased acetylation of proximal promoters of EMT-related genes have been observed [361]. Furthermore, a synergistic effect of sorafenib and resminostat has been found in mesenchymal HCC cell lines rather insensitive to sorafenib treatment. Moreover, resminostat treatment decreased the expression of mesenchymal markers in these cells and increased the expression of epithelial markers, whereas their stemness and invasive properties were decreased [342]. In this project we show, that treatment of HCC cell lines with pan-HDAC inhibitors alone already has an effect on the growth of the cell lines tested. Combinatorial treatment with sorafenib on intrinsically resistant cells resulted in a synergistic effect and seemed to affect cell morphology as well. This notion has to be further tested in the sorafenib-resistant cell lines established. Hence co-treatment with HDAC inhibitors might have a beneficial effect in treatment of HCC patients as well. Clearly, the interplay and interactions between HDACi, EMT and sorafenib resistance in our models merit further investigations.

3.5.3 Transcriptomic analysis of sorafenib resistance

RNA sequencing comparing parental sensitive to established resistant cells and intrinsically resistant cells demonstrates that the established resistant cells cluster together. The same is true for the intrinsically resistant cell lines. Hence there seem to be common mechanisms that might confer sorafenib resistance, which was further examined by functional enrichment analysis. Pathway analysis using Reactome revealed that amongst the pathways commonly upregulated in the established resistant cells are several that are involved in the extracellular matrix organisation and interactions which are associated with EMT. During EMT there are changes in the cell-

cell and cell-ECM interactions and also ECM components themselves are found to be regulated during an EMT [208, 362]. One pathway found to be commonly upregulated is the MET pathway which is known to be able to stimulate cancer cell motility. In this pathway the binding of HGF (hepatocyte growth factor) to the transmembrane receptor c-MET (MET or HGFR) is able to activate the RAS-MAPK and PI3K/AKT signaling pathways. Expression of MET has been found to be increased in HCC as compared to normal liver tissue and to correlate with poor prognosis [363]. Additionally, high levels of p-MET have been found to be associated with resistance to sorafenib treatment in mice [364]. *In vitro* experiments have revealed that sorafenib-resistant HCC cells were overexpressing *HGF* and *c-Met*. Treatment using c-Met inhibitors enhanced the effects of sorafenib and showed growth inhibition of sorafenib-resistant HCC cells [365]. Knockdown of *MET* in HCC cell lines has furthermore been found to reduce proliferation, colony formation and migration *in vitro* and tumor growth as well as angiogenesis and metastasis formation *in vivo* [364]. Furthermore, many downregulated genes in our study seem to be associated with epigenetic regulation, especially with histone modification and cell cycle control. These results are compatible with our *in vitro* observations. However, when looking at the genes commonly and significantly up- or downregulated within the previously observed alterations in EMT-related marker expression, only *N-cadherin* was found to be significantly upregulated. Not only the expression levels but also the localization of EMT markers like E-cadherin have to be considered. Therefore, IF staining would be needed to further evaluate the localisation of EMT-related markers in the established resistant cell lines. Moreover, expression of *AFP*, one of the clinical serum biomarkers for HCC, was not downregulated in all resistant cell lines, whereas *HSP70* and *GPC3* showed no change in expression levels. Similarly, the increased expression of *CD44* and *CD133* in the Huh7- and Hep3B I.R. cells by qRT-PCR was not found to be common for all the cell lines. Hence, mechanisms related to EMT and involving epigenetic changes might be shared, however, different genes might be affected and the common denominator conferring resistance still has to be identified. The PI3K pathway which has been previously reported to confer sorafenib resistance was not amongst the commonly altered pathways [291]. Also there are no ABC transporters amongst the common differentially expressed genes found that might promote sorafenib efflux [312, 314]. To further dissect these highly complex results, a synthetic lethal screen with shRNA libraries has been performed to narrow down the number of genes involved in

resistance development. The data is currently being analyzed and candidate genes are being tested *in vivo* and *in vitro*. It has to be further examined whether acquired sorafenib resistance is based on a similar or the same mechanism as the intrinsic resistance observed in some of our cell lines. Even though they do not cluster together, it is well possible and reasonable that they share common mechanisms of resistance development. One of these might involve epigenetic changes that promote EMT. Therefore, further and more stringent analysis of the RNA sequencing data and subsequent functional validation will be required to eventually pinpoint common denominators of sorafenib resistance in HCC cells. In conclusion, we demonstrate that sorafenib-resistant cell lines seem to undergo an EMT and become more migratory. The morphology as well as the sensitivity seems to be partially restored by treatment with HDACi. Furthermore, preliminary results show overlapping mechanisms between different cell lines.

3.6 Material and Methods

Antibodies and Reagents

Antibodies: Purified Mouse Anti-E-Cadherin (610182, BD Biosciences), ZO-1 Polyclonal (617300, Thermo Fisher Scientific), Vimentin (NB300-223, Novus Biologicals), Alexa Fluor™ 568 Phalloidin (A12380, Thermo Fisher Scientific), 4′,6-Diamidino-2-phenylindole (DAPI, D9542, Sigma-Aldrich),
HDAC inhibitors: Trichostatin A (T8552, Sigma-Aldrich), Entinostat (MS-275, S1053, Selleckchem), Pracinostat (SB939, S1515, Selleckchem).

Cell culture

The cell lines Huh6, Huh7, PLC/PRF/5, Hep3B, SNU-182, SNU-387, SNU-449, and HLE were kindly provided by Dr. Luca Quagliata (Institute of Pathology, University of Basel). The Huh1 cell lines was obtained from CellBank Australia. HepG2 (ATCC HB-8065), SNU-398 (ATCC CRL-2233), SNU-423 (ATCC CRL-2238), SNU475 (ATCC CRL-2236) cell lines were purchased from ATCC. The Huh6, Huh7 and the HLE cell lines were cultured in Dulbecco's Modified Eagle's Medium - high glucose (D5671, Sigma-Aldrich). Huh1 cells in Dulbecco's Modified Eagle's Medium - low glucose (D6046, Sigma-Aldrich), PLC, Hep3B and HepG2 in Minimum Essential Medium Eagle (, M8042, Sigma-Aldrich) and the SNU- cell lines in RPMI-1640 Medium (R8758, Sigma-Aldrich). All growth media were supplemented with 10% Fetal Bovine Serum (FBS, F7524; Sigma-Aldrich), 2 mM L-Glutamine (G7513, Sigma-Aldrich), 100 U penicillin and 0.1 mg/ml streptomycin (P4333, Sigma-Aldrich). All cell lines were grown at 37 °C, 5 % CO_2, 95 % humidity. For experiments with HDACi, the cell lines were treated every day with the mentioned concentrations for three days. For long-term treatment every second day for seven days.

Cell-IQ

We determine the IC50 of all HCC cell lines for sorafenib, therefore cells were seeded into 24-well plates in duplicates. On the next day the cells were treated with increasing doses of sorafenib and put into the Cell-IQ (Model v.2., Chip-Man Technologies). Pictures were taken every 4 hours (hr) for three days and sorafenib was added every

day. To generate the growth curves, the Cell IQ analysis software was used and the IC50 was calculated.

Development of sorafenib-resistant cell lines

Establishment of sorafenib-resistant cell lines was performed by slowly increasing concentrations over time with a starting concentration just below the measured IC50 value, or with constantly high concentrations of sorafenib. Control cell lines were treated simultaneously under the same conditions with either increasing or constant high DMSO concentrations. To establish sorafenib-resistant cell lines, two different approaches were executed. The indicated cell lines were either incubated with sorafenib concentrations just below their IC50 and the concentration was slowly increased during the following weeks and months. In the second approach, the cells were exposed to high sorafenib concentrations and maintained at this concentration to select for resistant cells to grow. As a control cells were treated the same way with the same DMSO oncentration and kept in culture as well. The established cell lines were then continuously cultured in the presence of DMSO (control) or sorafenib (resistant cells).

Viability assay

To determine the IC50 of the control (DMSO) and established resistant cells, the ApoTox-Glo™ Triplex Assay (G6320, Promega) was used. The cells were plated into a 96 well plate. On the next day, the cells were treated with increasing sorafenib concentrations and treated for three days by daily addition of sorafenib. The viability of the cells was then measured according to the manufacturer's instructions and the measurements were performed using a plate reader (SPECTRAmax Gemini EM, Bucher Biotec) with subsequent calculation of the IC50.

Immunofluorescence of cultured cells

Cells were grown on uncovered glass coverslips (#1, 12 mm round, Menzel–Glaser) and treated for 3 days with sorafenib. After treatment, the cells were washed with 1x PBS and fixed with 4% paraformaldehyde/PBS for 15 min at room temperature. Following PBS washes, the cells were permeabilized with 0.2% TritonX-100/PBS for 5 min. Subsequently, blocking was performed with 3% BSA/0.01% Triton X-100/PBS for

1 hour. The indicated primary antibodies was then added in the appropriate dilution in 3% BSA/ 0.2 % PBS-T for 2 hr at room temperature. Afterwards incubation with a fluorophore-coupled secondary antibody (Alexa Fluor, Invitrogen) was performed for 1 hr at room temperature in the dark. Cell nuclei were counterstained with DAPI (D9542, Sigma-Aldrich). After staining, the coverslips were washed and then mounted in Fluorescence Mounting Medium (S302380-2, Dako) on microscope slides and imaged using a fluorescence microscope (DMI 4000, Leica).

Transwell Boyden Chamber Migration Assay

Trypsinized and washed cells were resuspended in growth medium containing 0.2% FBS. 25,000 cells were suspended in 500 µl 0.2 % FBS/DMEM and seeded into 24-trans-well migration (Corning, 353097) inserts in duplicates. The bottom chambers were filled with 750 µl of 20 % FBS/DMEM to create a chemo-attractant gradient. The cells were incubated in a tissue culture incubator at 37 °C with 5% CO_2. After 16 hr, the inserts were washed and fixed with 4% PFA/PBS for 10 min. Cells that did not migrate were removed with a cotton swab, and the remaining migrated cells were stained with DAPI. Images of five fields per insert were taken with a Leica DMI 4000 microscope and stained cells were counted using an ImageJ software plugin developed in-house.

RNA isolation and real-time qPCR

Total RNA was isolated using the guanidine isothiocyanate and phenol/chloroform method from TRI reagent (T9424, Sigma-Aldrich) harvested cells. Reverse transcription was performed using the ImProm-II™ Reverse Transcription System (A3803, Promega) according to the manufacturer's instructions. mRNA expression was quantified by real-time quantitativePCR by using the PowerUp™ SYBR™ Green Master Mix (A25743, ThermoFisher Scientific) according to the manufacturer's instructions. Human Riboprotein L19 (hRPL19) primers were used for normalization. qPCR assays were performed in duplicates, and the fold change was calculated using the comparative Ct method (ΔΔCt). Primer sequences are listed in Supplementary Table S1.

RNA sequencing and analysis

Total RNA was extracted from the established resistant cell lines (Huh7 I.R., C.R., Hep3B I.R., C.R. and Huh1 I.R.) their respective control cell lines as well as the intrinsically resistant SNU-449 and SNU-475 cell lines using miRNeasy Mini Kit (Qiagen, 217004) with on-column DNAse digestion according to the manufacturer's instructions . Biological duplicates for Huh7 and Hep3B and triplicates for Huh1, SNU-449 and SNU-475 were prepared for RNA sequencing. RNA quality control was performed using RNA ScreenTape on the Agilent 4200 TapeStation and the concentration was measured by using the Quanti-iT RiboGreen RNA assay Kit (Life Technologies). Libraries preparation for sequencing was prepared with 200 ng total RNA input using the TruSeq Stranded mRNA Library Prep kit (Illumina) and the quality was checked using the Fragment Analyzer standard sensitivity NGS kit (AATI). SR51 sequencing was performed on an Illumina HiSeq2500 sequencing system (HiSeq SBS kit v4).

Analysis of RNA sequencing data

Obtained single-end RNA sequencing reads were mapped to the human genome assembly, version hg19, with RNA-STAR (PMID:23104886), with default parameters except for allowing only unique hits to genome (outFilterMultimapNmax=1) and filtering reads without evidence in spliced junction table (outFilterType="BySJout"). Using RefSeq mRNA coordinates from UCSC (genome.ucsc.edu, downloaded in December 2015) and the qCount function from QuasR package (version 3.12.1) (PMID:25417205) we quantified gene expression as the number of reads that started within any annotated exon of a gene. The differentially expressed genes were identified using the edgeR package (version 1.10.1) (PMID:19910308). Genes with fdr ≤ 0.05 and minimum log2 fold change of +/- 1.0 were considered statistically significant and used for downstream functional analysis.

Functional enrichment analysis

We performed functional enrichment analysis of differentially expressed genes for biological processes or pathways in R using several publicly available Bioconductor resources including GO.db (version 3.4.1), GOstats (version 2.42.0) (PMID: 17098774), KEGG.db (version 3.2.3) and ReactomePA (version 1.20.2) (PMID: 26661513). The

significance of each biological process or pathway identified was calculated using the hypergeometric test (equivalent to Fisher's exact test) and those with p values ≤0.05 were considered significant.

Statistical analysis

Statistical analyses and graphs were generated using GraphPad Prism 7.02 software. All data are presented as mean ± S.E.M.

3.7 Supplementary Data

Gene	Forward primer	Reverse primer
CDH1	AGAACGCATTGCCACATACACT	TCTGATCGGTTACCGTGATCAA
CDH2	TAGTCACCGTGGTCAAACCAAT	GTGCTGAATTCCCTTGGCTAAT
FN1	GAACTATGATGCCGACCAGAA	GGTTGTGCAGATTTCCTCGT
SNAI1	GCTGCAGGACTCTAATCCAGA	ATCTCCGGAGGTGGGATG
SNAI2	TGGTTGCTTCAAGGACACAT	GTTGCAGTGAGGGCAAGAA
ZEB1	GCCAACAGACCAGACAGTGTT	TCTTGCCCTTCCTTTCCTG
TWIST	AAGGCATCACTATGGACTTTCTCT	GCCAGTTTGATCCCAGTATTTT
AFP	TGTACTGCAGAGATAAGTTTAGCTGAC	TCCTTGTAAGTGGCTTCTTGAAC
HSP70	CAGCAGACACCAGCAGAAAA	CCTTGGATCCAGCTTGAGAG
GPC3	TGATGAAGATGAGTGCATTGG	GATCATAGGCCAGTTCTGCAA
Albumin	AGAGGTCTCAAGAAACCTAGGAAA	GGTTCAGGACCACGGATAGA
CD44	CTGCCGCTTTGCAGGTGTA	CATTGTGGGCAAGGTGCTATT
CD133	GGAAACTAAGAAGTATGGGAGAACA	CGATGCCACTTTCTCACTGAT
RPL19	GATGCCGGAAAAACACCTTG	TGGCTGTACCCTTCCGCTT

Supplementary Table 1. Primer sequences used for qRT-PCR (5'-3').

4. References

1. Christofori, G., *New signals from the invasive front.* Nature, 2006. **441**(7092): p. 444-50.
2. Egeblad, M., E.S. Nakasone, and Z. Werb, *Tumors as organs: complex tissues that interface with the entire organism.* Dev Cell, 2010. **18**(6): p. 884-901.
3. White, M.C., et al., *Age and cancer risk: a potentially modifiable relationship.* Am J Prev Med, 2014. **46**(3 Suppl 1): p. S7-15.
4. Wu, S., et al., *Evaluating intrinsic and non-intrinsic cancer risk factors.* Nat Commun, 2018. **9**(1): p. 3490.
5. Khan, N., F. Afaq, and H. Mukhtar, *Lifestyle as risk factor for cancer: Evidence from human studies.* Cancer Lett, 2010. **293**(2): p. 133-43.
6. Siegel, R.L., K.D. Miller, and A. Jemal, *Cancer statistics, 2018.* CA Cancer J Clin, 2018. **68**(1): p. 7-30.
7. Hanahan, D. and R.A. Weinberg, *The hallmarks of cancer.* Cell, 2000. **100**(1): p. 57-70.
8. Hanahan, D. and R.A. Weinberg, *Hallmarks of cancer: the next generation.* Cell, 2011. **144**(5): p. 646-74.
9. Veltmaat, J.M., et al., *Mouse embryonic mammogenesis as a model for the molecular regulation of pattern formation.* Differentiation, 2003. **71**(1): p. 1-17.
10. Kratochwil, K., *Organ specificity in mesenchymal induction demonstrated in the embryonic development of the mammary gland of the mouse.* Dev Biol, 1969. **20**(1): p. 46-71.
11. Hogg, N.A., C.J. Harrison, and C. Tickle, *Lumen formation in the developing mouse mammary gland.* J Embryol Exp Morphol, 1983. **73**: p. 39-57.
12. Williams, J.M. and C.W. Daniel, *Mammary ductal elongation: differentiation of myoepithelium and basal lamina during branching morphogenesis.* Dev Biol, 1983. **97**(2): p. 274-90.
13. Humphreys, R.C., et al., *Mammary gland development is mediated by both stromal and epithelial progesterone receptors.* Mol Endocrinol, 1997. **11**(6): p. 801-11.
14. Macias, H. and L. Hinck, *Mammary gland development.* Wiley Interdiscip Rev Dev Biol, 2012. **1**(4): p. 533-57.
15. Ball, S.M., *The development of the terminal end bud in the prepubertal-pubertal mouse mammary gland.* Anat Rec, 1998. **250**(4): p. 459-64.
16. Gouon-Evans, V. and J.W. Pollard, *Unexpected deposition of brown fat in mammary gland during postnatal development.* Mol Endocrinol, 2002. **16**(11): p. 2618-27.
17. Stein, T., et al., *Involution of the mouse mammary gland is associated with an immune cascade and an acute-phase response, involving LBP, CD14 and STAT3.* Breast Cancer Res, 2004. **6**(2): p. R75-91.
18. Dulbecco, R., et al., *Marker evolution during the development of the rat mammary gland: stem cells identified by markers and the role of myoepithelial cells.* Cancer Res, 1986. **46**(5): p. 2449-56.
19. Sun, P., et al., *Cytokeratin expression during mouse embryonic and early postnatal mammary gland development.* Histochem Cell Biol, 2010. **133**(2): p. 213-21.
20. Mikaelian, I., et al., *Expression of terminal differentiation proteins defines stages of mouse mammary gland development.* Vet Pathol, 2006. **43**(1): p. 36-49.
21. Visvader, J.E., *Keeping abreast of the mammary epithelial hierarchy and breast tumorigenesis.* Genes Dev, 2009. **23**(22): p. 2563-77.

22. Siegel, R.L., K.D. Miller, and A. Jemal, *Cancer Statistics, 2017.* CA Cancer J Clin, 2017. **67**(1): p. 7-30.
23. Kelsey, J.L., M.D. Gammon, and E.M. John, *Reproductive factors and breast cancer.* Epidemiol Rev, 1993. **15**(1): p. 36-47.
24. Titus-Ernstoff, L., et al., *Menstrual factors in relation to breast cancer risk.* Cancer Epidemiol Biomarkers Prev, 1998. **7**(9): p. 783-9.
25. Hsieh, C.C., et al., *Age at menarche, age at menopause, height and obesity as risk factors for breast cancer: associations and interactions in an international case-control study.* Int J Cancer, 1990. **46**(5): p. 796-800.
26. Miki, Y., et al., *A strong candidate for the breast and ovarian cancer susceptibility gene BRCA1.* Science, 1994. **266**(5182): p. 66-71.
27. Wooster, R., et al., *Identification of the breast cancer susceptibility gene BRCA2.* Nature, 1995. **378**(6559): p. 789-92.
28. Malone, K.E., et al., *Frequency of BRCA1/BRCA2 mutations in a population-based sample of young breast carcinoma cases.* Cancer, 2000. **88**(6): p. 1393-402.
29. Peto, J., et al., *Prevalence of BRCA1 and BRCA2 gene mutations in patients with early-onset breast cancer.* J Natl Cancer Inst, 1999. **91**(11): p. 943-9.
30. Friedenson, B., *The BRCA1/2 pathway prevents hematologic cancers in addition to breast and ovarian cancers.* BMC Cancer, 2007. **7**: p. 152.
31. van der Groep, P., E. van der Wall, and P.J. van Diest, *Pathology of hereditary breast cancer.* Cell Oncol (Dordr), 2011. **34**(2): p. 71-88.
32. Koren, S. and M. Bentires-Alj, *Breast Tumor Heterogeneity: Source of Fitness, Hurdle for Therapy.* Mol Cell, 2015. **60**(4): p. 537-46.
33. Bertos, N.R. and M. Park, *Breast cancer - one term, many entities?* J Clin Invest, 2011. **121**(10): p. 3789-96.
34. Dai, X., et al., *Breast cancer intrinsic subtype classification, clinical use and future trends.* Am J Cancer Res, 2015. **5**(10): p. 2929-43.
35. Sorlie, T., et al., *Gene expression patterns of breast carcinomas distinguish tumor subclasses with clinical implications.* Proc Natl Acad Sci U S A, 2001. **98**(19): p. 10869-74.
36. Prat, A., et al., *Phenotypic and molecular characterization of the claudin-low intrinsic subtype of breast cancer.* Breast Cancer Res, 2010. **12**(5): p. R68.
37. Perou, C.M., et al., *Molecular portraits of human breast tumours.* Nature, 2000. **406**(6797): p. 747-52.
38. Cheang, M.C., et al., *Ki67 index, HER2 status, and prognosis of patients with luminal B breast cancer.* J Natl Cancer Inst, 2009. **101**(10): p. 736-50.
39. de Azambuja, E., et al., *Ki-67 as prognostic marker in early breast cancer: a meta-analysis of published studies involving 12,155 patients.* Br J Cancer, 2007. **96**(10): p. 1504-13.
40. Jordan, V.C. and A.M. Brodie, *Development and evolution of therapies targeted to the estrogen receptor for the treatment and prevention of breast cancer.* Steroids, 2007. **72**(1): p. 7-25.
41. Verma, S., et al., *Trastuzumab emtansine for HER2-positive advanced breast cancer.* N Engl J Med, 2012. **367**(19): p. 1783-91.
42. Junttila, T.T., et al., *Ligand-independent HER2/HER3/PI3K complex is disrupted by trastuzumab and is effectively inhibited by the PI3K inhibitor GDC-0941.* Cancer Cell, 2009. **15**(5): p. 429-40.
43. Nishimura, R. and N. Arima, *Is triple negative a prognostic factor in breast cancer?* Breast Cancer, 2008. **15**(4): p. 303-8.

44. Onitilo, A.A., et al., *Breast cancer subtypes based on ER/PR and Her2 expression: comparison of clinicopathologic features and survival.* Clin Med Res, 2009. **7**(1-2): p. 4-13.
45. Ovcaricek, T., et al., *Triple negative breast cancer - prognostic factors and survival.* Radiol Oncol, 2011. **45**(1): p. 46-52.
46. Sharma, R.P. and V.L. Chopra, *Effect of the Wingless (wg1) mutation on wing and haltere development in Drosophila melanogaster.* Dev Biol, 1976. **48**(2): p. 461-5.
47. Nusslein-Volhard, C. and E. Wieschaus, *Mutations affecting segment number and polarity in Drosophila.* Nature, 1980. **287**(5785): p. 795-801.
48. Nusse, R. and H.E. Varmus, *Many tumors induced by the mouse mammary tumor virus contain a provirus integrated in the same region of the host genome.* Cell, 1982. **31**(1): p. 99-109.
49. Nusse, R., et al., *Mode of proviral activation of a putative mammary oncogene (int-1) on mouse chromosome 15.* Nature, 1984. **307**(5947): p. 131-6.
50. Rijsewijk, F., et al., *The Drosophila homolog of the mouse mammary oncogene int-1 is identical to the segment polarity gene wingless.* Cell, 1987. **50**(4): p. 649-57.
51. Willert, K., et al., *Wnt proteins are lipid-modified and can act as stem cell growth factors.* Nature, 2003. **423**(6938): p. 448-52.
52. Takada, R., et al., *Monounsaturated fatty acid modification of Wnt protein: its role in Wnt secretion.* Dev Cell, 2006. **11**(6): p. 791-801.
53. Komekado, H., et al., *Glycosylation and palmitoylation of Wnt-3a are coupled to produce an active form of Wnt-3a.* Genes Cells, 2007. **12**(4): p. 521-34.
54. Banziger, C., et al., *Wntless, a conserved membrane protein dedicated to the secretion of Wnt proteins from signaling cells.* Cell, 2006. **125**(3): p. 509-22.
55. Franch-Marro, X., et al., *Wingless secretion requires endosome-to-Golgi retrieval of Wntless/Evi/Sprinter by the retromer complex.* Nat Cell Biol, 2008. **10**(2): p. 170-7.
56. Herr, P. and K. Basler, *Porcupine-mediated lipidation is required for Wnt recognition by Wls.* Dev Biol, 2012. **361**(2): p. 392-402.
57. Clevers, H., *Wnt/beta-catenin signaling in development and disease.* Cell, 2006. **127**(3): p. 469-80.
58. Takada, S., et al., *Differences in the secretion and transport of Wnt proteins.* J Biochem, 2017. **161**(1): p. 1-7.
59. Port, F. and K. Basler, *Wnt trafficking: new insights into Wnt maturation, secretion and spreading.* Traffic, 2010. **11**(10): p. 1265-71.
60. Glinka, A., et al., *Dickkopf-1 is a member of a new family of secreted proteins and functions in head induction.* Nature, 1998. **391**(6665): p. 357-62.
61. Hsieh, J.C., et al., *A new secreted protein that binds to Wnt proteins and inhibits their activities.* Nature, 1999. **398**(6726): p. 431-6.
62. Kim, K.A., et al., *R-Spondin family members regulate the Wnt pathway by a common mechanism.* Mol Biol Cell, 2008. **19**(6): p. 2588-96.
63. Galli, L.M., et al., *Differential inhibition of Wnt-3a by Sfrp-1, Sfrp-2, and Sfrp-3.* Dev Dyn, 2006. **235**(3): p. 681-90.
64. Siar, C.H., et al., *Differential expression of canonical and non-canonical Wnt ligands in ameloblastoma.* J Oral Pathol Med, 2012. **41**(4): p. 332-9.
65. He, X., et al., *A member of the Frizzled protein family mediating axis induction by Wnt-5A.* Science, 1997. **275**(5306): p. 1652-4.
66. Mikels, A.J. and R. Nusse, *Purified Wnt5a protein activates or inhibits beta-catenin-TCF signaling depending on receptor context.* PLoS Biol, 2006. **4**(4): p. e115.
67. Sato, A., et al., *Wnt5a regulates distinct signalling pathways by binding to Frizzled2.* EMBO J, 2010. **29**(1): p. 41-54.

68. Grumolato, L., et al., *Canonical and noncanonical Wnts use a common mechanism to activate completely unrelated coreceptors.* Genes Dev, 2010. **24**(22): p. 2517-30.
69. Liu, G., A. Bafico, and S.A. Aaronson, *The mechanism of endogenous receptor activation functionally distinguishes prototype canonical and noncanonical Wnts.* Mol Cell Biol, 2005. **25**(9): p. 3475-82.
70. Rulifson, E.J., C.H. Wu, and R. Nusse, *Pathway specificity by the bifunctional receptor frizzled is determined by affinity for wingless.* Mol Cell, 2000. **6**(1): p. 117-26.
71. van Amerongen, R., A. Mikels, and R. Nusse, *Alternative wnt signaling is initiated by distinct receptors.* Sci Signal, 2008. **1**(35): p. re9.
72. Topol, L., et al., *Wnt-5a inhibits the canonical Wnt pathway by promoting GSK-3-independent beta-catenin degradation.* J Cell Biol, 2003. **162**(5): p. 899-908.
73. Yuzugullu, H., et al., *Canonical Wnt signaling is antagonized by noncanonical Wnt5a in hepatocellular carcinoma cells.* Mol Cancer, 2009. **8**: p. 90.
74. van Amerongen, R. and R. Nusse, *Towards an integrated view of Wnt signaling in development.* Development, 2009. **136**(19): p. 3205-14.
75. Valenta, T., G. Hausmann, and K. Basler, *The many faces and functions of beta-catenin.* EMBO J, 2012. **31**(12): p. 2714-36.
76. MacDonald, B.T. and X. He, *Frizzled and LRP5/6 receptors for Wnt/beta-catenin signaling.* Cold Spring Harb Perspect Biol, 2012. **4**(12).
77. Lustig, B., et al., *Negative feedback loop of Wnt signaling through upregulation of conductin/axin2 in colorectal and liver tumors.* Mol Cell Biol, 2002. **22**(4): p. 1184-93.
78. Hagen, T. and A. Vidal-Puig, *Characterisation of the phosphorylation of beta-catenin at the GSK-3 priming site Ser45.* Biochem Biophys Res Commun, 2002. **294**(2): p. 324-8.
79. Rubinfeld, B., et al., *Binding of GSK3beta to the APC-beta-catenin complex and regulation of complex assembly.* Science, 1996. **272**(5264): p. 1023-6.
80. Ikeda, S., et al., *Axin, a negative regulator of the Wnt signaling pathway, forms a complex with GSK-3beta and beta-catenin and promotes GSK-3beta-dependent phosphorylation of beta-catenin.* EMBO J, 1998. **17**(5): p. 1371-84.
81. Winston, J.T., et al., *The SCFbeta-TRCP-ubiquitin ligase complex associates specifically with phosphorylated destruction motifs in IkappaBalpha and beta-catenin and stimulates IkappaBalpha ubiquitination in vitro.* Genes Dev, 1999. **13**(3): p. 270-83.
82. Hart, M., et al., *The F-box protein beta-TrCP associates with phosphorylated beta-catenin and regulates its activity in the cell.* Curr Biol, 1999. **9**(4): p. 207-10.
83. Chitalia, V.C., et al., *Jade-1 inhibits Wnt signalling by ubiquitylating beta-catenin and mediates Wnt pathway inhibition by pVHL.* Nat Cell Biol, 2008. **10**(10): p. 1208-16.
84. Bilic, J., et al., *Wnt induces LRP6 signalosomes and promotes dishevelled-dependent LRP6 phosphorylation.* Science, 2007. **316**(5831): p. 1619-22.
85. Zeng, X., et al., *Initiation of Wnt signaling: control of Wnt coreceptor Lrp6 phosphorylation/activation via frizzled, dishevelled and axin functions.* Development, 2008. **135**(2): p. 367-75.
86. Zeng, X., et al., *A dual-kinase mechanism for Wnt co-receptor phosphorylation and activation.* Nature, 2005. **438**(7069): p. 873-7.

87. Daniels, D.L. and W.I. Weis, *Beta-catenin directly displaces Groucho/TLE repressors from Tcf/Lef in Wnt-mediated transcription activation.* Nat Struct Mol Biol, 2005. **12**(4): p. 364-71.
88. Cavallo, R.A., et al., *Drosophila Tcf and Groucho interact to repress Wingless signalling activity.* Nature, 1998. **395**(6702): p. 604-8.
89. Roose, J., et al., *Synergy between tumor suppressor APC and the beta-catenin-Tcf4 target Tcf1.* Science, 1999. **285**(5435): p. 1923-6.
90. Hovanes, K., et al., *Beta-catenin-sensitive isoforms of lymphoid enhancer factor-1 are selectively expressed in colon cancer.* Nat Genet, 2001. **28**(1): p. 53-7.
91. Filali, M., et al., *Wnt-3A/beta-catenin signaling induces transcription from the LEF-1 promoter.* J Biol Chem, 2002. **277**(36): p. 33398-410.
92. Willert, J., et al., *A transcriptional response to Wnt protein in human embryonic carcinoma cells.* BMC Dev Biol, 2002. **2**: p. 8.
93. Gonzalez-Sancho, J.M., et al., *The Wnt antagonist DICKKOPF-1 gene is a downstream target of beta-catenin/TCF and is downregulated in human colon cancer.* Oncogene, 2005. **24**(6): p. 1098-103.
94. Sasai, N., et al., *The neurotrophin-receptor-related protein NRH1 is essential for convergent extension movements.* Nat Cell Biol, 2004. **6**(8): p. 741-8.
95. Lu, W., et al., *Mammalian Ryk is a Wnt coreceptor required for stimulation of neurite outgrowth.* Cell, 2004. **119**(1): p. 97-108.
96. Lu, X., et al., *PTK7/CCK-4 is a novel regulator of planar cell polarity in vertebrates.* Nature, 2004. **430**(6995): p. 93-8.
97. Nishita, M., et al., *Filopodia formation mediated by receptor tyrosine kinase Ror2 is required for Wnt5a-induced cell migration.* J Cell Biol, 2006. **175**(4): p. 555-62.
98. Niehrs, C., *The complex world of WNT receptor signalling.* Nat Rev Mol Cell Biol, 2012. **13**(12): p. 767-79.
99. Komiya, Y. and R. Habas, *Wnt signal transduction pathways.* Organogenesis, 2008. **4**(2): p. 68-75.
100. Kuhl, M., et al., *Ca(2+)/calmodulin-dependent protein kinase II is stimulated by Wnt and Frizzled homologs and promotes ventral cell fates in Xenopus.* J Biol Chem, 2000. **275**(17): p. 12701-11.
101. Zhan, T., N. Rindtorff, and M. Boutros, *Wnt signaling in cancer.* Oncogene, 2017. **36**(11): p. 1461-1473.
102. Ozawa, M., H. Baribault, and R. Kemler, *The cytoplasmic domain of the cell adhesion molecule uvomorulin associates with three independent proteins structurally related in different species.* EMBO J, 1989. **8**(6): p. 1711-7.
103. Wieschaus, E., C. Nusslein-Volhard, and G. Jurgens, *Mutations affecting the pattern of the larval cuticle inDrosophila melanogaster : III. Zygotic loci on the X-chromosome and fourth chromosome.* Wilehm Roux Arch Dev Biol, 1984. **193**(5): p. 296-307.
104. Peifer, M. and E. Wieschaus, *The segment polarity gene armadillo encodes a functionally modular protein that is the Drosophila homolog of human plakoglobin.* Cell, 1990. **63**(6): p. 1167-76.
105. McCrea, P.D., C.W. Turck, and B. Gumbiner, *A homolog of the armadillo protein in Drosophila (plakoglobin) associated with E-cadherin.* Science, 1991. **254**(5036): p. 1359-61.
106. Xing, Y., et al., *Crystal structure of a full-length beta-catenin.* Structure, 2008. **16**(3): p. 478-87.

107. Huber, A.H. and W.I. Weis, *The structure of the beta-catenin/E-cadherin complex and the molecular basis of diverse ligand recognition by beta-catenin.* Cell, 2001. **105**(3): p. 391-402.
108. Pokutta, S. and W.I. Weis, *Structure of the dimerization and beta-catenin-binding region of alpha-catenin.* Mol Cell, 2000. **5**(3): p. 533-43.
109. Hoffmans, R. and K. Basler, *BCL9-2 binds Arm/beta-catenin in a Tyr142-independent manner and requires Pygopus for its function in Wg/Wnt signaling.* Mech Dev, 2007. **124**(1): p. 59-67.
110. Sampietro, J., et al., *Crystal structure of a beta-catenin/BCL9/Tcf4 complex.* Mol Cell, 2006. **24**(2): p. 293-300.
111. Brembeck, F.H., et al., *Essential role of BCL9-2 in the switch between beta-catenin's adhesive and transcriptional functions.* Genes Dev, 2004. **18**(18): p. 2225-30.
112. Piedra, J., et al., *Regulation of beta-catenin structure and activity by tyrosine phosphorylation.* J Biol Chem, 2001. **276**(23): p. 20436-43.
113. Maretzky, T., et al., *ADAM10 mediates E-cadherin shedding and regulates epithelial cell-cell adhesion, migration, and beta-catenin translocation.* Proc Natl Acad Sci U S A, 2005. **102**(26): p. 9182-7.
114. Reiss, K., et al., *ADAM10 cleavage of N-cadherin and regulation of cell-cell adhesion and beta-catenin nuclear signalling.* EMBO J, 2005. **24**(4): p. 742-52.
115. Gavert, N., et al., *Expression of L1-CAM and ADAM10 in human colon cancer cells induces metastasis.* Cancer Res, 2007. **67**(16): p. 7703-12.
116. Onder, T.T., et al., *Loss of E-cadherin promotes metastasis via multiple downstream transcriptional pathways.* Cancer Res, 2008. **68**(10): p. 3645-54.
117. Kuphal, F. and J. Behrens, *E-cadherin modulates Wnt-dependent transcription in colorectal cancer cells but does not alter Wnt-independent gene expression in fibroblasts.* Exp Cell Res, 2006. **312**(4): p. 457-67.
118. Herzig, M., et al., *Tumor progression induced by the loss of E-cadherin independent of beta-catenin/Tcf-mediated Wnt signaling.* Oncogene, 2007. **26**(16): p. 2290-8.
119. van de Wetering, M., et al., *Mutant E-cadherin breast cancer cells do not display constitutive Wnt signaling.* Cancer Res, 2001. **61**(1): p. 278-84.
120. Stepniak, E., G.L. Radice, and V. Vasioukhin, *Adhesive and signaling functions of cadherins and catenins in vertebrate development.* Cold Spring Harb Perspect Biol, 2009. **1**(5): p. a002949.
121. Mukherjee, A., et al., *Understanding How Wnt Influences Destruction Complex Activity and beta-Catenin Dynamics.* iScience, 2018. **6**: p. 13-21.
122. Liu, C., et al., *Control of beta-catenin phosphorylation/degradation by a dual-kinase mechanism.* Cell, 2002. **108**(6): p. 837-47.
123. Townsley, F.M., A. Cliffe, and M. Bienz, *Pygopus and Legless target Armadillo/beta-catenin to the nucleus to enable its transcriptional co-activator function.* Nat Cell Biol, 2004. **6**(7): p. 626-33.
124. Zhang, N., et al., *FoxM1 promotes beta-catenin nuclear localization and controls Wnt target-gene expression and glioma tumorigenesis.* Cancer Cell, 2011. **20**(4): p. 427-42.
125. Mosimann, C., G. Hausmann, and K. Basler, *Beta-catenin hits chromatin: regulation of Wnt target gene activation.* Nat Rev Mol Cell Biol, 2009. **10**(4): p. 276-86.
126. Kramps, T., et al., *Wnt/wingless signaling requires BCL9/legless-mediated recruitment of pygopus to the nuclear beta-catenin-TCF complex.* Cell, 2002. **109**(1): p. 47-60.

127. Sustmann, C., et al., *Cell-type-specific function of BCL9 involves a transcriptional activation domain that synergizes with beta-catenin.* Mol Cell Biol, 2008. **28**(10): p. 3526-37.
128. Kessler, R., G. Hausmann, and K. Basler, *The PHD domain is required to link Drosophila Pygopus to Legless/beta-catenin and not to histone H3.* Mech Dev, 2009. **126**(8-9): p. 752-9.
129. Song, N., et al., *pygopus 2 has a crucial, Wnt pathway-independent function in lens induction.* Development, 2007. **134**(10): p. 1873-85.
130. Carrera, I., et al., *Pygopus activates Wingless target gene transcription through the mediator complex subunits Med12 and Med13.* Proc Natl Acad Sci U S A, 2008. **105**(18): p. 6644-9.
131. Cantu, C., et al., *Pax6-dependent, but beta-catenin-independent, function of Bcl9 proteins in mouse lens development.* Genes Dev, 2014. **28**(17): p. 1879-84.
132. Thompson, B., et al., *A new nuclear component of the Wnt signalling pathway.* Nat Cell Biol, 2002. **4**(5): p. 367-73.
133. Li, B., et al., *Developmental phenotypes and reduced Wnt signaling in mice deficient for pygopus 2.* Genesis, 2007. **45**(5): p. 318-25.
134. Schwab, K.R., et al., *Pygo1 and Pygo2 roles in Wnt signaling in mammalian kidney development.* BMC Biol, 2007. **5**: p. 15.
135. Li, B., et al., *Cloning and developmental expression of mouse pygopus 2, a putative Wnt signaling component.* Genomics, 2004. **84**(2): p. 398-405.
136. Brack, A.S., et al., *BCL9 is an essential component of canonical Wnt signaling that mediates the differentiation of myogenic progenitors during muscle regeneration.* Dev Biol, 2009. **335**(1): p. 93-105.
137. Valenta, T., et al., *Probing transcription-specific outputs of beta-catenin in vivo.* Genes Dev, 2011. **25**(24): p. 2631-43.
138. Badders, N.M., et al., *The Wnt receptor, Lrp5, is expressed by mouse mammary stem cells and is required to maintain the basal lineage.* PLoS One, 2009. **4**(8): p. e6594.
139. Zeng, Y.A. and R. Nusse, *Wnt proteins are self-renewal factors for mammary stem cells and promote their long-term expansion in culture.* Cell Stem Cell, 2010. **6**(6): p. 568-77.
140. Yu, Q.C., E.M. Verheyen, and Y.A. Zeng, *Mammary Development and Breast Cancer: A Wnt Perspective.* Cancers (Basel), 2016. **8**(7).
141. Chu, E.Y., et al., *Canonical WNT signaling promotes mammary placode development and is essential for initiation of mammary gland morphogenesis.* Development, 2004. **131**(19): p. 4819-29.
142. Gu, B., et al., *Pygo2 expands mammary progenitor cells by facilitating histone H3 K4 methylation.* J Cell Biol, 2009. **185**(5): p. 811-26.
143. Lindvall, C., et al., *The Wnt co-receptor Lrp6 is required for normal mouse mammary gland development.* PLoS One, 2009. **4**(6): p. e5813.
144. Lane, T.F. and P. Leder, *Wnt-10b directs hypermorphic development and transformation in mammary glands of male and female mice.* Oncogene, 1997. **15**(18): p. 2133-44.
145. Tsukamoto, A.S., et al., *Expression of the int-1 gene in transgenic mice is associated with mammary gland hyperplasia and adenocarcinomas in male and female mice.* Cell, 1988. **55**(4): p. 619-25.
146. Howe, L.R. and A.M. Brown, *Wnt signaling and breast cancer.* Cancer Biol Ther, 2004. **3**(1): p. 36-41.
147. Barker, N. and H. Clevers, *Mining the Wnt pathway for cancer therapeutics.* Nat Rev Drug Discov, 2006. **5**(12): p. 997-1014.

148. Taniguchi, K., et al., *Mutational spectrum of beta-catenin, AXIN1, and AXIN2 in hepatocellular carcinomas and hepatoblastomas.* Oncogene, 2002. **21**(31): p. 4863-71.
149. Lin, S.Y., et al., *Beta-catenin, a novel prognostic marker for breast cancer: its roles in cyclin D1 expression and cancer progression.* Proc Natl Acad Sci U S A, 2000. **97**(8): p. 4262-6.
150. He, Y., et al., *Expression and significance of Wnt signaling components and their target genes in breast carcinoma.* Mol Med Rep, 2014. **9**(1): p. 137-43.
151. Brabletz, T., et al., *Expression of nuclear beta-catenin and c-myc is correlated with tumor size but not with proliferative activity of colorectal adenomas.* Am J Pathol, 2000. **156**(3): p. 865-70.
152. Said, A.H., J.P. Raufman, and G. Xie, *The role of matrix metalloproteinases in colorectal cancer.* Cancers (Basel), 2014. **6**(1): p. 366-75.
153. Bae, Y.K., et al., *Fibronectin expression in carcinoma cells correlates with tumor aggressiveness and poor clinical outcome in patients with invasive breast cancer.* Hum Pathol, 2013. **44**(10): p. 2028-37.
154. Barker, N., et al., *Crypt stem cells as the cells-of-origin of intestinal cancer.* Nature, 2009. **457**(7229): p. 608-11.
155. Barker, N., et al., *Lgr5(+ve) stem cells drive self-renewal in the stomach and build long-lived gastric units in vitro.* Cell Stem Cell, 2010. **6**(1): p. 25-36.
156. Barker, N., et al., *Lgr5(+ve) stem/progenitor cells contribute to nephron formation during kidney development.* Cell Rep, 2012. **2**(3): p. 540-52.
157. Plaks, V., et al., *Lgr5-expressing cells are sufficient and necessary for postnatal mammary gland organogenesis.* Cell Rep, 2013. **3**(1): p. 70-8.
158. McClanahan, T., et al., *Identification of overexpression of orphan G protein-coupled receptor GPR49 in human colon and ovarian primary tumors.* Cancer Biol Ther, 2006. **5**(4): p. 419-26.
159. Yamamoto, Y., et al., *Overexpression of orphan G-protein-coupled receptor, Gpr49, in human hepatocellular carcinomas with beta-catenin mutations.* Hepatology, 2003. **37**(3): p. 528-33.
160. Haegebarth, A. and H. Clevers, *Wnt signaling, lgr5, and stem cells in the intestine and skin.* Am J Pathol, 2009. **174**(3): p. 715-21.
161. Mani, M., et al., *BCL9 promotes tumor progression by conferring enhanced proliferative, metastatic, and angiogenic properties to cancer cells.* Cancer Res, 2009. **69**(19): p. 7577-86.
162. Deka, J., et al., *Bcl9/Bcl9l are critical for Wnt-mediated regulation of stem cell traits in colon epithelium and adenocarcinomas.* Cancer Res, 2010. **70**(16): p. 6619-28.
163. Zhang, S., et al., *Pygopus-2 promotes invasion and metastasis of hepatic carcinoma cell by decreasing E-cadherin expression.* Oncotarget, 2015. **6**(13): p. 11074-86.
164. Zhou, S.Y., et al., *Overexpression of Pygopus-2 is required for canonical Wnt activation in human lung cancer.* Oncol Lett, 2014. **7**(1): p. 233-238.
165. Takebe, N., et al., *Targeting Notch, Hedgehog, and Wnt pathways in cancer stem cells: clinical update.* Nat Rev Clin Oncol, 2015. **12**(8): p. 445-64.
166. Reya, T. and H. Clevers, *Wnt signalling in stem cells and cancer.* Nature, 2005. **434**(7035): p. 843-50.
167. Yue, Z., et al., *LGR4 modulates breast cancer initiation, metastasis, and cancer stem cells.* FASEB J, 2018. **32**(5): p. 2422-2437.
168. Valkenburg, K.C., et al., *Wnt/beta-catenin Signaling in Normal and Cancer Stem Cells.* Cancers (Basel), 2011. **3**(2): p. 2050-79.

169. Leng, Z., et al., *Lgr5+CD44+EpCAM+ Strictly Defines Cancer Stem Cells in Human Colorectal Cancer.* Cell Physiol Biochem, 2018. **46**(2): p. 860-872.
170. Merlos-Suarez, A., et al., *The intestinal stem cell signature identifies colorectal cancer stem cells and predicts disease relapse.* Cell Stem Cell, 2011. **8**(5): p. 511-24.
171. Hirsch, D., et al., *LGR5 positivity defines stem-like cells in colorectal cancer.* Carcinogenesis, 2014. **35**(4): p. 849-58.
172. Su, Y.J., et al., *An aberrant nuclear localization of E-cadherin is a potent inhibitor of Wnt/beta-catenin-elicited promotion of the cancer stem cell phenotype.* Oncogenesis, 2015. **4**: p. e157.
173. Junttila, M.R., et al., *Targeting LGR5+ cells with an antibody-drug conjugate for the treatment of colon cancer.* Sci Transl Med, 2015. **7**(314): p. 314ra186.
174. Al-Hajj, M., et al., *Prospective identification of tumorigenic breast cancer cells.* Proc Natl Acad Sci U S A, 2003. **100**(7): p. 3983-8.
175. Ahmed, K., et al., *A Second WNT for Old Drugs: Drug Repositioning against WNT-Dependent Cancers.* Cancers (Basel), 2016. **8**(7).
176. Krishnamurthy, N. and R. Kurzrock, *Targeting the Wnt/beta-catenin pathway in cancer: Update on effectors and inhibitors.* Cancer Treat Rev, 2018. **62**: p. 50-60.
177. Bui, T.D., et al., *A novel human Wnt gene, WNT10B, maps to 12q13 and is expressed in human breast carcinomas.* Oncogene, 1997. **14**(10): p. 1249-53.
178. Huguet, E.L., et al., *Differential expression of human Wnt genes 2, 3, 4, and 7B in human breast cell lines and normal and disease states of human breast tissue.* Cancer Res, 1994. **54**(10): p. 2615-21.
179. Veeck, J., et al., *Prognostic relevance of Wnt-inhibitory factor-1 (WIF1) and Dickkopf-3 (DKK3) promoter methylation in human breast cancer.* BMC Cancer, 2009. **9**: p. 217.
180. Suzuki, H., et al., *Frequent epigenetic inactivation of Wnt antagonist genes in breast cancer.* Br J Cancer, 2008. **98**(6): p. 1147-56.
181. Prasad, C.P., et al., *Epigenetic alterations of CDH1 and APC genes: relationship with activation of Wnt/beta-catenin pathway in invasive ductal carcinoma of breast.* Life Sci, 2008. **83**(9-10): p. 318-25.
182. Caldeira, J.R., et al., *CDH1 promoter hypermethylation and E-cadherin protein expression in infiltrating breast cancer.* BMC Cancer, 2006. **6**: p. 48.
183. Jin, Z., et al., *Adenomatous polyposis coli (APC) gene promoter hypermethylation in primary breast cancers.* Br J Cancer, 2001. **85**(1): p. 69-73.
184. Bjorklund, P., et al., *The internally truncated LRP5 receptor presents a therapeutic target in breast cancer.* PLoS One, 2009. **4**(1): p. e4243.
185. Dong, Y., et al., *Epigenetic silencing of NKD2, a major component of Wnt signaling, promotes breast cancer growth.* Oncotarget, 2015. **6**(26): p. 22126-38.
186. Nagahata, T., et al., *Amplification, up-regulation and over-expression of DVL-1, the human counterpart of the Drosophila disheveled gene, in primary breast cancers.* Cancer Sci, 2003. **94**(6): p. 515-8.
187. Watanabe, K., M. Fallahi, and X. Dai, *Chromatin effector Pygo2 regulates mammary tumor initiation and heterogeneity in MMTV-Wnt1 mice.* Oncogene, 2014. **33**(5): p. 632-42.
188. Toya, H., et al., *Immunohistochemical expression of the beta-catenin-interacting protein B9L is associated with histological high nuclear grade and immunohistochemical ErbB2/HER-2 expression in breast cancers.* Cancer Sci, 2007. **98**(4): p. 484-90.

189. Elsarraj, H.S., et al., *Expression profiling of in vivo ductal carcinoma in situ progression models identified B cell lymphoma-9 as a molecular driver of breast cancer invasion.* Breast Cancer Res, 2015. **17**: p. 128.
190. Chrzan, P., et al., *Amplification of c-myc gene and overexpression of c-Myc protein in breast cancer and adjacent non-neoplastic tissue.* Clin Biochem, 2001. **34**(7): p. 557-62.
191. Xu, J., Y. Chen, and O.I. Olopade, *MYC and Breast Cancer.* Genes Cancer, 2010. **1**(6): p. 629-40.
192. Rieger, M.E., et al., *The embryonic transcription cofactor LBH is a direct target of the Wnt signaling pathway in epithelial development and in aggressive basal subtype breast cancers.* Mol Cell Biol, 2010. **30**(17): p. 4267-79.
193. Yang, J., et al., *Twist, a master regulator of morphogenesis, plays an essential role in tumor metastasis.* Cell, 2004. **117**(7): p. 927-39.
194. Klauzinska, M., et al., *Rspo2/Int7 regulates invasiveness and tumorigenic properties of mammary epithelial cells.* J Cell Physiol, 2012. **227**(5): p. 1960-71.
195. Moor, A.E., et al., *BCL9/9L-beta-catenin Signaling is Associated With Poor Outcome in Colorectal Cancer.* EBioMedicine, 2015. **2**(12): p. 1932-43.
196. Zatula, N., et al., *The BCL9-2 proto-oncogene governs estrogen receptor alpha expression in breast tumorigenesis.* Oncotarget, 2014. **5**(16): p. 6770-87.
197. Andrews, P.G., et al., *Requirement of Pygopus 2 in breast cancer.* Int J Oncol, 2007. **30**(2): p. 357-63.
198. Talla, S.B. and F.H. Brembeck, *The role of Pygo2 for Wnt/ss-catenin signaling activity during intestinal tumor initiation and progression.* Oncotarget, 2016. **7**(49): p. 80612-80632.
199. Schaffner, F., et al., *Endothelial protein C receptor function in murine and human breast cancer development.* PLoS One, 2013. **8**(4): p. e61071.
200. Perurena, N., et al., *EPCR promotes breast cancer progression by altering SPOCK1/testican 1-mediated 3D growth.* J Hematol Oncol, 2017. **10**(1): p. 23.
201. Baum, B., J. Settleman, and M.P. Quinlan, *Transitions between epithelial and mesenchymal states in development and disease.* Semin Cell Dev Biol, 2008. **19**(3): p. 294-308.
202. Lamouille, S., J. Xu, and R. Derynck, *Molecular mechanisms of epithelial-mesenchymal transition.* Nat Rev Mol Cell Biol, 2014. **15**(3): p. 178-96.
203. Thiery, J.P., et al., *Epithelial-mesenchymal transitions in development and disease.* Cell, 2009. **139**(5): p. 871-90.
204. Wheelock, M.J., et al., *Cadherin switching.* J Cell Sci, 2008. **121**(Pt 6): p. 727-35.
205. Cavallaro, U., B. Schaffhauser, and G. Christofori, *Cadherins and the tumour progression: is it all in a switch?* Cancer Lett, 2002. **176**(2): p. 123-8.
206. Christofori, G., *Changing neighbours, changing behaviour: cell adhesion molecule-mediated signalling during tumour progression.* EMBO J, 2003. **22**(10): p. 2318-23.
207. Shibue, T. and R.A. Weinberg, *EMT, CSCs, and drug resistance: the mechanistic link and clinical implications.* Nat Rev Clin Oncol, 2017. **14**(10): p. 611-629.
208. Kalluri, R. and R.A. Weinberg, *The basics of epithelial-mesenchymal transition.* J Clin Invest, 2009. **119**(6): p. 1420-8.
209. Nieto, M.A., *Epithelial plasticity: a common theme in embryonic and cancer cells.* Science, 2013. **342**(6159): p. 1234850.
210. Tiwari, N., et al., *EMT as the ultimate survival mechanism of cancer cells.* Semin Cancer Biol, 2012. **22**(3): p. 194-207.

211. Saxena, M., et al., *Transcription factors that mediate epithelial-mesenchymal transition lead to multidrug resistance by upregulating ABC transporters.* Cell Death Dis, 2011. **2**: p. e179.
212. Klein, C.A., *Parallel progression of primary tumours and metastases.* Nat Rev Cancer, 2009. **9**(4): p. 302-12.
213. Diepenbruck, M. and G. Christofori, *Epithelial-mesenchymal transition (EMT) and metastasis: yes, no, maybe?* Curr Opin Cell Biol, 2016. **43**: p. 7-13.
214. Kallergi, G., et al., *Epithelial to mesenchymal transition markers expressed in circulating tumour cells of early and metastatic breast cancer patients.* Breast Cancer Res, 2011. **13**(3): p. R59.
215. Yu, M., et al., *Circulating breast tumor cells exhibit dynamic changes in epithelial and mesenchymal composition.* Science, 2013. **339**(6119): p. 580-4.
216. Aktas, B., et al., *Stem cell and epithelial-mesenchymal transition markers are frequently overexpressed in circulating tumor cells of metastatic breast cancer patients.* Breast Cancer Res, 2009. **11**(4): p. R46.
217. Berx, G. and F. Van Roy, *The E-cadherin/catenin complex: an important gatekeeper in breast cancer tumorigenesis and malignant progression.* Breast Cancer Res, 2001. **3**(5): p. 289-93.
218. Cowin, P., T.M. Rowlands, and S.J. Hatsell, *Cadherins and catenins in breast cancer.* Curr Opin Cell Biol, 2005. **17**(5): p. 499-508.
219. Grosse-Wilde, A., et al., *Stemness of the hybrid Epithelial/Mesenchymal State in Breast Cancer and Its Association with Poor Survival.* PLoS One, 2015. **10**(5): p. e0126522.
220. Zhou, B.P., et al., *Dual regulation of Snail by GSK-3beta-mediated phosphorylation in control of epithelial-mesenchymal transition.* Nat Cell Biol, 2004. **6**(10): p. 931-40.
221. Yook, J.I., et al., *A Wnt-Axin2-GSK3beta cascade regulates Snail1 activity in breast cancer cells.* Nat Cell Biol, 2006. **8**(12): p. 1398-406.
222. Sanchez-Tillo, E., et al., *beta-catenin/TCF4 complex induces the epithelial-to-mesenchymal transition (EMT)-activator ZEB1 to regulate tumor invasiveness.* Proc Natl Acad Sci U S A, 2011. **108**(48): p. 19204-9.
223. Xu, J., S. Lamouille, and R. Derynck, *TGF-beta-induced epithelial to mesenchymal transition.* Cell Res, 2009. **19**(2): p. 156-72.
224. Qin, Q., et al., *Normal and disease-related biological functions of Twist1 and underlying molecular mechanisms.* Cell Res, 2012. **22**(1): p. 90-106.
225. De Langhe, S.P., et al., *Dickkopf-1 (DKK1) reveals that fibronectin is a major target of Wnt signaling in branching morphogenesis of the mouse embryonic lung.* Dev Biol, 2005. **277**(2): p. 316-31.
226. Brabletz, T., et al., *beta-catenin regulates the expression of the matrix metalloproteinase-7 in human colorectal cancer.* Am J Pathol, 1999. **155**(4): p. 1033-8.
227. Malliri, A., et al., *The rac activator Tiam1 is a Wnt-responsive gene that modifies intestinal tumor development.* J Biol Chem, 2006. **281**(1): p. 543-8.
228. Gilles, C., et al., *Transactivation of vimentin by beta-catenin in human breast cancer cells.* Cancer Res, 2003. **63**(10): p. 2658-64.
229. Gavert, N., et al., *L1, a novel target of beta-catenin signaling, transforms cells and is expressed at the invasive front of colon cancers.* J Cell Biol, 2005. **168**(4): p. 633-42.

230. Conacci-Sorrell, M.E., et al., *Nr-CAM is a target gene of the beta-catenin/LEF-1 pathway in melanoma and colon cancer and its expression enhances motility and confers tumorigenesis.* Genes Dev, 2002. **16**(16): p. 2058-72.
231. van der Velden, J.L., et al., *Induction of a mesenchymal expression program in lung epithelial cells by wingless protein (Wnt)/beta-catenin requires the presence of c-Jun N-terminal kinase-1 (JNK1).* Am J Respir Cell Mol Biol, 2012. **47**(3): p. 306-14.
232. Polyak, K. and R.A. Weinberg, *Transitions between epithelial and mesenchymal states: acquisition of malignant and stem cell traits.* Nat Rev Cancer, 2009. **9**(4): p. 265-73.
233. Perlman, R.L., *Mouse models of human disease: An evolutionary perspective.* Evol Med Public Health, 2016. **2016**(1): p. 170-6.
234. Kersten, K., et al., *Genetically engineered mouse models in oncology research and cancer medicine.* EMBO Mol Med, 2017. **9**(2): p. 137-153.
235. Fantozzi, A. and G. Christofori, *Mouse models of breast cancer metastasis.* Breast Cancer Res, 2006. **8**(4): p. 212.
236. Guy, C.T., R.D. Cardiff, and W.J. Muller, *Induction of mammary tumors by expression of polyomavirus middle T oncogene: a transgenic mouse model for metastatic disease.* Mol Cell Biol, 1992. **12**(3): p. 954-61.
237. Maglione, J.E., et al., *Transgenic Polyoma middle-T mice model premalignant mammary disease.* Cancer Res, 2001. **61**(22): p. 8298-305.
238. Lin, E.Y., et al., *Progression to malignancy in the polyoma middle T oncoprotein mouse breast cancer model provides a reliable model for human diseases.* Am J Pathol, 2003. **163**(5): p. 2113-26.
239. Gordon, M.D. and R. Nusse, *Wnt signaling: multiple pathways, multiple receptors, and multiple transcription factors.* J Biol Chem, 2006. **281**(32): p. 22429-33.
240. Warner, D.R., R.M. Greene, and M.M. Pisano, *Cross-talk between the TGFbeta and Wnt signaling pathways in murine embryonic maxillary mesenchymal cells.* FEBS Lett, 2005. **579**(17): p. 3539-46.
241. Akhmetshina, A., et al., *Activation of canonical Wnt signalling is required for TGF-beta-mediated fibrosis.* Nat Commun, 2012. **3**: p. 735.
242. Zhang, J., X.J. Tian, and J. Xing, *Signal Transduction Pathways of EMT Induced by TGF-beta, SHH, and WNT and Their Crosstalks.* J Clin Med, 2016. **5**(4).
243. Berry, D.C., L. Levi, and N. Noy, *Holo-retinol-binding protein and its receptor STRA6 drive oncogenic transformation.* Cancer Res, 2014. **74**(21): p. 6341-51.
244. Szeto, W., et al., *Overexpression of the retinoic acid-responsive gene Stra6 in human cancers and its synergistic induction by Wnt-1 and retinoic acid.* Cancer Res, 2001. **61**(10): p. 4197-205.
245. Yan, Q., et al., *Prevalence of protein C receptor (PROCR) is associated with inferior clinical outcome in Breast invasive ductal carcinoma.* Pathol Res Pract, 2017. **213**(9): p. 1173-1179.
246. Wang, D., et al., *Protein C receptor stimulates multiple signaling pathways in breast cancer cells.* J Biol Chem, 2018. **293**(4): p. 1413-1424.
247. Klein, E.A. and R.K. Assoian, *Transcriptional regulation of the cyclin D1 gene at a glance.* J Cell Sci, 2008. **121**(Pt 23): p. 3853-7.
248. Busby, M., M.T. Hallett, and I. Plante, *The Complex Subtype-Dependent Role of Connexin 43 (GJA1) in Breast Cancer.* Int J Mol Sci, 2018. **19**(3).
249. van der Heyden, M.A., et al., *Identification of connexin43 as a functional target for Wnt signalling.* J Cell Sci, 1998. **111 (Pt 12)**: p. 1741-9.
250. Heuberger, J. and W. Birchmeier, *Interplay of cadherin-mediated cell adhesion and canonical Wnt signaling.* Cold Spring Harb Perspect Biol, 2010. **2**(2): p. a002915.

251. Micalizzi, D.S., S.M. Farabaugh, and H.L. Ford, *Epithelial-mesenchymal transition in cancer: parallels between normal development and tumor progression.* J Mammary Gland Biol Neoplasia, 2010. **15**(2): p. 117-34.
252. He, X., *Unwinding a path to nuclear beta-catenin.* Cell, 2006. **127**(1): p. 40-2.
253. Wagner, K.U., et al., *Cre-mediated gene deletion in the mammary gland.* Nucleic Acids Res, 1997. **25**(21): p. 4323-30.
254. Brault, V., et al., *Inactivation of the beta-catenin gene by Wnt1-Cre-mediated deletion results in dramatic brain malformation and failure of craniofacial development.* Development, 2001. **128**(8): p. 1253-64.
255. Cortazar, D., et al., *Embryonic lethal phenotype reveals a function of TDG in maintaining epigenetic stability.* Nature, 2011. **470**(7334): p. 419-23.
256. Llovet, J.M., et al., *Hepatocellular carcinoma.* Nat Rev Dis Primers, 2016. **2**: p. 16018.
257. Bartosch, B., et al., *Hepatitis C virus-induced hepatocarcinogenesis.* J Hepatol, 2009. **51**(4): p. 810-20.
258. Tarocchi, M., et al., *Molecular mechanism of hepatitis B virus-induced hepatocarcinogenesis.* World J Gastroenterol, 2014. **20**(33): p. 11630-40.
259. Testino, G., S. Leone, and P. Borro, *Alcohol and hepatocellular carcinoma: a review and a point of view.* World J Gastroenterol, 2014. **20**(43): p. 15943-54.
260. Zoller, H. and H. Tilg, *Nonalcoholic fatty liver disease and hepatocellular carcinoma.* Metabolism, 2016. **65**(8): p. 1151-60.
261. Forner, A., J.M. Llovet, and J. Bruix, *Hepatocellular carcinoma.* Lancet, 2012. **379**(9822): p. 1245-55.
262. El-Serag, H.B. and K.L. Rudolph, *Hepatocellular carcinoma: epidemiology and molecular carcinogenesis.* Gastroenterology, 2007. **132**(7): p. 2557-76.
263. Global Burden of Disease Liver Cancer, C., et al., *The Burden of Primary Liver Cancer and Underlying Etiologies From 1990 to 2015 at the Global, Regional, and National Level: Results From the Global Burden of Disease Study 2015.* JAMA Oncol, 2017. **3**(12): p. 1683-1691.
264. Thorgeirsson, S.S. and J.W. Grisham, *Molecular pathogenesis of human hepatocellular carcinoma.* Nat Genet, 2002. **31**(4): p. 339-46.
265. Sun, V.C. and L. Sarna, *Symptom management in hepatocellular carcinoma.* Clin J Oncol Nurs, 2008. **12**(5): p. 759-66.
266. Arrieta, O., et al., *The progressive elevation of alpha fetoprotein for the diagnosis of hepatocellular carcinoma in patients with liver cirrhosis.* BMC Cancer, 2007. **7**: p. 28.
267. Bai, D.S., et al., *The prognostic correlation of AFP level at diagnosis with pathological grade, progression, and survival of patients with hepatocellular carcinoma.* Sci Rep, 2017. **7**(1): p. 12870.
268. Llovet, J.M., C. Bru, and J. Bruix, *Prognosis of hepatocellular carcinoma: the BCLC staging classification.* Semin Liver Dis, 1999. **19**(3): p. 329-38.
269. Kinoshita, A., et al., *Staging systems for hepatocellular carcinoma: Current status and future perspectives.* World J Hepatol, 2015. **7**(3): p. 406-24.
270. Bruix, J., M. Sherman, and D. American Association for the Study of Liver, *Management of hepatocellular carcinoma: an update.* Hepatology, 2011. **53**(3): p. 1020-2.
271. Geschwind, J.F., *Locoregional Therapy for Patients With Hepatocellular Carcinoma.* Gastroenterol Hepatol (N Y), 2015. **11**(10): p. 698-700.
272. Waghray, A., A.R. Murali, and K.N. Menon, *Hepatocellular carcinoma: From diagnosis to treatment.* World J Hepatol, 2015. **7**(8): p. 1020-9.

273. Wilhelm, S.M., et al., *BAY 43-9006 exhibits broad spectrum oral antitumor activity and targets the RAF/MEK/ERK pathway and receptor tyrosine kinases involved in tumor progression and angiogenesis.* Cancer Res, 2004. **64**(19): p. 7099-109.
274. Llovet, J.M., et al., *Sorafenib in advanced hepatocellular carcinoma.* N Engl J Med, 2008. **359**(4): p. 378-90.
275. Escudier, B., et al., *Sorafenib in advanced clear-cell renal-cell carcinoma.* N Engl J Med, 2007. **356**(2): p. 125-34.
276. Ezzoukhry, Z., et al., *EGFR activation is a potential determinant of primary resistance of hepatocellular carcinoma cells to sorafenib.* Int J Cancer, 2012. **131**(12): p. 2961-9.
277. Zhu, Y.J., et al., *New knowledge of the mechanisms of sorafenib resistance in liver cancer.* Acta Pharmacol Sin, 2017. **38**(5): p. 614-622.
278. Ito, Y., et al., *Expression and clinical significance of erb-B receptor family in hepatocellular carcinoma.* Br J Cancer, 2001. **84**(10): p. 1377-83.
279. Blivet-Van Eggelpoel, M.J., et al., *Epidermal growth factor receptor and HER-3 restrict cell response to sorafenib in hepatocellular carcinoma cells.* J Hepatol, 2012. **57**(1): p. 108-15.
280. Zhang, Z., et al., *Phosphorylated ERK is a potential predictor of sensitivity to sorafenib when treating hepatocellular carcinoma: evidence from an in vitro study.* BMC Med, 2009. **7**: p. 41.
281. Abou-Alfa, G.K., et al., *Phase II study of sorafenib in patients with advanced hepatocellular carcinoma.* J Clin Oncol, 2006. **24**(26): p. 4293-300.
282. Hagiwara, S., et al., *Activation of JNK and high expression level of CD133 predict a poor response to sorafenib in hepatocellular carcinoma.* Br J Cancer, 2012. **106**(12): p. 1997-2003.
283. Horwitz, E., et al., *Human and mouse VEGFA-amplified hepatocellular carcinomas are highly sensitive to sorafenib treatment.* Cancer Discov, 2014. **4**(6): p. 730-43.
284. Wong, C.M., S.T. Fan, and I.O. Ng, *beta-Catenin mutation and overexpression in hepatocellular carcinoma: clinicopathologic and prognostic significance.* Cancer, 2001. **92**(1): p. 136-45.
285. Colnot, S., et al., *Liver-targeted disruption of Apc in mice activates beta-catenin signaling and leads to hepatocellular carcinomas.* Proc Natl Acad Sci U S A, 2004. **101**(49): p. 17216-21.
286. Sohn, B.H., et al., *Glutamine synthetase mediates sorafenib sensitivity in beta-catenin-active hepatocellular carcinoma cells.* Exp Mol Med, 2018. **50**(1): p. e421.
287. Bae, J.S., et al., *Serum response factor induces epithelial to mesenchymal transition with resistance to sorafenib in hepatocellular carcinoma.* Int J Oncol, 2014. **44**(1): p. 129-36.
288. Chen, Y.L., et al., *Sorafenib inhibits transforming growth factor beta1-mediated epithelial-mesenchymal transition and apoptosis in mouse hepatocytes.* Hepatology, 2011. **53**(5): p. 1708-18.
289. Zhang, J., et al., *Sorafenib inhibits epithelial-mesenchymal transition through an epigenetic-based mechanism in human lung epithelial cells.* PLoS One, 2013. **8**(5): p. e64954.
290. van Malenstein, H., et al., *Long-term exposure to sorafenib of liver cancer cells induces resistance with epithelial-to-mesenchymal transition, increased invasion and risk of rebound growth.* Cancer Lett, 2013. **329**(1): p. 74-83.
291. Dong, J., et al., *Activation of phosphatidylinositol 3-kinase/AKT/snail signaling pathway contributes to epithelial-mesenchymal transition-induced multi-drug*

resistance to sorafenib in hepatocellular carcinoma cells. PLoS One, 2017. **12**(9): p. e0185088.
292. Zhang, H., et al., *Inhibition of the PI3K/Akt signaling pathway reverses sorafenib-derived chemo-resistance in hepatocellular carcinoma.* Oncol Lett, 2018. **15**(6): p. 9377-9384.
293. Rudalska, R., et al., *In vivo RNAi screening identifies a mechanism of sorafenib resistance in liver cancer.* Nat Med, 2014. **20**(10): p. 1138-46.
294. Mani, S.A., et al., *The epithelial-mesenchymal transition generates cells with properties of stem cells.* Cell, 2008. **133**(4): p. 704-15.
295. Phillips, T.M., W.H. McBride, and F. Pajonk, *The response of CD24(-/low)/CD44+ breast cancer-initiating cells to radiation.* J Natl Cancer Inst, 2006. **98**(24): p. 1777-85.
296. Yin, S., et al., *CD133 positive hepatocellular carcinoma cells possess high capacity for tumorigenicity.* Int J Cancer, 2007. **120**(7): p. 1444-50.
297. Ma, S., et al., *Aldehyde dehydrogenase discriminates the CD133 liver cancer stem cell populations.* Mol Cancer Res, 2008. **6**(7): p. 1146-53.
298. Zhu, Z., et al., *Cancer stem/progenitor cells are highly enriched in CD133+CD44+ population in hepatocellular carcinoma.* Int J Cancer, 2010. **126**(9): p. 2067-78.
299. Fernando, J., et al., *A mesenchymal-like phenotype and expression of CD44 predict lack of apoptotic response to sorafenib in liver tumor cells.* Int J Cancer, 2015. **136**(4): p. E161-72.
300. Chen, X., et al., *Epithelial mesenchymal transition and hedgehog signaling activation are associated with chemoresistance and invasion of hepatoma subpopulations.* J Hepatol, 2011. **55**(4): p. 838-45.
301. van Zijl, F., et al., *A human model of epithelial to mesenchymal transition to monitor drug efficacy in hepatocellular carcinoma progression.* Mol Cancer Ther, 2011. **10**(5): p. 850-60.
302. Brown, L.M., et al., *Reversing hypoxic cell chemoresistance in vitro using genetic and small molecule approaches targeting hypoxia inducible factor-1.* Mol Pharmacol, 2006. **69**(2): p. 411-8.
303. Tak, E., et al., *Human carbonyl reductase 1 upregulated by hypoxia renders resistance to apoptosis in hepatocellular carcinoma cells.* J Hepatol, 2011. **54**(2): p. 328-39.
304. Liang, Y., et al., *Hypoxia-mediated sorafenib resistance can be overcome by EF24 through Von Hippel-Lindau tumor suppressor-dependent HIF-1alpha inhibition in hepatocellular carcinoma.* Hepatology, 2013. **57**(5): p. 1847-57.
305. Comerford, K.M., et al., *Hypoxia-inducible factor-1-dependent regulation of the multidrug resistance (MDR1) gene.* Cancer Res, 2002. **62**(12): p. 3387-94.
306. Shimizu, S., et al., *Inhibition of autophagy potentiates the antitumor effect of the multikinase inhibitor sorafenib in hepatocellular carcinoma.* Int J Cancer, 2012. **131**(3): p. 548-57.
307. Namisaki, T., et al., *Differential expression of drug uptake and efflux transporters in Japanese patients with hepatocellular carcinoma.* Drug Metab Dispos, 2014. **42**(12): p. 2033-40.
308. Herraez, E., et al., *Expression of SLC22A1 variants may affect the response of hepatocellular carcinoma and cholangiocarcinoma to sorafenib.* Hepatology, 2013. **58**(3): p. 1065-73.
309. Sukowati, C.H., et al., *Gene and functional up-regulation of the BCRP/ABCG2 transporter in hepatocellular carcinoma.* BMC Gastroenterol, 2012. **12**: p. 160.

310. Kato, A., et al., *Multidrug resistance gene (MDR-1) expression as a useful prognostic factor in patients with human hepatocellular carcinoma after surgical resection.* J Surg Oncol, 2001. **78**(2): p. 110-5.
311. Zollner, G., et al., *Hepatobiliary transporter expression in human hepatocellular carcinoma.* Liver Int, 2005. **25**(2): p. 367-79.
312. Shibayama, Y., et al., *Multidrug resistance protein 2 implicates anticancer drug-resistance to sorafenib.* Biol Pharm Bull, 2011. **34**(3): p. 433-5.
313. Tomonari, T., et al., *MRP3 as a novel resistance factor for sorafenib in hepatocellular carcinoma.* Oncotarget, 2016. **7**(6): p. 7207-15.
314. Huang, W.C., et al., *BCRP/ABCG2 inhibition sensitizes hepatocellular carcinoma cells to sorafenib.* PLoS One, 2013. **8**(12): p. e83627.
315. Coradini, D. and A. Speranza, *Histone deacetylase inhibitors for treatment of hepatocellular carcinoma.* Acta Pharmacol Sin, 2005. **26**(9): p. 1025-33.
316. Graff, J.R., et al., *E-cadherin expression is silenced by DNA hypermethylation in human breast and prostate carcinomas.* Cancer Res, 1995. **55**(22): p. 5195-9.
317. Bird, A., *DNA methylation patterns and epigenetic memory.* Genes Dev, 2002. **16**(1): p. 6-21.
318. Anestopoulos, I., et al., *Epigenetic therapy as a novel approach in hepatocellular carcinoma.* Pharmacol Ther, 2015. **145**: p. 103-19.
319. Nass, S.J., et al., *Aberrant methylation of the estrogen receptor and E-cadherin 5' CpG islands increases with malignant progression in human breast cancer.* Cancer Res, 2000. **60**(16): p. 4346-8.
320. Matsumura, T., R. Makino, and K. Mitamura, *Frequent down-regulation of E-cadherin by genetic and epigenetic changes in the malignant progression of hepatocellular carcinomas.* Clin Cancer Res, 2001. **7**(3): p. 594-9.
321. Feng, Q., et al., *DNA methylation changes in normal liver tissues and hepatocellular carcinoma with different viral infection.* Exp Mol Pathol, 2010. **88**(2): p. 287-92.
322. Glozak, M.A. and E. Seto, *Histone deacetylases and cancer.* Oncogene, 2007. **26**(37): p. 5420-32.
323. Seto, E. and M. Yoshida, *Erasers of histone acetylation: the histone deacetylase enzymes.* Cold Spring Harb Perspect Biol, 2014. **6**(4): p. a018713.
324. Yang, X.J. and E. Seto, *HATs and HDACs: from structure, function and regulation to novel strategies for therapy and prevention.* Oncogene, 2007. **26**(37): p. 5310-8.
325. Arzumanyan, A., et al., *Epigenetic repression of E-cadherin expression by hepatitis B virus x antigen in liver cancer.* Oncogene, 2012. **31**(5): p. 563-72.
326. Kouzarides, T., *Chromatin modifications and their function.* Cell, 2007. **128**(4): p. 693-705.
327. Bannister, A.J. and T. Kouzarides, *Regulation of chromatin by histone modifications.* Cell Res, 2011. **21**(3): p. 381-95.
328. Pogribny, I.P., et al., *The role of epigenetic events in genotoxic hepatocarcinogenesis induced by 2-acetylaminofluorene.* Mutat Res, 2011. **722**(2): p. 106-13.
329. Wang, H., et al., *SIRT1 promotes tumorigenesis of hepatocellular carcinoma through PI3K/PTEN/AKT signaling.* Oncol Rep, 2012. **28**(1): p. 311-8.
330. Buurman, R., et al., *Histone deacetylases activate hepatocyte growth factor signaling by repressing microRNA-449 in hepatocellular carcinoma cells.* Gastroenterology, 2012. **143**(3): p. 811-820 e15.
331. Noh, J.H., et al., *Aberrant regulation of HDAC2 mediates proliferation of hepatocellular carcinoma cells by deregulating expression of G1/S cell cycle proteins.* PLoS One, 2011. **6**(11): p. e28103.

332. Kanno, K., et al., *Overexpression of histone deacetylase 6 contributes to accelerated migration and invasion activity of hepatocellular carcinoma cells.* Oncol Rep, 2012. **28**(3): p. 867-73.
333. Quint, K., et al., *Clinical significance of histone deacetylases 1, 2, 3, and 7: HDAC2 is an independent predictor of survival in HCC.* Virchows Arch, 2011. **459**(2): p. 129-39.
334. Liu, T.P., Y.H. Hong, and P.M. Yang, *In silico and in vitro identification of inhibitory activities of sorafenib on histone deacetylases in hepatocellular carcinoma cells.* Oncotarget, 2017. **8**(49): p. 86168-86180.
335. Suraweera, A., K.J. O'Byrne, and D.J. Richard, *Combination Therapy With Histone Deacetylase Inhibitors (HDACi) for the Treatment of Cancer: Achieving the Full Therapeutic Potential of HDACi.* Front Oncol, 2018. **8**: p. 92.
336. Wang, Y.C., et al., *Effects of SAHA on proliferation and apoptosis of hepatocellular carcinoma cells and hepatitis B virus replication.* World J Gastroenterol, 2013. **19**(31): p. 5159-64.
337. Sun, W.J., et al., *Romidepsin induces G2/M phase arrest via Erk/cdc25C/cdc2/cyclinB pathway and apoptosis induction through JNK/c-Jun/caspase3 pathway in hepatocellular carcinoma cells.* Biochem Pharmacol, 2017. **127**: p. 90-100.
338. Lachenmayer, A., et al., *Combination therapy for hepatocellular carcinoma: additive preclinical efficacy of the HDAC inhibitor panobinostat with sorafenib.* J Hepatol, 2012. **56**(6): p. 1343-50.
339. Zhang, G., et al., *Vorinostat and sorafenib synergistically kill tumor cells via FLIP suppression and CD95 activation.* Clin Cancer Res, 2008. **14**(17): p. 5385-99.
340. Fu, M., et al., *Activation of mPTP-dependent mitochondrial apoptosis pathway by a novel pan HDAC inhibitor resminostat in hepatocellular carcinoma cells.* Biochem Biophys Res Commun, 2016. **477**(4): p. 527-533.
341. Bitzer, M., et al., *Resminostat plus sorafenib as second-line therapy of advanced hepatocellular carcinoma - The SHELTER study.* J Hepatol, 2016. **65**(2): p. 280-8.
342. Soukupova, J., et al., *Resminostat induces changes in epithelial plasticity of hepatocellular carcinoma cells and sensitizes them to sorafenib-induced apoptosis.* Oncotarget, 2017. **8**(66): p. 110367-110379.
343. Smith, M.A. and P. Houghton, *A proposal regarding reporting of in vitro testing results.* Clin Cancer Res, 2013. **19**(11): p. 2828-33.
344. Wahid, B., et al., *New Insights into the Epigenetics of Hepatocellular Carcinoma.* Biomed Res Int, 2017. **2017**: p. 1609575.
345. Conacci-Sorrell, M., et al., *Autoregulation of E-cadherin expression by cadherin-cadherin interactions: the roles of beta-catenin signaling, Slug, and MAPK.* J Cell Biol, 2003. **163**(4): p. 847-57.
346. Zhang, L., et al., *Resistance of renal cell carcinoma to sorafenib is mediated by potentially reversible gene expression.* PLoS One, 2011. **6**(4): p. e19144.
347. Zhai, B., et al., *Reduced expression of E-cadherin/catenin complex in hepatocellular carcinomas.* World J Gastroenterol, 2008. **14**(37): p. 5665-73.
348. Lee, T.K., et al., *Twist overexpression correlates with hepatocellular carcinoma metastasis through induction of epithelial-mesenchymal transition.* Clin Cancer Res, 2006. **12**(18): p. 5369-76.
349. Coulouarn, C., V.M. Factor, and S.S. Thorgeirsson, *Transforming growth factor-beta gene expression signature in mouse hepatocytes predicts clinical outcome in human cancer.* Hepatology, 2008. **47**(6): p. 2059-67.

350. Wang, Z., M. Wang, and B.I. Carr, *Involvement of receptor tyrosine phosphatase DEP-1 mediated PI3K-cofilin signaling pathway in sorafenib-induced cytoskeletal rearrangement in hepatoma cells.* J Cell Physiol, 2010. **224**(2): p. 559-65.
351. Dong, S., et al., *Sorafenib suppresses the epithelial-mesenchymal transition of hepatocellular carcinoma cells after insufficient radiofrequency ablation.* BMC Cancer, 2015. **15**: p. 939.
352. Cheung, S.T., et al., *Albumin mRNA in plasma predicts post-transplant recurrence of patients with hepatocellular carcinoma.* Transplantation, 2008. **85**(1): p. 81-7.
353. Jeng, K.S., I.S. Sheen, and Y.C. Tsai, *Circulating messenger RNA of alpha-fetoprotein: a possible risk factor of recurrence after resection of hepatocellular carcinoma.* Arch Surg, 2004. **139**(10): p. 1055-60.
354. Ataide, E.C., et al., *Immunoexpression of Heat Shock Protein 70, Glypican 3, Glutamine Synthetase, and Beta-Catenin in Hepatocellular Carcinoma After Liver Transplantation: Association Between Positive Glypican 3 and Beta-Catenin With the Presence of Larger Nodules.* Transplant Proc, 2017. **49**(4): p. 858-862.
355. Carr, B.I. and V. Guerra, *Serum albumin levels in relation to tumor parameters in hepatocellular carcinoma patients.* Int J Biol Markers, 2017. **32**(4): p. e391-e396.
356. Di Tommaso, L., et al., *Diagnostic value of HSP70, glypican 3, and glutamine synthetase in hepatocellular nodules in cirrhosis.* Hepatology, 2007. **45**(3): p. 725-34.
357. Di Tommaso, L., et al., *The application of markers (HSP70 GPC3 and GS) in liver biopsies is useful for detection of hepatocellular carcinoma.* J Hepatol, 2009. **50**(4): p. 746-54.
358. Davalos, V., et al., *Dynamic epigenetic regulation of the microRNA-200 family mediates epithelial and mesenchymal transitions in human tumorigenesis.* Oncogene, 2012. **31**(16): p. 2062-74.
359. Chang, R., et al., *Snail acetylation by histone acetyltransferase p300 in lung cancer.* Thorac Cancer, 2017. **8**(3): p. 131-137.
360. Yokomizo, C., et al., *High expression of p300 in HCC predicts shortened overall survival in association with enhanced epithelial mesenchymal transition of HCC cells.* Cancer Lett, 2011. **310**(2): p. 140-7.
361. Kong, D., et al., *Histone deacetylase inhibitors induce epithelial-to-mesenchymal transition in prostate cancer cells.* PLoS One, 2012. **7**(9): p. e45045.
362. Chen, Q.K., et al., *Extracellular matrix proteins regulate epithelial-mesenchymal transition in mammary epithelial cells.* Differentiation, 2013. **86**(3): p. 126-32.
363. Dika, I.E. and G.K. Abou-Alfa, *Treatment options after sorafenib failure in patients with hepatocellular carcinoma.* Clin Mol Hepatol, 2017. **23**(4): p. 273-279.
364. Xiang, Q., et al., *Cabozantinib suppresses tumor growth and metastasis in hepatocellular carcinoma by a dual blockade of VEGFR2 and MET.* Clin Cancer Res, 2014. **20**(11): p. 2959-70.
365. Han, P., et al., *Dual inhibition of Akt and c-Met as a second-line therapy following acquired resistance to sorafenib in hepatocellular carcinoma cells.* Mol Oncol, 2017. **11**(3): p. 320-334.

5. Acknowledgements

In the end I would like to thank all the people who contributed either directly or indirectly to this thesis. In particular I would like to thank Prof. Dr. Gerhard Christofori for giving me the opportunity to join his lab. Under his guidance I was able to develop and follow a project independently however had his support whenever needed. I am grateful for the inspiring discussions, the encouragement and highly instructive time I was able to spend in his laboratory with a wonderful atmosphere.

Furthermore I would like to thank my committee members Prof. Dr. Markus Heim and Prof. Dr. Markus Affolter for their insightful comments, discussions and their encouragement.

I would also like to thank all former and present members of the Christofori group who supported me and shared their knowledge and skills, for their inspiration, giving me helpful advices, who made it possible to work in a joyful atmosphere, for their precious support as well as making my past years in Basel in- as well as outside of the laboratory a fun and a memorable experience. Especially I would like to thank Meera, Feng, Marco and Helena who helped me a lot, spent a lot of time for discussions and for their friendship.

Finally, I am tremendously thankful to my beloved family and friends, for their love, support and encouragements at any moment as well as for always being there for me. In particular I would like to thank Stephanie for her patience, love, support, joyfulness and also critical questions whenever needed within the past years. I would not have been possible without you.

THANK YOU

6. Curriculum Vitae

David Martin Büchel

Date of birth:	25.08.1989
Address:	Oetlingerstrasse 45, Basel
E-Mail:	davidbchel@yahoo.de
Phone number:	+41 79 718 40 94
Marital status:	Single
Home town:	Rüthi (SG)

Education

PhD at the University of Basel 2014 - present
Department of Biomedicine
Laboratory of Prof. Dr. Gerhard Christofori
Titel of the thesis: *Wnt/β-catenin signaling in malignant mammary tumor progression and metastasis formation & Mechanisms of evasive resistance to sorafenib in hepatocellular carcinoma*

Applied methods:
Mouse handling (LTK1 course), breeding and dissection.
Further applied methods: tissue histology, cell culture handling, establishment of cell lines from mouse mammary tumors, transfection, viral infection, Luciferase reporter assay, immunofluorescent staining, imaging DNA/RNA extraction, PCR, qRT-PCR, migration and invasion assays, FACS analysis, Immunoblotting, Co-IP, ChIP, Microscopy.

Master of Science in Molecular Life Sciences 2011 - 2013
with special qualification in cell and molecular biology
University of Bern
Laboratory of Prof. Dr. Eduardo Moreno,
Supervised by Dr. Marisa M. Merino
Titel of the thesis: *Genetic and functional analysis of the EF-Hand protein Ahuizotl (Azot)*

Applied methods:
Generation of a knock-out by ends-out gene targeting and an HA-tagged version of the uncharacterized gene *azot*. Further applied methods: cloning, PCR, imaging, primer design, antibody staining and dissections of *D. melanogaster*.

Bachelor of Science in Biology 2008 - 2011
with special qualification in Cell Biology

University of Bern,
Laboratory of Prof. Dr. Daniel Schümperli

Supervised by Dr. Qing Huo
Titel of the thesis: *Validation of ten top-splicing-changes of a SMA microarray study*

Applied methods:
Validation of splicing changes using self-designed primers recognizing alternative splicing within specific genes. Further applied methods: Transfection of a Nb2a cell culture, Transformation, RNA extraction, Reverse Transcription-PCR

Matriculation

Gymnasium Köniz-Lerbermatt 2005 – 2008
Major subject: economics and law
Matriculation project in biology: *Lungenkrebs, Herstellung und Analyse histologischer Krebspräparate / Lung cancer, preparation and analysis of histological cancer specimens*

Publications

Merino MM, Rhiner C, Lopez-Gay JM, Buechel D, Hauert B and Moreno E. *Elimination of unfit cells maintains tissue health and prolongs life span*., Cell, 2015 Jan 29;160(3):461-76

Buechel, David; Saxena, Meera; Rubinstein, Natalia; Kalathur, Ravi Kiran Reddy; Valenta, Tomas; Hausmann, George; Cantù, Claudio; Basler, Konrad; Christofori, Gerhard. β-catenin signaling function vs. adhesion: *Role in epithelial-mesenchymal Transition (EMT) and malignant mammary tumor progression*. (in preparation)

Fengyuan Tang, Ruize Gao, Beena Jeevan-Raj, Christof B. Wyss, Ravi Kiran Reddy Kalathur, Salvatore Piscuoglio, Charlotte K.Y. Ng, Eva Dazert, Shuang Song, David Buechel, Marco F. Morini, Alexander Hergovich, Patrick Matthias, Dae-Sik Lim, Luigi M. Terracciano, Markus H. Heim, Michael N. Hall, and Gerhard Christofori. *LATS1 but not LATS2 represses therapy-induced autophagy by a kinase-independent scaffold function*. (in preparation)

Teaching

Supervising civil service candidates 2014 - 2018

Master thesis supervisor of a medical master student Feb. 2015 - July 2015
During doctoral studies
Titel: *Phenotypic Characterization of the β-catenin/BCL9 Signaling in Breast Cancer malignant Tumor Progression and Metastasis Formation in vivo*

Teaching of medical students at the Faculty of Medicine, 2014 and 2018
TSCR Tutoriat
University of Basel, Switzerland

Conferences

ISREC Conference Sep. 2018
Horizons of Cancer Biology and Therapy
Lausanne, Switzerland (Poster presentation)

DBM Research Day Jan. 2018
Basel, Switzerland

Basel Breast Consortium (BBC) second annual meeting Nov. 2017
Personalized breast cancer treatment 2
Basel, Switzerland

SGV Meeting Sep. 2016
Basel, Switzerland

Annual Basel Stem Cell Network (BSCN) Meeting Apr. 2016
Basel, Switzerland

SFB850
Control of Cell Motility in Development and Cancer Mar. 2015
Freiburg, Germany
Basel, Switzerland

Targeting the Kinome III Meeting Sep. 2014
Basel, Switzerland

European Cancer Center Symposium (EuCC) May 2014
Basel, Switzerland

Language skills

German:	native speaker
English:	fluent in writing and speaking
French:	good in writing and speaking

IT- skills

Adobe Illustrator
Clone Manager
Excel
Leica Application Suite (LAS)
MS-Office
End Note X6
Image J